

**A PRACTICAL FRAMEWORK TO ACHIEVE
PERCEPTUALLY SEAMLESS MULTI-PROJECTOR DISPLAYS**

by
ADITI MAJUMDER

A dissertation submitted to the faculty of the University of North Carolina at Chapel Hill in partial fulfillment of the requirements for the degree of Doctor of Philosophy in the Department of Computer Science.

Chapel Hill
2003

Approved by:

Advisor: Greg Welch

Advisor: Rick Stevens

Reader: Herman Towles

Member: Anselmo Lastra

Member: Gary Bishop

Member: Henry Fuchs

© 2003
Aditi Majumder
ALL RIGHTS RESERVED

ABSTRACT

ADITI MAJUMDER:

A Practical Framework to Achieve Perceptually Seamless Multi-Projector Displays

(Under the direction of Prof. Greg Welch and Prof. Rick Stevens)

Arguably the most vexing problem remaining for planar multi-projector displays is that of color seamlessness between and within projectors. While researchers have explored approaches that strive for strict color uniformity, this goal typically results in severely compressed dynamic range and generally poor image quality.

In this dissertation, I introduce the emineoptic function that models the color variations in multi-projector displays. I also introduce a general goal of color seamlessness that seeks to balance perceptual uniformity and display quality. These two provide a comprehensive generalized framework to study and solve for color variation in multi-projector displays.

For current displays, usually built with same model projectors, the variation in chrominance (hue) is significantly less than in luminance (brightness). Further, humans are at least an order of magnitude more sensitive to variations in luminance than in chrominance. So, using this framework of the emineoptic function I develop a new approach to solve the restricted problem of luminance variation across multi projector displays. My approach *reconstructs* the emineoptic function efficiently and *modifies* it based on a perception-driven goal for luminance seamlessness. Finally I use the graphics hardware to *reproject* the modified function at interactive rates by manipulating only the projector inputs. This method has been successfully demonstrated on three different displays made of 5×3 array of fifteen projectors, 3×2 array of six projectors and 2×2 array of four projectors at the Argonne National Laboratory. My approach is efficient, accurate, automatic and scalable – requiring only a digital camera and a photometer. To the best of my knowledge, this is the first approach and system that addresses the luminance problem in such a comprehensive fashion and generates truly seamless displays with high dynamic range.

PREFACE

Many thanks to

My parents, for being a constant source of support, inspiration, encouragement and active participation in everything that I did.

The Link Foundation and Argonne National Laboratory for funding my research for the past three years.

Eastman Kodak Company for the many high fidelity, high resolution images used in the different experiments relevant to this research.

Rick Stevens, for giving me the opportunity to work at Argonne, guiding me through my research, and finding the time to work with me even in his very busy schedule.

Greg Welch, for being there always helping me in almost all ways he can. He had truly been a friend, philosopher and guide.

Herman Towles, for helping me to gain hands on experience in graphics during my first days in graphics research, and for taking great pains to read my thesis meticulously.

Henry Fuchs, for introducing me to computer graphics and large area displays in 1998 and introducing me to the problem of color seamlessness across such displays.

Gary Bishop, for spending time with me on many discussions at the inception of my idea. His technical insights have been of great help many a times.

Anselmo Lastra, for agreeing to be in my committee and helping me with valuable advice many a times.

Many fellow grad students with whom I spent so much time, especially Ramesh Raskar, Ashes Ganguly, Anand Srinivasan, Chandna Bhatnagar, Deepak Bandyopadhyay, Mike Brown, Praveen Patnala, Ruigang Yang, Wei-Chao Chen, Benjamin Lok, Gentaro Hirota, and many others. These are all the people who made Chapel Hill a home to live in.

Many fellow researchers in Argonne, Mark Hereld, Michael Papka, Ivan Judson and others, for helping me with my experiments at Argonne and making my stay at Argonne a pleasant experience.

The graphics research groups in UNC and Argonne, for providing me with the thriving environment and exposing me to this exciting field of computer graphics.

The staff and faculty of the UNC computer science department for being a very warm and caring family to us away from home.

Last but not the least, my husband Gopi Meenakshisundaram, without whose patience, constant encouragement, determination, support and active participation through all these years, this thesis would not have been possible.

TABLE OF CONTENTS

LIST OF TABLES	x
LIST OF FIGURES	xi
CHAPTER 1: Introduction	1
1.1 Large Tiled Displays	1
1.2 Building Large Tiled Displays	3
1.3 Multi Projector Display Seamlessness	4
1.4 Previous Work	5
1.5 The Problem: Color Variation Across Multi-Projector Displays	7
1.6 Main Innovations	8
1.6.1 <i>Modeling Color Variation Across Multi-Projector Displays</i>	8
1.6.2 <i>Definition of Color Seamlessness</i>	9
1.6.3 <i>A Practical Algorithm to Achieve Photometric Seamlessness</i>	10
1.6.4 <i>Thesis Statement</i>	11
1.7 Dissertation Outline	12
CHAPTER 2: Projection Based Displays	13
2.1 Projection Technologies	13
2.1.1 <i>Cathode Ray Tube (CRT)</i>	14
2.1.2 <i>Liquid Crystal Device (LCD)</i>	15
2.1.3 <i>Digital Micromirror Device (DMD)</i>	16
2.2 Comparison of Different Projection Technologies	17
2.3 Optical Elements	18
2.3.1 <i>Filters</i>	18
2.3.2 <i>Mirrors and Prisms</i>	19
2.3.3 <i>Integrators</i>	20
2.3.4 <i>Projection Screens</i>	21

2.3.5	<i>Projector Lamps</i>	21
2.4	Projection Architectures	22
2.4.1	<i>CRT Projectors</i>	22
2.4.2	<i>Light Valve Projectors</i>	22
2.5	Multi Projector Displays	26
2.5.1	<i>Front and Rear Projection Systems</i>	27
2.5.2	<i>Projector Configuration</i>	28
2.5.3	<i>Color Variation</i>	29
2.5.4	<i>Overlapping Regions</i>	30
CHAPTER 3:	Perception	35
3.1	Perception	35
3.2	Human Visual System	36
3.3	Visual Limitations and Capabilities	37
3.3.1	<i>Luminance and chrominance sensitivity</i>	37
3.3.2	<i>Lower Color Acuity in Peripheral Vision</i>	38
3.3.3	<i>Lower Color Acuity in Dark</i>	38
3.3.4	<i>Lower Resolution in Dark</i>	38
3.3.5	<i>Lateral Inhibition</i>	38
3.3.6	<i>Spatial Frequency Sensitivity</i>	39
3.3.7	<i>Contrast Sensitivity Function</i>	40
3.4	Relationship to Tiled Displays	41
3.4.1	<i>Resolution</i>	41
3.4.2	<i>Black Offset</i>	41
3.4.3	<i>Spatial Luminance Variation</i>	41
3.4.4	<i>Visual Acuity</i>	42
3.4.5	<i>Flicker</i>	42
CHAPTER 4:	Color Variation in Multi-Projector Displays	44
4.1	Measurement	45
4.1.1	<i>Measuring Devices</i>	45
4.1.2	<i>Screen Material and View Dependency</i>	46
4.1.3	<i>Ambient Light</i>	47

4.2	Our Notation	47
4.2.1	<i>Color Operators</i>	47
4.2.2	<i>Ideal Displays</i>	48
4.3	Intra-Projector Variation	49
4.3.1	<i>Input Variation</i>	49
4.3.2	<i>Spatial Variation</i>	52
4.3.3	<i>Temporal Variation</i>	56
4.4	Projector Parameters that Change Color Properties	56
4.4.1	<i>Position</i>	57
4.4.2	<i>Projector Controls</i>	58
4.5	Inter-Projector Variation	61
4.6	Luminance Variation is the Primary Cause of Color Variation	62
CHAPTER 5: The Emineoptic Function		63
5.1	Definitions	63
5.2	The Emineoptic Function	64
5.2.1	<i>Emineoptic Function for a Single Projector</i>	64
5.2.2	<i>Emineoptic Function for a Multi-Projector Display</i>	65
5.3	Relationship with Color Variation	65
5.4	Model Verification	68
CHAPTER 6: A Framework for Achieving Color Seamlessness		71
6.1	The Framework	71
6.2	Color Seamlessness	72
6.3	Unifying Previous Work	73
6.3.1	<i>Manual Manipulation of Projector Controls</i>	74
6.3.2	<i>Gamut Matching</i>	74
6.3.3	<i>Using the same lamp for all projectors</i>	74
6.3.4	<i>Blending</i>	75
6.3.5	<i>Luminance Matching</i>	76
CHAPTER 7: An Algorithm to Achieve Photometric Seamlessness		77
7.1	Reconstruction	78
7.1.1	<i>Reconstruction Overview</i>	78

7.1.2	<i>Reconstruction Process</i>	79
7.2	Modification	82
7.2.1	<i>Choosing a Common Display Transfer Function</i>	82
7.2.2	<i>Modifying Display Luminance Functions</i>	82
7.2.3	<i>Constrained Gradient Based Smoothing</i>	85
7.3	Reprojection	90
7.3.1	<i>Retaining Actual Luminance Functions</i>	91
7.3.2	<i>Retaining Actual Transfer Function</i>	91
7.4	Chrominance	92
7.5	Enhancements to Address Chrominance	93
CHAPTER 8:	System	94
8.1	Calibration	95
8.1.1	<i>Geometric Calibration</i>	95
8.1.2	<i>Measuring Channel Intensity Response of Camera</i>	95
8.1.3	<i>Measuring Channel Transfer Function of Projector</i>	95
8.1.4	<i>Data Capture for Measuring the Luminance Functions</i>	96
8.1.5	<i>Measuring Projector Luminance Functions</i>	96
8.1.6	<i>Display Luminance Surface Generation</i>	98
8.1.7	<i>Smoothing Map Generation</i>	98
8.1.8	<i>Projector Smoothing Map Generation</i>	98
8.1.9	<i>Image Correction</i>	100
8.2	Results	100
8.3	Smoothing Parameter	102
8.4	Scalability	103
8.5	Other Issues	104
8.5.1	<i>Black Offset</i>	104
8.5.2	<i>View Dependency</i>	104
8.5.3	<i>White Balance</i>	105
8.5.4	<i>Dynamic Range</i>	105
8.5.5	<i>Accuracy of Geometric Calibration</i>	105

CHAPTER 9: Evaluation Metrics	106
9.1 Goal	107
9.2 Overview	107
9.2.1 <i>Capturing Data</i>	107
9.2.2 <i>Photometric Comparability</i>	108
9.2.3 <i>Error Images Generation</i>	110
9.2.4 <i>Error Metric</i>	110
9.2.5 <i>Evaluation Results</i>	110
CHAPTER 10: Conclusion	114
APPENDIX A: Color and Measurement	116
A.1 Color	116
A.2 Measuring Color	118
A.2.1 <i>Light Sources</i>	118
A.2.2 <i>Objects</i>	119
A.2.3 <i>Color Stimuli</i>	119
A.2.4 <i>Human Color Vision</i>	119
A.2.5 <i>Color Mixtures</i>	121
A.2.6 <i>Colorimetry</i>	123
A.2.7 <i>Chromaticity Diagram</i>	125
BIBLIOGRAPHY	128

LIST OF TABLES

4.1	Chromaticity Coordinates of the primaries of different brands of projectors	60
9.1	Results for the images shown in Figure 9.3	111
9.2	Results for the images shown in Figure 9.4	112
9.3	Results for the images shown in Figure 9.5	112

LIST OF FIGURES

1.1	A Large Area Display at Argonne National Laboratory.	1
1.2	Large Tiled Display at Argonne National Laboratory: 5×3 array of fifteen projectors.	2
1.3	Components of a Large Tiled Display System.	3
1.4	Left: Abutting Projectors; Right: Overlapping Projectors.	4
1.5	Geometric Misalignment Across Projector Boundaries. Note the area marked by the yellow square where the fender of the bike is broken across the projector boundaries.	5
1.6	Fifteen projector tiled display at Argonne National Laboratory: before blending (left), after software blending (middle), and after optical blending using physical mask (right).	6
1.7	Digital Photograph of a 5×3 array of 15 projectors. Left: Before Correction. Right: After absolute photometric uniformity (Matching only luminance).	9
2.1	Schematic of CRT projection system.	13
2.2	Schematic representation of a light valve projection system.	14
2.3	A Cathode Ray Tube.	14
2.4	Left: Schematic representation of DMD. Right: A DLP projector made of DMDs.	16
2.5	The convergence problem of the CRT projectors (left) when compared with a light valve projector (right).	18
2.6	Three CRT single lens architecture.	22
2.7	Three Panel Equal Path Architecture.	23
2.8	Three Panel Unequal Path Architecture.	24
2.9	Principle of Angular Color Separation in Single Panel Light Valve Projectors.	25
2.10	Left: The twenty dollar bill on a tiled display at the University of North Carolina at Chapel Hill. Right: Zoomed in to show that we can see details invisible to the naked eye.	27
2.11	Left: Rear Projection System at Princeton University. Right: Front Projection System at University of North Carolina at Chapel Hill.	27
2.12	Shadows formed in front projection systems.	28
2.13	Office of the Future: Conception at the University of North Carolina at Chapel Hill.	28

2.14	Left: Projection systems with mirrors on computer controlled pan tilt units for reconfigurable display walls at the University of North Carolina at Chapel Hill. Right: Zoomed in picture of a single projector.	29
2.15	Top Row: Left: Tiled displays not restricted to rectangular arrays. Right: Tiled display on a non-planar surface.(Both at the University of North Carolina at Chapel Hill) . . .	30
2.16	Frequency response for overlapped shifted combs. Top left: Response of a comb of width T . Others: Response of a comb of width T added in space with a similar comb but shifted by $T/2$ (top left), $T/4$ (bottom left) and $T/8$ (bottom right).	32
3.1	The Human Eye.	36
3.2	The distribution of the sensors on the retina. The eye on the left indicates the locations of the retina in degrees relative to the fovea. This is repeated as the x axis of the chart on the right.	37
3.3	Left: Mach Band Effect. Right: Schematic Explanation.	39
3.4	The Contrast Sensitive Function for Human Eye.	40
3.5	Left: This shows the plot of the distance of the viewer from the screen d vs the minimum resolution r required by a display	42
4.1	Left: Luminance Response of the three channels; Right: Chromaticity x for the three channels. The shape of the curves for chromaticity y are similar. The dotted lines show the chromaticity coordinates when the black offset was removed from all the readings.	50
4.2	Left: Gamut Contour as the input changes from 0 to 255 at intervals of 32; Right: Channel Constancy of DLP projectors with white filter.	50
4.3	Left: Luminance Response of the red channel plotted against input at four different spatial locations; Right: Luminance Variation of different inputs of the red channel plotted against spatial location. The responses are similar for other channels.	52
4.4	Left: Color gamut at four different spatial locations of the same projector; Right: Spatial variation in luminance of a single projector for input $(1, 0, 0)$	53
4.5	Spatial Variation in chromaticity coordinates x (left) and y (right) for maximum input of green in a single projector.	53
4.6	Left: Per channel non-linear luminance response of red and blue channel; Right: Luminance Response of the green channel at four different bulb ages	56
4.7	Left: Luminance Response of the green channel as the distance from the wall is varied along the axis of projection; Middle: Luminance Response of the red channel with varying axis of projection; Right: Luminance response of different inputs in the green channel plotted against the spatial location along the projector diagonal for oblique axis of projection.	57

4.8	Left: Luminance Response of the green channel with varying brightness settings; Middle: Luminance Response of the green channel with varying brightness settings zoomed near the lower input range to show the change in the black offset; Right: Chrominance Response of the green channel with varying brightness settings.	58
4.9	Left: Luminance Response of the green channel with varying contrast settings; Middle: Luminance Response of the green channel with varying contrast settings zoomed near the lower luminance region to show that there is no change in the black offset; Right: Chrominance Response of the green channel with varying contrast settings.	59
4.10	Left: Chrominance Response of the green channel with varying green brightness settings for white balance; Middle: Chrominance Response of the red channel with varying red contrast settings for white balancing; Right: Luminance Response of the red channel with varying red brightness settings in white balance.	60
4.11	Left: Peak luminance of green channel for fifteen different projectors of the same model with same control settings; Right: Color gamut of 5 different projectors of the same model. Compare the large variation in luminance in Figure 4.11 with small variation in chrominance.	61
4.12	Left: Chrominance response of a display wall made of four overlapping projectors of same model; Right: Color gamut of projectors of different models.	62
5.1	Projector and display coordinate space.	63
5.2	Left: Color blotches on a single projector. Right: Corresponding percentage deviation in the shape of the blue and green channel luminance functions.	66
5.3	Reconstructed luminance (left) and chrominance y (right), measured from a camera image, for the emineoptic function at input $(1, 1, 0)$ of a four projector tiled display.	68
5.4	A 2×2 array of four projectors. Left Column: Predicted Response. Right Column: Real Response.	69
6.1	Left: A flat green image displayed on a single-projector display. Right: The luminance response for the left image. Note that it is not actually flat.	72
7.1	Left: Projector channel input transfer function; Middle: Projector channel linearization function; Right: Composition of the channel input transfer function and the channel linearization function.	80
7.2	Left: The maximum luminance function for green channel and the black luminance function for a single projector. This figure gives an idea about their relative scales. Left: Zoomed in view of the black luminance surface.	81

7.3	Left: The maximum luminance function for green channel and the black luminance function for a display made of 5×3 array of fifteen projectors. This figure gives an idea about their relative scales. Right: A zoomed in view of the black luminance surface for the whole display	83
7.4	Reconstructed display luminance function of green channel for a 2×2 array of projectors (left) and 3×5 array of projectors (right). The high luminance regions correspond to the overlap regions across different projectors.	83
7.5	Left: Reconstructed display luminance function of green channel for a 3×5 array of projectors Right: Smooth display function for green channel achieved by applying the smoothing algorithm on the display luminance function in the left figure.	84
7.6	The problem: The left figure shows the reconstructed maximum luminance function, the middle figure shows the image to be displayed and the right figure shows the image seen by the viewer. Note that this image is distorted by the luminance variation of the display.	85
7.7	Photometric uniformity: The left figure shows the modified luminance function, and the right shows the image seen by the viewer. Note that the image seen by the viewer though similar to image to be displayed, it has significant reduction in dynamic range.	85
7.8	Optimization problem: The display luminance response is modified to achieve perceptual uniformity with minimal loss in display quality.	86
7.9	This shows the smooth luminance surface for different smoothing parameters. Left: Reconstructed display luminance function of green channel for a 2×2 array of projectors Middle: Smooth display function for green channel achieved by applying the smoothing algorithm on the display luminance function with $\lambda = 400$. Right: Smoothing applied with a higher smoothing parameter of $\lambda = 800$ to generate a smoother display surface.	87
8.1	System pipeline	94
8.2	To compute the maximum display luminance surface for green channel, we need only four pictures. Top: Pictures taken for a display made of a 2×2 array of 4 projectors. Bottom: The pictures taken for a display made of a 3×5 array of 15 projectors.	96
8.3	Left: Result with no edge attenuation. Right: Edge attenuation of the maximum luminance function of a single projector.	97
8.4	Left: Display attenuation map for a 3×5 projector array. Right: The projector attenuation map for one projector.	99
8.5	Image Correction Pipeline.	99
8.6	Left: Image from a single projector before correction. Right: Image after correction. Note that the boundaries of the corrected image which overlaps with other projectors are darker to compensate for the higher brightness in the overlap region.	100

8.7	Digital photographs of actual displays made of 3×5 , 2×2 and 2×3 array of projectors. Left: Before correction. Right: After constrained gradient based luminance smoothing.	101
8.8	Digital photographs of a fifteen projector tiled display. Left: Before any correction. Middle: After photometric uniformity. Right: After constrained gradient based luminance smoothing.	101
8.9	Digital Photograph of a fifteen projector tiled display. Left: Before any correction. Middle: Results with smoothing parameter of $\lambda = 400$. Right: Results with smoothing parameter of $\lambda = 800$.	102
8.10	Left: The camera and projector set up for our scalable algorithm; Right: Seams visible when the display is viewed from oblique angles due to non-Lambertian characteristics of the display surface.	103
8.11	Digital photograph of eight projector tiled display showing the result of our scalable algorithm. The display luminance function for the left and right four projector configurations are reconstructed from two different orientations. The display luminance surface for the eight projectors is stitched from these. Left: Before correction. Right: After correction.	104
9.1	Left: Reference image. Middle: Result image. Right: The recaptured image corresponding to the result image in the middle.	108
9.2	Top Row: Left: Reference image. Middle: Recaptured image for uncorrected display. Right: Recaptured image with a photometrically seamlessness display. Middle Row: Left: Comparable reference image. Middle: Comparable recaptured image for uncorrected display. Right: Comparable recaptured image for photometrically seamless display. Bottom Row: Middle: Error of the comparable recaptured image for uncorrected display from the comparable reference image. Right: Error of the comparable recaptured image for photometrically seamless display from the comparable reference image.	109
9.3	Top Row from left: (1) The reference image R . (2) Recaptured image before correction (O_1) (3) Recaptured image after photometric uniformity (O_2). (4) Recaptured image after achieving photometric seamlessness with smoothing parameter 400 (O_3). Bottom Row from left: (2) Error image for uncorrected display (E_1). (3) Error image for photometric uniformity (E_2). (4) Error image for photometric seamlessness with smoothing parameter 200. (E_3).	111
9.4	Top Row from Left: (1) Recaptured image with uncorrected display (O_1) (2) Recaptured image after photometric uniformity (O_2). (3) Recaptured image after photometric seamlessness with smoothing parameter 400 (O_3). Bottom Row from left: (4) E_1 . (5) E_2 . (6) E_3 .	111
9.5	Top Row from Left: (1) Recaptured image with uncorrected display (O_1) (2) Recaptured image after photometric seamlessness with smoothing parameter 400 (O_2). (3) Recaptured image after photometric seamlessness with smoothing parameter 800 (O_3). Bottom Row from left: (4) E_1 . (5) E_2 . (6) E_3 .	112

9.6	Error vs Smoothing Parameter.	113
A.1	The color spectrum of light for different wavelength	117
A.2	Spectrum of a red color	117
A.3	Comparison of the relative power distributions for spectral power distribution of a fluorescent (solid line) and a tungsten (dotted line) light sources	118
A.4	Calculation of the spectral power distribution of a Cortland apple illuminated with fluorescent light	119
A.5	Estimated spectral sensitivities of ρ , γ and β photo-receptors of the eye	120
A.6	Left: Color stimuli from ageratum flower appearing blue to the human eye. Right: Color stimuli from a particular fabric sample looking green to the human eye.	120
A.7	Subtractive Color Mixture	121
A.8	Additive Color Mixture	122
A.9	A set of color matching functions adopted by the CIE to define a Standard Colorimetric Observer	124
A.10	Calculation of CIE tristimulus values	124
A.11	CIE Chromaticity Diagram	125
A.12	CIE diagram showing three different color gamuts	126
A.13	Least amount of change in color required to produce a change in hue and saturation	127

CHAPTER 1

Introduction

1.1 Large Tiled Displays



Figure 1.1: *A Large Area Display at Argonne National Laboratory.*

In 1980s, Alan Kay, the father of object oriented programming, envisioned a dream computer with a megahertz processor, megabytes of memory and a display of several mega pixels. Today, after two decades, we have reached the milestones of a gigahertz processor and gigabytes of memory. But we are still limited to small monitors with approximately one mega pixels (1000×1000) only.

Present day desktop monitors have low resolution and small field of view. The limitation of such monitors is the inability to offer scale and details at the same time. Imagine such a display being used by a scientist to study a large high resolution data. While seeing the details in high resolution, he loses sight of his location in the data. Large high resolution displays offer life-size scale and high resolution,

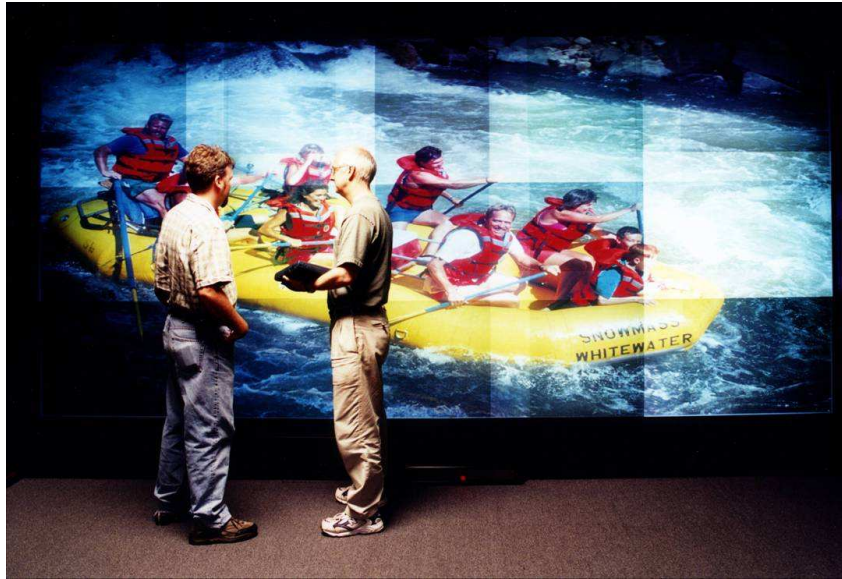


Figure 1.2: *Large Tiled Display at Argonne National Laboratory: 5×3 array of fifteen projectors.*

both of which are desirable for applications like scientific visualization and tele-collaboration. Several such displays are used at Sandia National Laboratory, Lawrence Livermore National Laboratory and Argonne National Laboratory for visualizing very large scientific data, in the order of petabytes (10^{15} bytes) and higher (10^{18} bytes), and also for holding meetings between collaborators located all around the country. Such displays are also used to create high quality virtual reality (VR) environments used to simulate sophisticated training environments for pilots. Such VR environments are also used for entertainment purpose, for example, by Disney. Fraunhofer Institute of Germany, located only a few miles away from the Mercedes manufacturing station at Stuttgart, has at least six such displays, all of which are used to visualize large data sets generated during the design of automobiles or for virtual auto crash tests. Similar such displays are investigated at Princeton University, the University of North Carolina at Chapel Hill, Stanford University, The University of Kentucky and the National Center for Supercomputing (NCSA) at the University of Illinois at Urbana Champaign.

Figure 1.1 shows one such display at the Argonne National Laboratory. Compared to a 19 inch monitor with 60 pixels per inch resolution, such a display would cover a large area of about 15×10 feet in size and would have a resolution of 100 – 300 pixels per inch. Thus such displays would have as many as 140 – 420 million pixels.

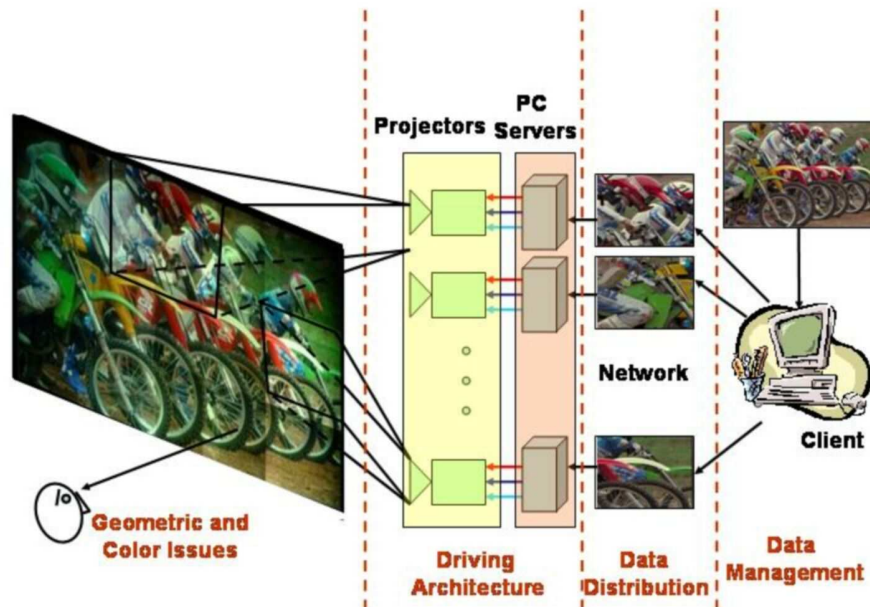


Figure 1.3: *Components of a Large Tiled Display System.*

1.2 Building Large Tiled Displays

There is no single display existing today that can meet such taxing demands. The largest display available today is about 60 inches in diagonal and has about four million pixels (2000×2000). Further, even if such a display is available in the future, it is not possible to have either the flexibility or the scalability in terms of resolution and the number of pixels.

Hence, the way to build flexible large-area high-resolution displays is to tile projectors to create one giant display. Figure 1.2 shows such a display at Argonne National Laboratory. It is made of a 3×5 array of fifteen projectors, which is 10×8 feet in size and 35 pixels per inch in resolution. In such a tiled display, scaling the number of pixels would mean using more projectors and changing the pixel density would mean changing the display field-of-view (FOV) of the projectors.

The projectors in a tiled multi projector display can be arranged in two different ways as shown in Figure 1.4. First, the projectors can be arranged carefully to abut each other. In this configuration, a slight mechanical movement in the projector position leads to a seam at the projector boundary. To avoid this mechanical rigidity, the projectors can be arranged so that they overlap at their boundaries. However, this leads to the introduction of high brightness overlap regions.

The rendering process on such display is different and more complicated than rendering on a desktop. Figure 1.3 shows one such pipeline of an image being rendered on such a display. The large

high resolution image that is to be displayed on the tiled display is divided into several smaller images by a centralized or a distributed client. In case of 3D scenes, this may mean distributing 3D geometric primitives to the servers. These smaller images or the 3D primitives are fed to PC servers which drive the projectors. The projectors project or render these on the display screen which is then viewed by a viewer.

There are several different issues that are important in this rendering pipeline. Handling and processing the hundreds of millions of pixels demand efficient data management techniques at the client end. Shipping this large amount of data efficiently to the different PC servers demands sophisticated data distribution. Efficient server architecture is essential for interactive systems. Finally, the display needs to be perfectly “seamless” and undistorted, in terms of geometry and color.

The data management, distribution and driving server architecture problems have been addressed in [Samanta99, Humphreys00, Buck00, Humphreys01, Humphreys99]. The main concentration of this dissertation is the issue of making these displays “seamless” in color.

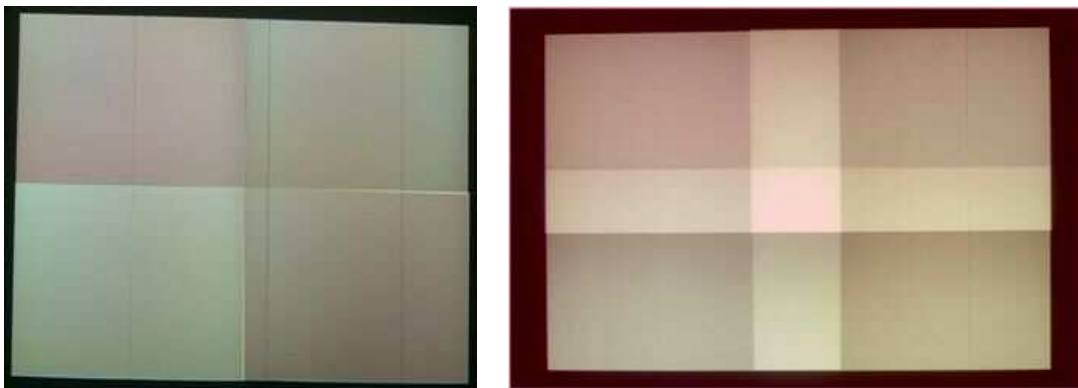


Figure 1.4: *Left: Abutting Projectors; Right: Overlapping Projectors.*

1.3 Multi Projector Display Seamlessness

There are two primary challenges faced while building a seamless multi projector display. These are *geometric misalignment* and *color variation*.

1. **Geometric Misalignment:** The final overall image of a tiled display is (by definition) formed from multiple individual display devices. Hence, they may not be aligned at their boundaries. This is illustrated in Figure 1.5. Note that the fender of the bike appears broken at the boundary between two projectors. In addition, the non linear radial distortion of the projection



Figure 1.5: *Geometric Misalignment Across Projector Boundaries.* Note the area marked by the yellow square where the fender of the bike is broken across the projector boundaries.

lens complicates the process further. There are several geometric registration algorithms [Raskar98, Raskar99b, Hereld02, Li00, Yang01] that address both these issues.

2. **Color Variation:** In Figure 1.4, while every pixel is driven with the same input value, the corresponding final colors on the display surface are not the same. This illustrates the general problem of color variation in multi-projector displays. Even in the presence of perfect geometric alignment, the color variation is sufficient to break the illusion of a single seamless display as shown in Figure 1.2. This problem can be caused by device-dependent conditions like *intra-projector color variation* (color variation within a single projector) and *inter-projector color variation* (color variation across different projectors) or by other device-independent conditions such as non-Lambertian display surface, overlaps between projectors and inter-reflections [Majumder00, Stone1a, Stone1b]. This dissertation addresses the color variation problem.

1.4 Previous Work

In the past, there had been quite a bit of work on geometric registration [Raskar98, Raskar99b, Yang01, Hereld02, Raskar99a, CN93, Chen02]. Manual methods of manipulating the projector controls are often extremely time consuming even for small displays made of two or four projectors. Furthermore,



Figure 1.6: Fifteen projector tiled display at Argonne National Laboratory: before blending (left), after software blending (middle), and after optical blending using physical mask (right).

it is difficult for humans to manage so many variables and arrive at an acceptable solution. Having a common lamp for different projectors [Pailthorpe01] is labor-intensive and unscalable. Some other methods [Majumder00, Stone1a, Stone1b, Cazes99] try to match the color gamut or luminance responses across different projectors by linear transformations of color spaces or luminance responses. Further, all these address only the color variation across different projectors. They do not address the variation within a single projector or in the overlap regions and hence cannot achieve entirely seamless displays. Blending or feathering techniques address only the overlap regions and aim to smooth color transitions across the overlap regions, as shown in Figure 1.6. This can be achieved in three different ways. First, it can be done in software by using carefully controlled linear or cosine functions, for example [Raskar98]. Second, it can be done optically with the inclusion of physical masks (apertures) mounted at the projector boundaries [Li00]. This is called *aperture blending*. Finally, the analog signals from the projectors can be manipulated to achieve seamlessness [Chen01]. This is called *optical blending*. Software blending often assumes linear response projectors and hence shows bands in the overlap regions. The aperture and optical blending techniques do not have enough control of the blending functions to produce the accuracy required for the blending to be imperceptible. Thus all the blending techniques result in softening the seams in the overlapping region, rather than removing them. Some other methods have tried to match the brightness response of every pixel with the response of the worst possible pixel on the display [Majumder02a]. Such methods suffer from poor image quality due to low dynamic range and color reproducing capabilities (Figure 8.8).

Thus, the problem of color variation in tiled multi-projector displays has not been studied in a structured and comprehensive manner. Further, there is no clear way to trade off the available projector capabilities and create high quality displays. Hence, there exists no prototype that addresses the different types of color variations in a unified manner and generates truly seamless displays. Thus, this is probably the most vexing problem that still needs to be addressed to achieve seamless displays.

1.5 The Problem: Color Variation Across Multi-Projector Displays

The problem of color variation across different devices is not entirely new. Color management systems have tried to match colors across a few devices in a laboratory setting in the past. However, the problem of color variation across the multi-projector display is much more daunting for many reasons.

First, just the *scale* of the problem is much larger than any other system developed before. Managing color across two or three laboratory devices like monitor, printer and scanner has proved to be a complicated problem [ea97, Katoh96, Nakauchi96]. This is because some colors produced by one device may not be produced by another. For multi-projector displays the complexity of the problem is increased by the fact that we want a solution that can easily scale to tens of projectors.

The traditional way to match colors across several devices in a color management system has been built on the assumption that the spatial color variation across each device is negligible. Thus, the problem is reduced to matching four or five different 3D color spaces. However, the projectors are different from most other display devices because their display space is separated from their physical space. This leads to several physical phenomena like distance attenuation of light, lens magnification and non-diffused nature of the display screen that cause severe spatial variation across the display. This becomes more acutely visible when they are tiled side by side. In addition, there are large sudden spatial luminance changes when the display transitions from a non-overlap to an overlap region. Thus, each pixel of each projection device behaves as a different device with its own different 3D color space. Thus, the problem of matching the color across the display needs *matching hundreds of millions of color spaces*, one for each pixel.

The problem of color management in the past aimed at matching the images from different devices. Note that these images were viewed by users at different points in time. This is called *temporal comparative* color. However, the images put up from different projection devices in a multi-projector display are viewed at the same time, but in a different space (i.e. side by side). This is called *spatial comparative* color. It has been shown by different perceptual studies [Valois88, Goldstein01, CC86] that humans are more sensitive to spatial comparative color than to temporal comparative color. Thus, a *higher accuracy* than the previous color management systems is needed while correcting the color variation problem in multi-projector displays.

Finally, there is *no model* that captures such a severe color variation across multi-projector displays accurately. As an analogy, existing geometric models of projectors and cameras help define

clearly the goal of achieving geometric registration. Such a model does not exist for the color seamlessness problem. Further, there is no formal definition of *color seamlessness*.

1.6 Main Innovations

This dissertation makes the first effort to address the daunting problem of color variation in a structured fashion. We present a comprehensive model that captures the color variation across multi-projector displays. This helps us define a formal general goal of color seamlessness. Finally, we present a practical algorithm to generate seamless high quality, tiled displays.

Color can be represented in many ways. One such representation is based on the way the humans perceive color. In this representation, color is defined using two properties, *luminance* and *chrominance*. Luminance, measured in cd/m^2 , is a one-dimensional property and indicates the *brightness* of a color. Chrominance is a two-dimensional property and describes the *hue* and *saturation* of a color. Hence, the range of luminance and chrominance reproduced by a device can be represented by a three dimensional volume that defines the *color space* of the device. The *dynamic range* of a device is defined as the ratio of the maximum and the minimum luminance that can be produced by the device. All the different hues and saturation that can be represented by a device can be represented by a two dimensional space called the *color gamut*. Note that this does not include luminance. A detailed treatise on this is available in Appendix A.

1.6.1 Modeling Color Variation Across Multi-Projector Displays

In this dissertation, I first develop a function that comprehensively models the variation in *both luminance and chrominance* across a multi-projector display. I call this function the *emineoptic function*. In Latin “*eminens*” means *projected light* and “*optic*” means *pertaining to vision*. Combining these, “*emineoptic*” signifies *viewing projected light*. This function provides us with a unifying framework within which all existing methods for multi-projector color correction can be explained. In addition, this function can also be used in the future to aid in the design of other methods to correct multi-projector display color variations. Thus, this function provides a fundamental tool to model *both the luminance and chrominance* variation across multi-projector displays. This is explained in detail in Chapters 5 and 6.



Figure 1.7: Digital Photograph of a 5×3 array of 15 projectors. Left: Before Correction. Right: After absolute photometric uniformity (Matching only luminance).

1.6.2 Definition of Color Seamlessness

The emineoptic function helps us to provide a formal definition of color seamlessness. We define achieving *absolute color uniformity* as matching the 3D color space at every pixel of the display to the others. We show that this approach has severe practical limitations.

1. As mentioned before, the severe spatial variation of color in projection based devices makes each pixel of the display vary significantly in 3D color space from its neighboring pixels. Thus, the problem of matching 3D color spaces of hundreds of millions of pixels is intractable.
2. Matching largely differing gamuts across small spatial distances using existing gamut mapping algorithms may not give us the accuracy demanded by the human visual sensitiveness towards comparative color differences. In fact, it may be practically impossible to achieve such a matching given the fact that the color produced by one pixel may be impossible to reproduce at another.
3. Finally, matching of the 3D color spaces across all pixels of the display strictly would match the response of all the pixels to the pixel on the display that has the worst color property, i.e. the smallest color gamut and the lowest dynamic range, ignoring the good pixels which are very much in majority. Given the fact that the spatial color variation is acute in multi-projector displays, the worst pixel can have really poor color properties like contrast, brightness and color gamut. So, by achieving an absolute color uniformity, the display quality will be severely degraded. Just to give a flavor of the problem, Figure 1.7 shows the result of an algorithm that matches *just the luminance* of every pixel to the worst one. And hence, I end up with a display that is severely compressed in contrast or dynamic range.

However, several perceptual studies [Goldstein01, Valois88, Lloyd02] confirm that it may not be necessary to achieve absolute color uniformity to generate the *perception* of color uniformity. The human vision system has limited capabilities in perceiving color, brightness and spatial frequency. This can be exploited to achieve *perceptual uniformity* which does not imply a *strict* color uniformity. For example, humans cannot detect a smooth spatial variation in color [Lloyd02, Goldstein01, Valois88]. Hence, we can retain smooth *imperceptible* color variations in the multi-projector display without degrading the display quality. In fact, allowing some imperceptible variation can increase the overall display quality. Further, this can enable us to relax the severe requirements for absolute color uniformity and make the problem tractable. Along these lines, I provide a general definition of perceptual uniformity using the emineoptic function in Chapter 6. The generality of this definition lies in the fact that it need not be limited to the single factor we have pointed out here but can incorporate different perceptual, user and task dependent factors.

Further, I formulate a general goal of achieving color seamlessness as an *optimization problem* that retains *maximal imperceptible color variation* while *minimizing the degradation in the display quality*. Such a goal helps me achieve *perceptually uniform high quality displays* as opposed to *absolutely uniform displays*. This general formal definition is derived from the emineoptic function in Chapter 6.

1.6.3 A Practical Algorithm to Achieve Photometric Seamlessness

Though we have a formal definition of color seamlessness, the optimization mentioned in the preceding section require the optimization of a five dimensional function. These five dimensions include three dimensions of color (one for luminance and two for chrominance) and two spatial dimensions. This is a daunting problem by itself. So, I simplify this problem while designing the algorithm using some practical observations as follows.

1. From analyzing the luminance and chrominance properties of multi-projector displays in Chapter 4, I make a very important observation that the chrominance is relatively constant spatially across all pixels of a single projector. Further, chrominance across different projectors of the *same model* vary negligibly. This indicates that for display walls made of the same model projectors, the spatial variation in chrominance is negligible. On the other hand, luminance variation is very significant.

2. The second important observation is made from several perceptual studies [Valois88, Valois90, Chorley81] that show that the humans are at least an order of magnitude more sensitive to variation in luminance than to variation in chrominance.

Given these two observations, I address only the luminance variation problem in our algorithm, assuming that the chrominance is spatially constant across the display. This helps me in two ways. First, when dealing with both chrominance and luminance, it is possible to be in a situation where there is no common 3D color space that is shared by all the projectors or pixels. This makes the problem of achieving a perceptual or an absolute uniformity an intractable optimization problem [Bern03, Stone1a, Stone1b]. Second, treating only the luminance reduces the problem from a five dimensional optimization problem to a simpler three dimensional optimization problem. Since our algorithm only addresses the luminance, we say that it achieves *photometric seamlessness* as opposed to *color seamlessness*. This algorithm and its implementation are presented in Chapter 7 and 8. We also present a metric to characterize and evaluate the photometric seamlessness achieved by a display in Chapter 9.

1.6.4 Thesis Statement

To summarize, the central claims of this research is as follows.

- *The color variation in multi-projector displays can be modeled by the emineoptic function.*
- *Achieving color seamlessness is an optimization problem that can be defined using the emineoptic function.*
- *Perceptually uniform high quality displays can be achieved by realizing a desired emineoptic function that satisfies the following two conditions.*
 1. *The variation in the desired emineoptic function is controlled to be imperceptible.*
 2. *The desired emineoptic function differs minimally from the original high quality emineoptic function of the display, thus avoiding the severe overall loss in display quality resulting from global uniformity.*

1.7 Dissertation Outline

In Appendix A, I provide a brief background on color and perception, as related to my thesis. Chapter 2 provides a brief introduction to projectors, different projection technologies with their advantages and disadvantages, projector architectures with their respective advantages and disadvantages. This chapter provides the necessary engineering knowledge to understand the source of the problem of color variation. A reader educated in these areas can skip most of these chapters. However the last section of Chapter 2 provides useful insights on the display properties for multi-projector displays which may not be available in any standard text books. In Chapter 3, we provide a brief introduction to human visual systems and discuss several relevant perceptual capabilities and limitations. This knowledge helps in optimally managing resources while designing multi-projector displays. A reader proficient with the area of human perception can skip most of this chapter. However, the last section of this chapter discusses the relevance of these perceptual limitations while dealing with properties of multi-projector displays and can provide interesting insights.

Chapter 4 provides a detailed analysis and classification of the color variation problem in multi-projector displays along with the possible reasons for these variations. This analysis and study leads to the development of the emineoptic function in Chapter 5 that models the color variation in multi-projector displays. Chapter 6 presents the definition of color seamlessness and the framework for achieving color seamlessness as derived from the emineoptic function. Chapter 7 presents the algorithm derived from the emineoptic function to achieve *photometric* seamlessness across multi-projector displays. Chapter 8 presents the detailed implementation and results of this algorithm. Chapter 9 presents an evaluation metric to evaluate the results of our algorithm. Finally we conclude in Chapter 10 with a few future problems.

CHAPTER 2

Projection Based Displays

Projection-based displays have been used for a long time for a variety of purposes starting from individual presentation to cinema. Though large tiled displays open up a completely new way to use projectors, it is still important to know the engineering details of a projection device to understand the problem of color variation in multi projector displays. A detailed treatise of this is available at [Stupp99].

2.1 Projection Technologies

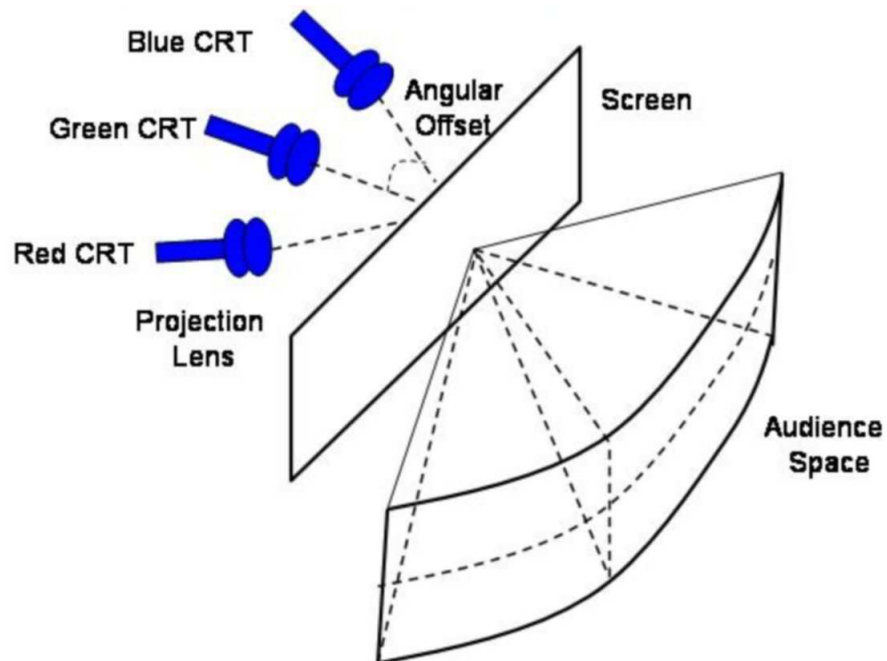


Figure 2.1: Schematic of CRT projection system.

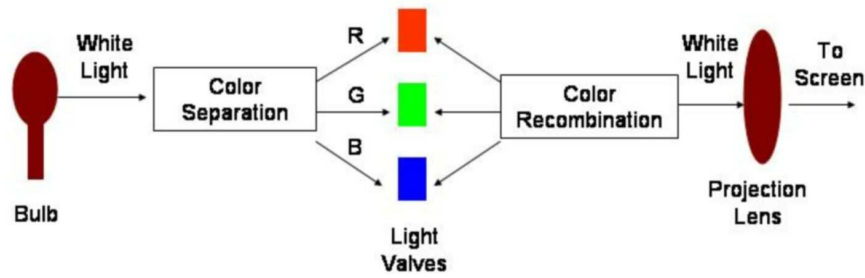


Figure 2.2: Schematic representation of a light valve projection system.

Projectors can be designed using two basic technologies. It can be a *emissive image source* technology like cathode ray tube (CRT) and laser or *light valve* technology like liquid crystal devices (LCD), digital micro-mirror devices (DMD), and digital image light amplifier (DILA). The former is light on-demand technology where appropriate amount of light is generated for varying signal strengths. On the other hand, the latter are light attenuating technology where light is continuously generated at peak strength and then the appropriate amount of light is blocked out based on the desired output intensity. These are illustrated in Figure 2.1 and 2.2.

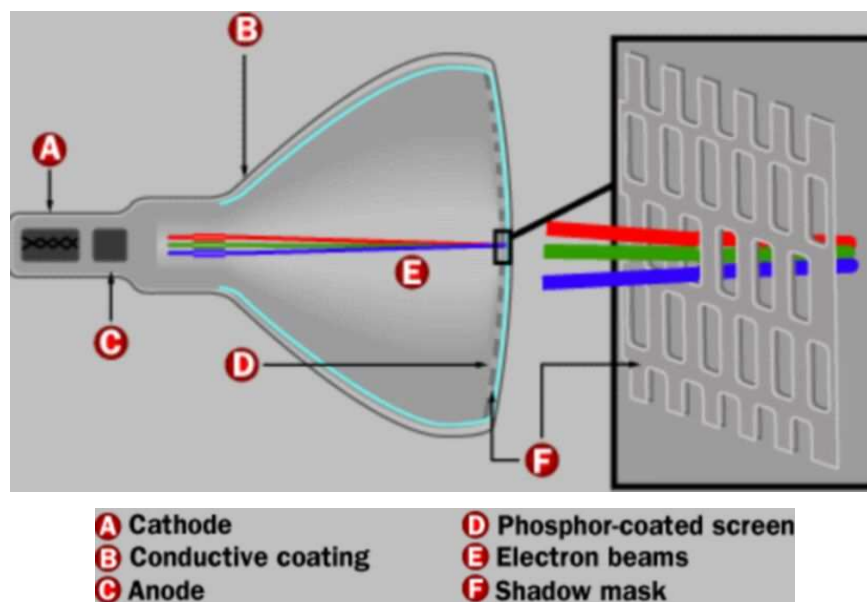


Figure 2.3: A Cathode Ray Tube.

2.1.1 Cathode Ray Tube (CRT)

The emissive image source in these kinds of devices is made of a cathode ray tube. A cathode ray tube is illustrated in Figure 2.3. In a cathode ray tube, the *cathode* is a heated filament (not unlike

the filament in a normal light lamp). The heated filament is in a vacuum created inside a glass *tube*. The *ray* is a stream of electrons that naturally pour off a heated cathode into the vacuum. Electrons are negative. The anode is positive, so it attracts the electrons pouring off the cathode. The stream of electrons is focused by a focusing anode into a tight beam and then accelerated by an accelerating anode. This tight, high-speed beam of electrons flies through the vacuum in the tube and hits the flat screen face at the other end of the tube. This screen is coated with phosphor, which glows when struck by the beam. This screen coated with phosphor is also called *faceplate*. To direct the beam at different locations in the phosphor coated screen, the tube is typically wrapped in coils of wires called the *steering coils*. These coils are able to create magnetic fields inside the tube, and the electron beam responds to the fields. One set of coils creates a magnetic field that moves the electron beam vertically, while another set moves the beam horizontally. By controlling the voltages in the coils, you can position the electron beam at any point on the screen.

In CRT projectors, as shown in Figure 2.1, a separate CRT is generally used for each color channel. The light from the faceplates are directed to a projection lens system which projects the magnified image on the wall.

2.1.2 Liquid Crystal Device (LCD)

The liquid crystal projector is based on light valve technology and is illustrated in Figure 2.2. This consists of a beam separator that splits the white light from the lamp into red, green and blue; the split beams then pass through the three light valve panels that attenuate the amount of light at each display location differently as per the image input; and finally the beam combiner combines these split beams from where it is projected through the projection lens.

The light valves in the LCD projection devices are made of liquid crystal pixels addressed by active matrix devices. The voltages applied changes the liquid crystal transmissive and dielectric properties, which in turn changes the polarization of light.

Liquid crystals (LC) are in an intermediate phase, called mesophase, between crystalline solids and isotropic fluid. When the LC is cooled, it will turn to a solid and at high temperatures, it will turn to a liquid.

Amongst all kinds of LC material, the nematic one is most commonly used. These are rod shaped liquid crystals aligned in one predominant direction called the *director*. Usually the LCs are sandwiched between two alignment layers called the polarizer and analyzer.

The LCD technology can be designed in two ways. The first is *driven to white* mode. Here, with no voltage, the unpolarized light gets polarized by the polarizer, changes direction of polarization when passing through the liquid crystal and then gets blocked by the analyzer. With applied voltage, the amount of light blocked by the analyzer decreases, thus increasing the intensity of the projected light. Since the minimum is produced with no voltage and applying voltage drives it towards the maximum intensity, this type of projectors are said to be driven to white.

In the *driven to black* mode, the polarizer and analyzer are orthogonal to each other or are at an angle so that the liquid crystals undergo a twist. These are called twisted nematic (TN) cells. Here, with no voltage, the maximum intensity is passed by the analyzer. With applied voltage, the amount of light blocked increases and at very high voltages, the whole light is blocked. Since these produce less and less light with more and more voltage, these are said to be driven to black.

The polymer dispersed liquid crystal (PDLC) does not need a polarizer or analyzer. The electro-optic material has liquid crystals suspended in them. Without voltage, light is not polarized and scattered in all directions. With voltage, it is polarized to different partial level. A schlieren optical system is then used to separate the scattered and the polarized light directing the polarized light on to the projection lens.

2.1.3 Digital Micromirror Device (DMD)

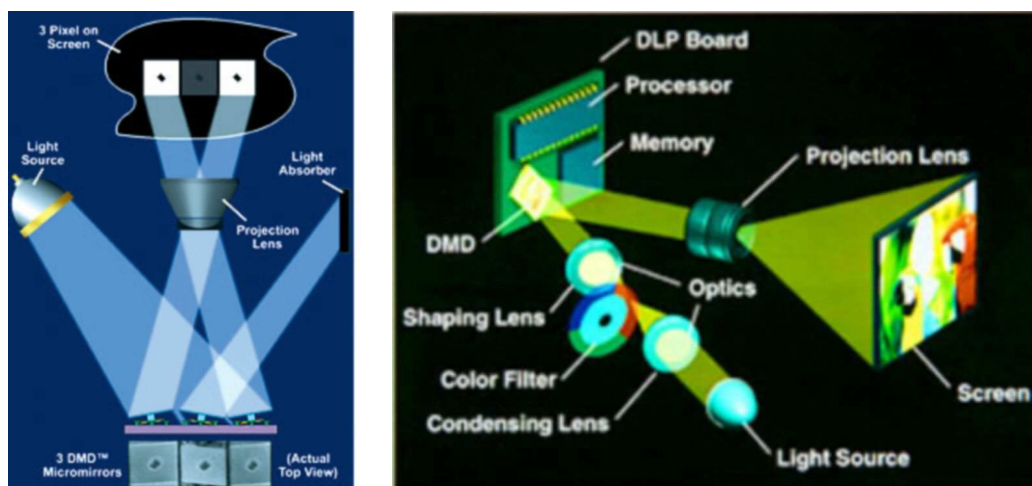


Figure 2.4: Left: Schematic representation of DMD. Right: A DLP projector made of DMDs.

In these, each pixel consists of a micro-mirror on a torsion-hinge-suspended yoke. The mirror can be deflected in a $+10$ or -10 degrees. In one position, the light falling on the mirror is reflected on

to the projection lens. In the other, it does not reflect on to the lens. The gray scale imagery is created by binary weighted pulse width modulation. This is illustrated in Figure 2.4. In single chip systems, color imagery is produced by using a rotating color filter to present the images for different channels sequentially.

2.2 Comparison of Different Projection Technologies

The different projection technologies mentioned in the preceding sections have different advantages and disadvantages which we will be discussing in this section.

1. **Brightness:** The brightness of the CRT projectors are often limited by the properties of the phosphors. With increasing beam currents, after a certain threshold, the phosphors do not increase the emission. This is significant for blue phosphors. However, this may be compensated by what is called *beam blooming*, the increase in the beam diameter at higher beam currents. This compensates the saturation problem to some extent. Further, there is the problem of thermal quenching. At very high temperatures the emissivity of phosphors decreases with increase in the beam current. A liquid cooling is coupled with the faceplate to avoid this problem. However, the brightness is limited by the phosphorus properties. Unlike this, increasing the power of the lamp can easily increase the brightness of the light valve projectors. Of course, this also brings in the need of cooling the system which is often achieved by a fan in the projector.
2. **Contrast:** Inherently, CRT projectors produce light under demand, can be adjusted to produce no discernable light for black. Thus, these projectors usually have very high dynamic range. On the other hand, since the light valve projectors use light blocking technology, it is impossible to eliminate the amount of leakage light that is projected at all times. This reduces the contrast of the projectors.
3. **Resolution:** Usually, the system shown in Figure 2.1 have the three different axis of projection for the different channels leading to different keystoneing for different channels. This needs to be converged by non-linear adjustments to the deflection. However, this often almost impossible to achieve. This is shown in Figure 2.5. Second, The focus of the electron beam also contributes to the resolution. Usually, the beam is best focused as constant distance from the center of deflection. So ideally, one should have convex face plate. But that leads to complex projection optics design and also some problems therein. Hence, such faceplates are avoided at cost of



Figure 2.5: *The convergence problem of the CRT projectors (left) when compared with a light valve projector (right).*

resolution. For light valve projectors, a phenomenon called coma is experienced when the light travels through the thick glass that makes the filter substrates or the projection lens. In such cases, some ghost images decrease the resolution of the picture. Often the orientation of light valve panels needs to be adjusted to correct for this.

4. **Light Efficacy:** Usually, the light efficacy of the light valve projectors are very low because light is continuously produced and the unwanted light is blocked out. This is especially low for LCD projectors since only light polarized in a particular direction is allowed to pass through the LCD panels.

2.3 Optical Elements

In this section, we discuss briefly the different optical elements of a projector. This will help us understand the contribution of these elements to the color variation in a multi-projector display. The different optical elements primarily include filters, mirrors and prisms, integrators, lamps and screens.

2.3.1 Filters

Filters are used in the optical path of light valve projectors to split the white light to red, green and blue ones and then recombine them back after passing through the light valves. The important properties of the filters are its spectral response, transmissivity and reflectivity. Usually these responses vary with polarization of light and angle of incidence and can cause different aberrations that needs to be compensated.

There are two kinds of filters, *absorptive* or *dichroic*. Both the filters are made by several layers of materials alternating with high and low dielectric constant and sandwiched between two substrates of glass.

Dichroic filters

Note that dichroic filters cannot combine beams of the same color or polarization. So, it can combine green and red beams together but not two red beams.

The biggest advantage for dichroic filters is that they absorb almost no light. Hence, almost all light is transmitted (about 96% at normal incidence). This also means negligible heating or thermal stress on the filters. Usually, it is pretty easy to design dichroic filters with good spectral characteristics.

Usually the spectral characteristics vary with angle of incidence. For non-normal incidence, especially at more than 20 degrees, the spectral band shows a significant shift to the left. In most projectors, the dichroic filters receive non-telecentric light where the angle of incidence on one side is different than at the other end. This leads to a color shift from one end of the projector to another that may be noticeable. Usually, non-telecentric light leads to compact design and smaller projectors. The angle also has effects in the transmissivity and hence often there is a luminance gradient from one side to other of a projector. As a solution, often a gradient is built in the dichroic filter to compensate for these effects.

Absorptive Filters

These are not used much for three primary reasons.

1. Since they absorb wavelengths selectively to split the light, they are often heated up highly or are thermally stressed. This leads to lower life of the filters.
2. They usually have low transmission capabilities, about 65%. This not only reduces the efficiency of the system, but the stray light generated often reduces the contrast by increasing the black offset.
3. Finally, it is difficult to design band pass or short wavelength pass filters. So the blue and green primaries often are not saturated leading to lower color gamuts. Long wavelength passing filters (red filters) are reasonably easy to make.

2.3.2 *Mirrors and Prisms*

Mirrors and prisms are used in the optical path to move the beam around as required. Reflection from mirrors and total internal reflections in prisms are used for this purpose. Usually, first surface mirrors are used. Second surface mirrors produce ghost images which reduce the projector resolution.

2.3.3 Integrators

The integrators have two functions. First, they make the luminance uniform and second they change the circular cross section of the lamp beam to the rectangular cross section beam required for the light valves.

Since the lamp is a point source of light, often the illumination of the light valves show a severe fall off from center to fringe. Further, due to the same reason, the efficiency of the system is often reduced since much of the light does not actually make it to the projection lens. And finally, this wasted light can end up causing low contrast displays.

Integrators alleviate all these problems. There are two types of integrators.

Lenslet integrators

This usually has two lenslet arrays following the lamp-reflector assembly. The second array is combined with an auxiliary lens. The lenslet changes the single source into a array of sources. However, the number of lenslets used is critical. With too few lenses, the illumination is not sufficiently uniform. But with too many lenslets, there is no transition region between adjacent lenslets creating some step artifacts.

Rod Integrators

This is made of a pair of square plates placed perpendicular to the lamp reflector assembly. The beam from the lamp gets reflected back and forth across these plates before reaching the light valve. If the rod is long enough, this means that the spatial correlation of the beams are lost by the time they reach at the end of the rod integrator creating a more uniform illumination. In fact, with a sufficiently long rod, a perfectly uniform field can be achieved. However, there are three main reasons why the lenslet integrators are more popular.

1. The optical path length can be pretty long leading to less compact design.
2. The multiple reflections can result in significant loss in light, reducing the overall system efficiency.
3. It is difficult to use it with polarized light usually used in LCDs because it can cause in partial change in polarization of light.

2.3.4 Projection Screens

Screen is a passive device but can redirect energy in an efficient manner to increase the visual experience. The gain of a screen is defined by the ratio of the light reflected by a screen towards a viewer perpendicular to it to that reflected by a Lambertian screen in the same direction. Thus, screens with high gain have directional light reflection properties while a Lambertian screen has a gain of 1.0.

2.3.5 Projector Lamps

There are two major types of lamps used for light valve projection devices, namely tungsten halogen lamps and high-intensity discharge (HID) lamps that include xenon lamps, metal halide lamps and the UHP lamps.

The HID lamps are filled with some material at room temperature. This vaporizes at high temperatures to emit light. However, when cold, the typical pressure of the lamp is 10 – 13 atmospheres. When operating, this is near 50 – 59 atmospheres which increase lamp explosion hazard. Usually, it is in a safe chamber while operating but this does not reduce the chance of an explosion while changing the lamp.

Metal halide lamps usually have a metal fill with halide doping. Most metals have excellent spectral emission in gaseous state. Unfortunately they have a very low vapor pressure and very few atoms are in the free gaseous state to emit light. In fact, they condense in the relatively cold quartz. To increase their vapor pressure, a halide doping is used. Iodine is usually a very good doping element. Using this leaves the metal atom in gaseous state near the arc and they emit due to the higher temperatures near the arc.

One of the most important lamp artifacts includes spectral emission lines. Some lamps emit light near the yellow and blue which cannot be blocked by the filters and reduces the saturation of either the green or red reducing the color gamut. Further, manufacturing errors make it difficult to predict whether the yellow will be included in the green or the red. Thus different projectors using the same lamp can show different characteristics of the primaries. The same problem near the blue-green region is not nearly as serious because of the considerable overlap in the blue and green spectrums.

2.4 Projection Architectures

The projector architecture usually differs in the number of projection lenses used and whether the three channels are multiplexed in time or space. In this section, we will first discuss the different CRT architectures and then the light valve projector architectures.

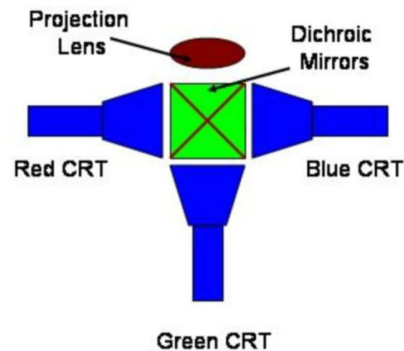


Figure 2.6: *Three CRT single lens architecture.*

2.4.1 CRT Projectors

Most CRT projectors have a three CRT three lens architecture as shown in Figure 2.1. As mentioned earlier, convergence of pixels from different channels is a significant issue. So, an one lens architecture is often used as shown in Figure 2.6. Here, the output of the three tubes is combined using dichroic filters which are then passed through the projection lens. The different keystone distortions of different channels are avoided. Thus convergence is much better. Further, the convergence need not be adjusted with change in the distance from the screen. The convergence can be factory set instead.

2.4.2 Light Valve Projectors

The light valve projectors differ in architecture depending on the number of panels used. Usually, panels are very expensive. Hence, lesser number of panels means lesser cost. Almost always a single lens is used for projection.

Three panel systems are the most dominant architecture by may have some convergence problem. For single panel projectors, color field sequential systems or color micro-filters systems or angular color separation systems are used.

Some two panel systems have also been designed due to engineering issues. Due to system or device limitations, sometimes a panel can modulate two colors satisfactorily and not the third. This calls for a second panel. Or, if the lamp is deficient in one color, it needs to be projected a greater percentage of time.

Three Panel Systems

This is the most dominant architecture. It uses three valves, single lens and single lamp. Each panel is dedicated to one color. This enables maximal usage of the available light. There are two types of three valve systems.

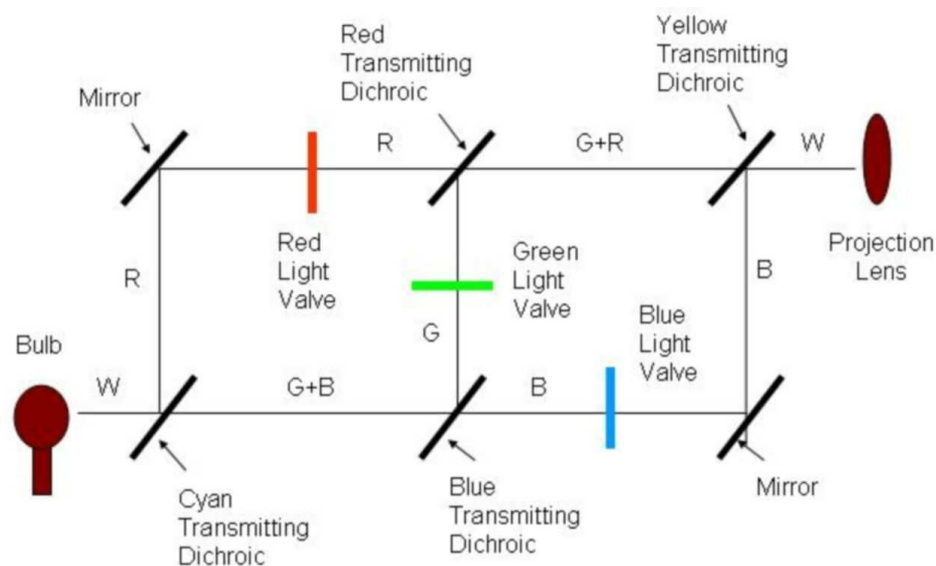


Figure 2.7: *Three Panel Equal Path Architecture.*

1. *Equal Path Systems:* In this system, the three colors have equal optical path as shown in Figure 2.7. Further, the path from the lamp to the light valves and from the light valves to the lens are also equal for every channel. However, the number of dichroic filters traversed and the number of mirror reflections undergone by the colors are not equal. Usually at least two of the three light valves are provided with six axis adjustments to achieve convergence. These adjustments should be shock resistant to maintain the convergence.

This architecture has a few disadvantages. First is the convergence issue. Second, the large distance from the lamp to the projection lens reduces the light efficiency thus demanding the use of expensive lens to get acceptable image quality. Third. the number of dichroic filters passed

is not same for every color which introduces different amount of coma for each of them. This leads to more convergence. Two colors undergo odd number of reflections that laterally invert the optical path while the other undergo even number of reflection. Thus, the optical path of the color with odd number of reflections needs to be inverted by electronics.

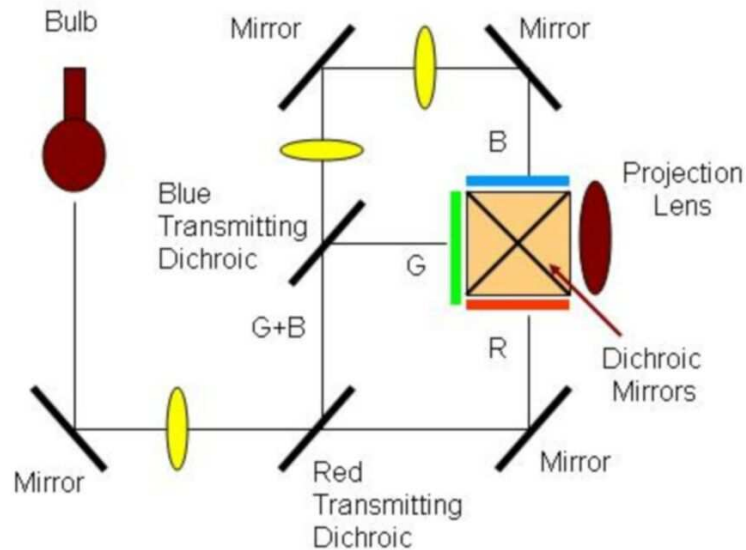


Figure 2.8: *Three Panel Unequal Path Architecture.*

2. **Unequal Path Systems:** In this architecture, crossed dichroic filters mounted on the inner diagonal of the prism is used for recombination of the light. The three panels are mounted on the three sides of the prism and the projection lens is mounted on the fourth side. This is illustrated in Figure 2.8.

There are some advantages of this system. First, the shorter optical path length from the lamp to the lens leads to less expensive lens, which in turn reduces the cost of the projector. Also, this yield more compact designs. Second, the panels are mounted on the prism which makes them easily shock resistant. Thus the six axis adjustments can be done in the factory to produce convergence. Often this eliminates the requirement of providing the users with these controls.

However, there are some disadvantages. First, the light hitting the dichroic filter is not telecentric. And since these filters are sensitive to angle of incidence, this often gives rise to left to right color shift. Due to the unequal path lengths, additional relay and field lens (shown in yellow in Figure 2.8) are required in the longer path to get similar illumination.

One Panel Systems

The one panel systems are less expensive and naturally convergent. However, these also have some problems. First, the cost to be paid is in terms of higher data rates (for time sequential operation) or higher resolution panels (sub pixelated panels with three times the resolution). Second, the energy falling on the panel is three times of that in three panel systems. Often some polarizers are unable to take this stress. Thus, extra thermal load on the polarizer may restrict the lamp power used in these projectors.

There are different kinds of one panel systems depending on how the three colors are managed.

1. **Sub-pixelated:** Usually, color micro-filters are used before the panel. They have micro-filter that produces the different colors in the sub pixel level. Further the light does not need to be recombined after the panel. This removes many of the expensive recombination optics after the panel also. However, the magnification should be kept low enough so that the eye cannot resolve the pixels for the different colors. Unable to achieve this creates artifacts called the *jaggies*, the step wise approximating of the lines of one or more colors.

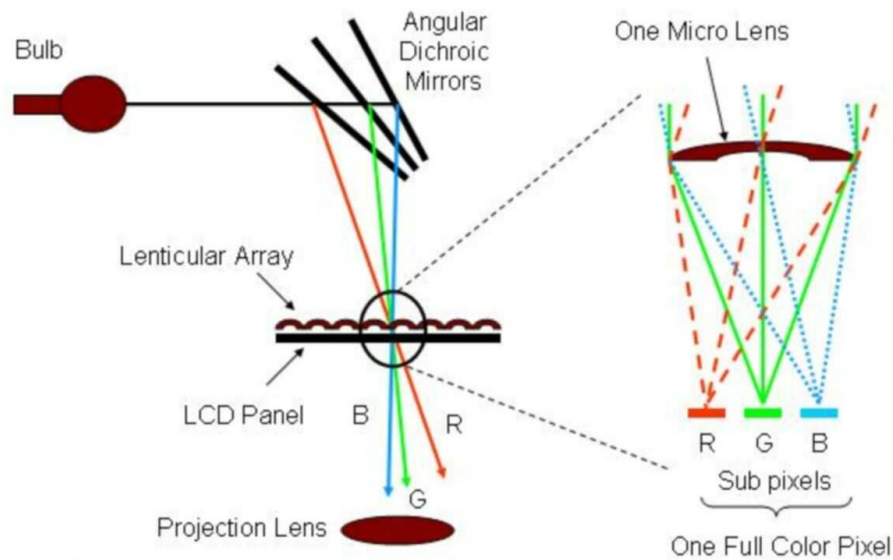


Figure 2.9: Principle of Angular Color Separation in Single Panel Light Valve Projectors.

2. **Angular Color Separation:** In this architecture, as shown in Figure 2.9, three dichroic mirrors, separate the incoming light from the lamp to three angularly separated beams. Each pixel consists of three subpixels for the three colors. And the angularly separated light passes through

micro-lenses (one for each pixel) which bring the different colored lights to focus on appropriate subpixels. This happens because the refractive index of the lens is different for different wavelength lights. Thus, these do not need the filters and use all the light thus increasing the efficiency of the device.

The problem in this system is that the dichroic mirrors need to be very flat to avoid distortion since this can easily lead to ‘cross-talk’ within colors. The angles of illumination in these filters can create color gradients. Second, the micro lenses also need to be accurately manufactured. Finally, here also we need larger panels.

3. **Field Sequential:** In this architecture, a motor rotates a color wheel and presents the red, green and blue filters in succession to the lamp. Thus at any time one of the color lights the panels. Unlike the other one panel system, the information that is presented to the panel in consecutive time frames may be highly uncorrelated. Thus, there may be big changes. To do these changes effectively, often a quite time is required between subsequent frames which leads to energy loss and reduction in lamp efficiency. Further, the switching time also may pose a limitation for many LCD panels. However, they have been successfully used in DMD systems.

However, one important point to note here is, some of the recent DLP projectors use a clear filter on the color wheel to project the grays. Thus, they use a four filter wheel. With this clear filter, the projector ceases to behave as a normal three primary system. So, the basic assumption that the light projected at any input is the optical superposition of the contributions from the red, green and blue primaries is no longer valid. As we will see later in this thesis, this can be a significant problem while modeling and correcting the color variation across multi-projector displays.

2.5 Multi Projector Displays

As mentioned in Chapter 1, the goal of multi projector is to produce life size and very high resolution images. The resolution that we are trying to achieve is demonstrated in Figure 2.10. For example, when we use them to display a twenty dollar bill, we can see high resolution details that are invisible even to the naked eye. In this section we will discuss the general setup of such multi projector displays and several issues thereof.

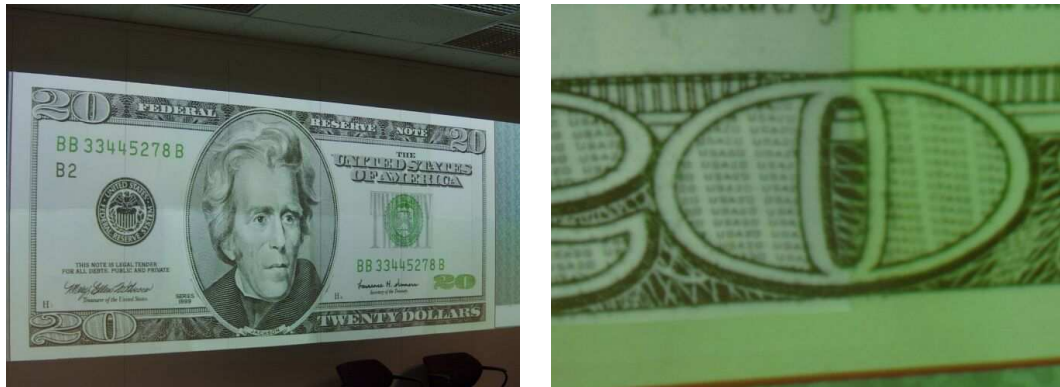


Figure 2.10: Left: The twenty dollar bill on a tiled display at the University of North Carolina at Chapel Hill. Right: Zoomed in to show that we can see details invisible to the naked eye.

2.5.1 Front and Rear Projection Systems



Figure 2.11: Left: Rear Projection System at Princeton University. Right: Front Projection System at University of North Carolina at Chapel Hill.

The tiled display may use front or rear projection. Figure 2.11 shows two examples. There are advantages and disadvantages for both of them. For rear projection system, an extra space is needed behind the screen which cannot be used for any other purpose. So, these have bigger space requirement. On the other hand, in front projection systems, the projectors are hung from the ceiling and do not need any extra dedicated space. But, in this case, it is easy to block the light from the projector thus creating shadows on the display as shown in Figure 2.12. Further, the light from projectors can blind the users at times. The second issue is with display screens. Usually such displays are built to accommodate many moving users. So, Lambertian screens are ideal as they do not amplify the spatial variation in color. However, very few rear projection screens are available that have screen gain of close to 1.0. So, typically, rear projection screens show larger luminance variation. But at



Figure 2.12: *Shadows formed in front projection systems.*

the same time, the diffused nature of the front projection screen allows light to spill from one pixel to another. Thus, rear projection screens produce crisper pictures than front projection screens.



Figure 2.13: *Office of the Future: Conception at the University of North Carolina at Chapel Hill.*

2.5.2 Projector Configuration

As mentioned in Chapter 1, the projectors can be arranged in both abutting and overlapping configuration. However, it is evident from the previous sections of this chapter that the projectors

would show considerable brightness fall off from center to the fringes. Thus the abutting configuration would show severe spatial variation, especially for rear projection systems. Our analysis shows that this can be as large as 20% of the peak luminance. The overlapping configuration not only alleviates the problem of mechanical rigidity of projector arrangements, but also compensates for some of the radial fall off along the projector fringes by overlapping projectors near the boundaries.

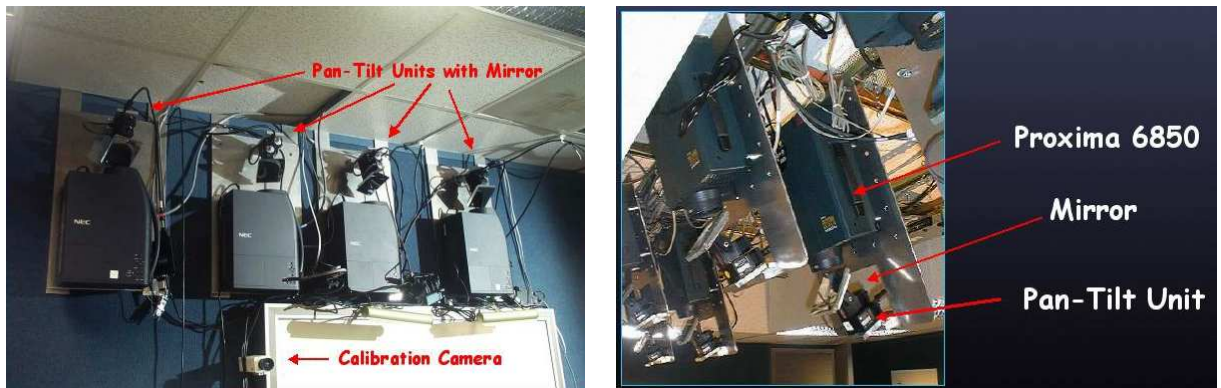


Figure 2.14: Left: Projection systems with mirrors on computer controlled pan tilt units for reconfigurable display walls at the University of North Carolina at Chapel Hill. Right: Zoomed in picture of a single projector.

In fact, for some applications, even the restriction rectangular projection or planar displays can be prohibitive. For example, *office of the future* application, as illustrated in Figure 2.13, proposes the use of the walls of everyday office space as displays. Thus, we would have “pixels everywhere” which we can use for something as complex as 3D visualization and teleconferencing applications or something as simple as our desktop. The Department of Energy (DOE) is supporting recent research directed towards what is called *reconfigurable displays*, where the projectors can be moved around to create different types of displays based on the user’s requirements. In such cases, often mirrors mounted on computer controlled pan tilt units are used to move the projectors projection area around, as shown in Figure 2.14. Thus, we can create displays which do not have projectors projecting in rectangular fashion only, or on planar displays only as shown in Figure 2.15.

2.5.3 Color Variation

The color variation problem has been introduced in Chapter 1. In this section, we will provide some insights as to how some projector configurations may alleviate the color variation problem to some extent. As evident from the previous sections of this chapter, projectors show radial spatial fall off in brightness. This can be accentuated in rear projection systems by the nature of the display

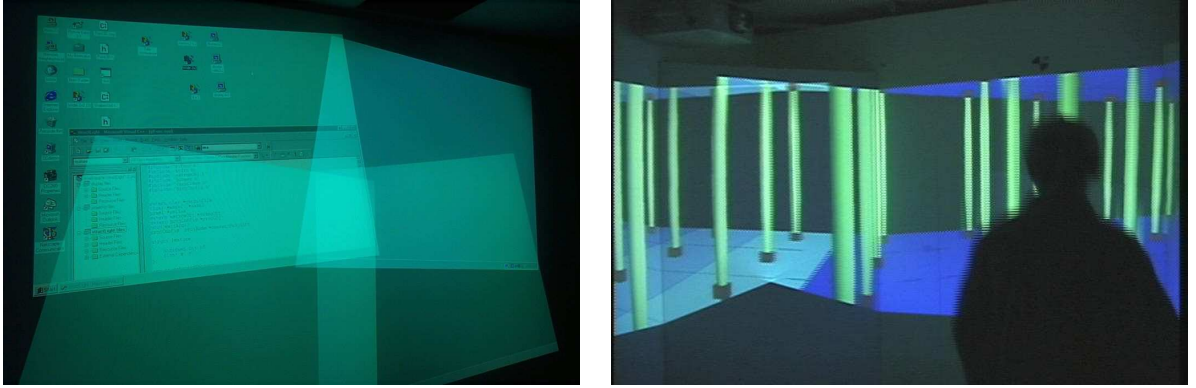


Figure 2.15: *Top Row: Left: Tiled displays not restricted to rectangular arrays. Right: Tiled display on a non-planar surface.(Both at the University of North Carolina at Chapel Hill)*

screen. Our analysis shows that this fall off can be as large as 60% of the peak luminance. Thus, overlapping projectors across the boundaries alleviate the problem to some extent by compensating the low luminance at the fringes by overlapping projectors. Further, this clearly indicates that tiling projectors in an abutting fashion not only leads to a rigid system but also a display which shows severe variation in color. Based on these observations, several innovative projector configurations have been suggested to alleviate this problem. Some of these include arranging projectors in honeycomb fashion or overlapping projectors. Some of these have been investigated [Majumder01] and it would be interesting to investigate more on such arrangements in the future.

2.5.4 Overlapping Regions

The overlapping regions in multi-projector displays raise several issues like what happens to the brightness, contrast and resolution in this region? Do we really enter a regime where we can get better contrast, brightness and resolution in the overlap region? Does that mean that we can just overlap projectors and get better displays? In this section, for the sake of completeness, we address these issues briefly.

We address these issues from a signal processing point of view. Let us consider a signal P with maximum at P_{max} and minimum at P_{min} . The brightness (mean) of this signal is defined as

$$P_{brightness} = \frac{P_{max} + P_{min}}{2}.$$

The contrast of the signal is defined by Michelson's contrast as

$$P_{contrast} = \frac{P_{max} - P_{min}}{P_{max} + P_{min}}.$$

Let us now look at the overlap region formed by two such signals P_1 and P_2 . Let the combined signal be called P_c .

Brightness

The brightness of P_c is the addition of the brightness of the two separate projectors. Thus we get higher brightness in the overlap region. In the general case of n projector overlaps, the brightness is the sum of the brightness of all the n projectors.

Contrast

However, note that for contrast this is not the case. First, because of the black offset ($P_{min} \neq 0$), the projectors do not have the ideal contrast of 1.0. Further, contrast is proportional to the ratio of the range and the mean of the signal. Thus, if we are dealing with projectors with similar contrast, the contrast in the overlapping region will not change significantly. However, it may show slight changes depending on the variation of range and brightness of the projectors.

Spatial Resolution

The next important issue is the resolution. It may seem that we can overlap projectors, we can achieve higher resolution in this region by using super resolution images. Let us investigate if this is really possible.

Let the sampling frequency be f_s . This defines the resolution at which the image to be projected is sampled. Now, this means that the analog signal sampled in this image must be band limited to $\frac{f_s}{2}$, to avoid aliasing effects. Further, the point spread function of the pixels of each projector should have a width of $f_p = \frac{f_s}{2}$ in the frequency domain for faithful reconstruction. If f_p is larger (pixels are sharper in the spatial domain), some low frequencies will show up as high frequency. This will lead to screen door effect or pixelization. If f_p is lower (wider pixels), some high frequency will be lost leading to blurred pictures. This is what happens for a non-overlapped projector. Let me mention as a side remark here, that this is the reason we see blurred pixels near the fringes of projectors set up in highly oblique fashion. The f_p is much lower leading to lost high frequencies.

Let us now consider an overlap of two projectors. Let us assume that the analog signal is band limited to f_s instead of $\frac{f_s}{2}$. This assures that the resolution in the overlap region is not limited by the

frequency content of the signal itself. In fact, this basically assured that we are trying to project a super resolution image.

Now let us assume that the pixels of the two projectors are offset by exactly half a pixel. Under the assumption that the computer to projector interface is digital, this increases the sampling frequency from f_s to $2f_s$. Now, if the point spread function is still f_p , while reconstruction, frequencies only till f_s will be passed and all the higher frequencies generated by the super resolution image will be discarded. Thus, if we have the same point spread function, having super resolution will *not* increase the resolution, but at the same time it cannot reduce the resolution either. However, if f_p is increased (pixels are made sharper), then higher frequencies will be passed leading to higher resolution.

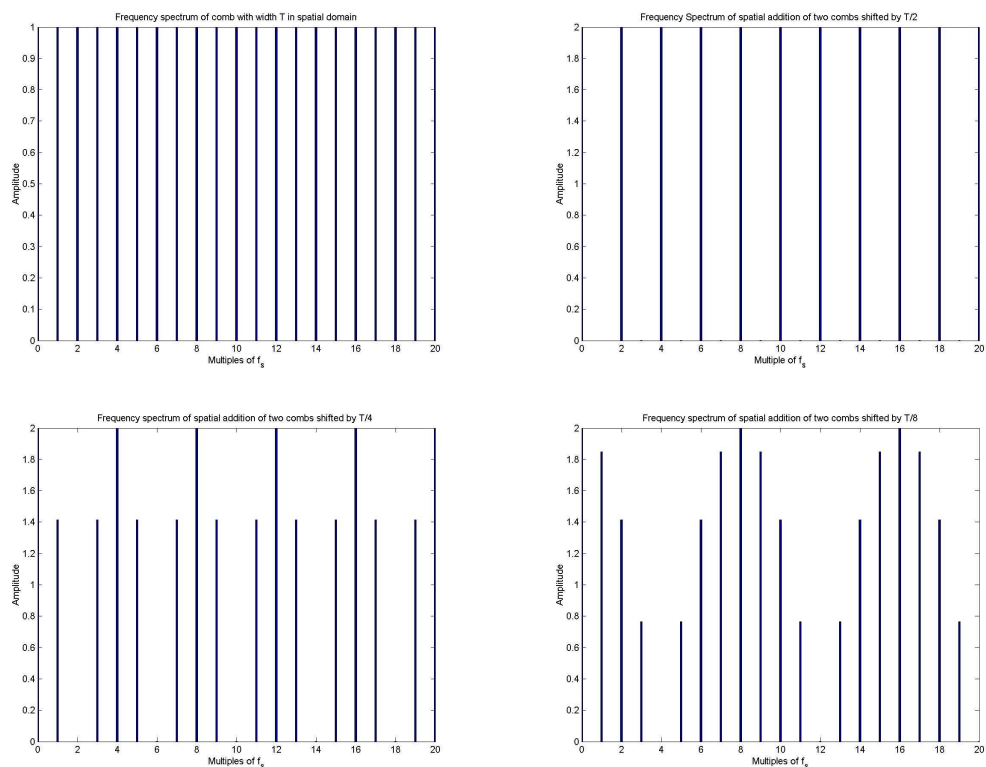


Figure 2.16: Frequency response for overlapped shifted combs. Top left: Response of a comb of width T . Others: Response of a comb of width T added in space with a similar comb but shifted by $T/2$ (top left), $T/4$ (bottom left) and $T/8$ (bottom right).

Now let us consider the more general case where the offset is not exactly half the pixel width. In this context, let us first investigate, why adding up two comb functions (used to sample the analog image) shifted by an amount which is half the width between the combs, results in a comb of higher frequency in the frequency domain (i.e. higher sampling frequency)? Let the width between the combs

be T . Therefore, the width of corresponding frequency domain comb is $1/T$. What happens in the spatial domain when we add two signals is interference. If the original signal has a frequency spectrum of $A(f)$, the signal obtained by adding the same signal shifted by s to it gives a frequency spectrum $B(f)$

$$B(f) = 2A(f)\cos 2\pi f s$$

where $f = \frac{1}{T}$.

Now note that for a comb (Figure 2.16), the spectrum is defined for only $f = \frac{n}{T}$ where n is an integer. Now, when $s = \frac{T}{2}$ (the shift is half the pixel width) $B(f)$ becomes zero at odd n . Thus the sampling frequency doubles. But for a more general T , instead of all the odd frequencies disappearing completely, some frequencies get modulated while others disappear. This is illustrated in Figure 2.16. For example, for $s = T/4$, $4n + 2$ frequencies disappear, while all the odd frequencies are multiplied by $\sqrt{2}$. In that case, having the same $f_p = \frac{f_s}{2}$ can result in two effects.

1. If the frequency component for $n = 1$ is absent (only happens when shift is $\frac{T}{2}$), then we would get the same resolution as the overlaps, but amplified. This is the special case of when the two projectors overlap at an offset of half the pixel. However, in this case, as mentioned before, if we make f_p higher, we can get higher resolution. Note that this means that we will see pixelization in the non-overlap region.
2. If the frequency component for $n = 1$ is modulated due to spatial interference, we would see aliasing, though we will not lose resolution. So, in order to avoid aliasing, we should not use supersampling.

In summary, we can use super resolution only if the pixels are offset by exactly half the pixel width and the reconstruction kernel is narrowed by half. For all other cases, super resolution is not achievable. In fact, it can degrade image quality by introducing aliasing artifacts.

Color Resolution

For each channel of the projector, the intensity resolution is defined as intensity per unit level. So for a single projector display with n discrete levels (n is usually 256 for 8 bit projector depths), the intensity resolution can be defined as brightness per unit level,

$$P_{res} = \frac{P_{brightness}}{n}$$

Here is the proof of the higher intensity resolution achieved from a CGO display. Assume that we have two projectors P_1 and P_2 , with same number of levels for each channel, n , making up the CGO. For simplicity, let us assume that projectors have linear response of luminance. Further, let the projectors have the black and white levels as $I_1(0) = L_1, I_2(0) = L_2$ and $I_1(n - 1) = H_1, I_2(n - 1) = H_2$ respectively. For any other input k , ($0 \leq k \leq n - 1$), because of the linear response, $I(k) = L + sk$, where s is the slope of the linear response. Thus for a two projector overlap,

$$I_c(i, j) = I_1(i) + I_2(j).$$

Rearranging the terms, we get

$$I_c(i, j) = L_1 + L_2 + s_1(i + jr)$$

, where $r = \frac{s_2}{s_1}$. Clearly the number of unique, discrete levels, I_c can take is the number of unique values $k = i + jr$, $0 \leq i, j \leq n - 1$ can take. It can be proved that $(2n - 1) \leq n_{CGO} \leq n^2$. Similar calculations can be done for the three different channels of color projectors and for more than two projectors. Thus the number of levels for a CGO with m projectors can be minimum of $O(nm)$ and maximum of $O(n^m)$. But note that, the brightness also multiplies. So, the minimum resolution can be identical to the non-overlapping case when the number of levels is $O(nm)$ and can go up if the slope of the channel responses are different. This says that if we use projectors with different channel gamma functions, we can have some higher channel intensity resolution and therefore higher color resolution, but we do not lose any color resolution by having projectors with same gamma functions.

CHAPTER 3

Perception

The end users of these large high resolution displays are humans. In order to succeed in making the humans use these displays effectively need to know about the capabilities and limitations of human vision. This will help us in two ways.

1. It will help us define the minimal requirements of such displays in terms of properties like resolution, brightness and so on. Thus, we can build cost effective display. Note that we are dealing with expensive resources and building displays with super optimal capabilities would only increase the total cost of the system thus making them cost prohibitive.
2. Sometimes knowing the limitations of human visual system can help us solve for certain problems easily. For example, we mentioned in Chapter 1 that a perceptual uniformity instead of color uniformity can achieve displays with higher dynamic range.

In this chapter, we discuss briefly the human visual system and a few relevant visual capabilities and phenomena. These are selective relevant material compiled from various references like [Goldstein01, Valois90, Chorley81]. Then we study the impact of these visual limitations and capabilities in several processes and choices made while building tiled displays.

3.1 Perception

Before describing the human visual system, we will briefly visit the basic laws of perception. The *difference threshold* is the smallest amount of difference between two stimuli that a human can detect. Weber law says that the ratio of the difference threshold and the intensity stimuli is constant. This threshold is dependent on many factors like distance from the stimuli, ambient light etc, and usually varies between 1 – 10%.

Starting from this point, Fechner showed that the magnitude of the perceived sensation is often not linearly related with the magnitude of the stimulus. Later, Steven proved that these two are related by a power function. This is *Steven's Power Law* and is given by

$$PerceivedSensation = K(Stimulus)^\gamma$$

This is true for human perception of luminance. If $\gamma < 1.0$, then the change in response is more rapid than the change in stimulus. Such responses are *expansive*. For example, human response to an electric shock stimuli is expansive. On the other hand, if $\gamma > 1.0$, then the change in response is less rapid than the change in stimuli. These responses are *compressive*. For example, the response of the human eye to intensity of light is compressive.

3.2 Human Visual System

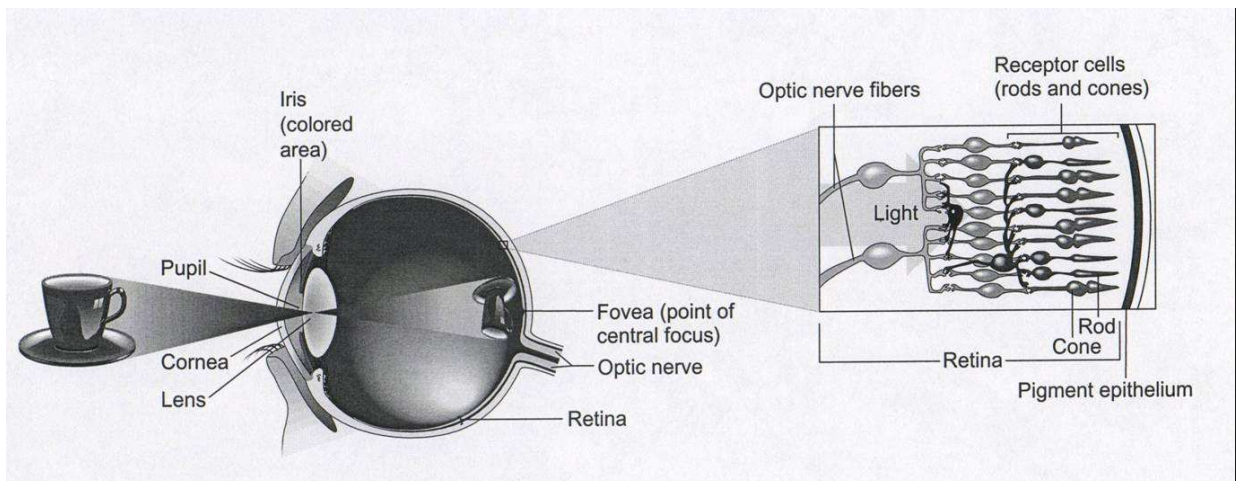


Figure 3.1: *The Human Eye.*

The human visual system comprises the sensor eye and the regions of the brain, namely lateral geniculate nucleus, striate cortex and extra cortex regions. Figure 3.1 shows the eye. The light enters the eye through the cornea and the lens. These two act as the focusing elements of the eye. The light is focussed on the retina, which lines the back in eye and is enriched with sensors and retina. The sensors are activated when light falls on the retina. These trigger electrical signals which then flow through the neurons to the different regions of the brain where it is decoded and interpreted.

The iris muscles that attach the lens to the cornea are responsible for what is called the *accommodation*. When the eye is focused at different depths these muscles lengthen or shorten the

lens, letting the eye to focus at different distances. Thus, these muscles help the eye to act as a lens with variable focal length. However, the eye fails to focus beyond and before a certain distance which are called the *depth of focus* and the *near point* of the eye respectively.

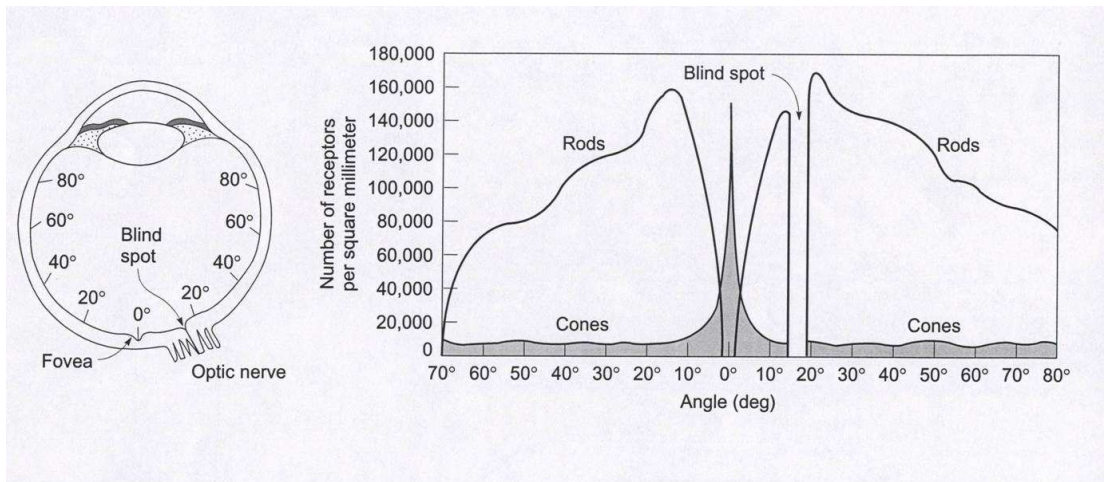


Figure 3.2: The distribution of the sensors on the retina. The eye on the left indicates the locations of the retina in degrees relative to the fovea. This is repeated as the x axis of the chart on the right.

The retina contains two types of sensors distributed in it, *rods* and the *cones*. These sensors are connected to cells in the retina called the ganglions. The ganglion cell fibers join together to form the optic nerve. The place where the optic nerve leaves the retina is devoid of any sensors and is called the *blind spot*. There is one area on the retina that contains only the cones. This is called the *fovea*. Figure 3.2 shows the distribution of the sensors on the retina. There are about 120 million rods but they are distributed mostly in the periphery of the eye. The cones are about 5 million in number and are mostly concentrated near the fovea. The cones response to different wavelengths of light while rods response to brightness of light. Thus, cones are responsible for color vision and rods are sensitive to brightness.

3.3 Visual Limitations and Capabilities

In this section we will see how the nature of the sensors and their distribution explain different visual limitations and capabilities that we explain in everyday life.

3.3.1 Luminance and chrominance sensitivity

Just by the sheer number of the rods, it is evident that the eye is much more sensitive to luminance than to chrominance. In fact, several studies show that the eye is at least an order of magnitude more

sensitive to luminance than to chrominance. This observation has been used to advantage in the design of analog color television standards and digital image compression algorithms like JPEG and MPEG.

3.3.2 Lower Color Acuity in Peripheral Vision

Since cones are sparsely distributed on the peripheral and dense only at the fovea, our peripheral vision is mostly black and white with very low color sensitivity.

3.3.3 Lower Color Acuity in Dark

There are a limited number of ganglion cells in the eye. These cells trigger only if the strength of the stimulus is greater than a threshold. Since rods are almost 25 times more in number than the cones, the number of rods attached to a ganglion cell is much higher than the number of cones. The number of sensors attached with a single ganglion cell is called its convergence. Just by the virtue of large numbers, the convergence of the rods are much higher than the cones. At night, each of the sensors receive very low light i.e. very low stimulus. But since the convergence of the rods is high, the sum of the stimulus converging on a ganglion from the rods can make it go beyond the threshold and trigger the ganglion. However, due to the low convergence of the cones, they do not succeed to trigger the ganglions at such low intensity of the stimulus.

3.3.4 Lower Resolution in Dark

The sensitivity of the eye reduces in the dark also due to the same reason. We detect a spatial resolution when two different ganglion cells are excited. Due to the higher convergence of the rods, even when different rod sensors are excited, it may mean that only one ganglion cell is triggered. However, due to low convergence of the cones, triggering a few cones is sufficient to trigger many ganglions. Since at dark, the stimulus on the cones cannot meet the threshold required to trigger the ganglion cells, we do not see high resolution in dark.

3.3.5 Lateral Inhibition

When a stimulus is imaged on the eye, it affects a region of the retina called the *receptive fields*. All the ganglions in the receptive field of the retina are affected by the stimulus. However, it has been found that all the ganglions are not affected similarly. The ganglions near the center are excited while

the ones in the periphery are inhibited. This phenomenon of excitatory center and inhibitory surround is called lateral inhibition and creates many visual artifacts.

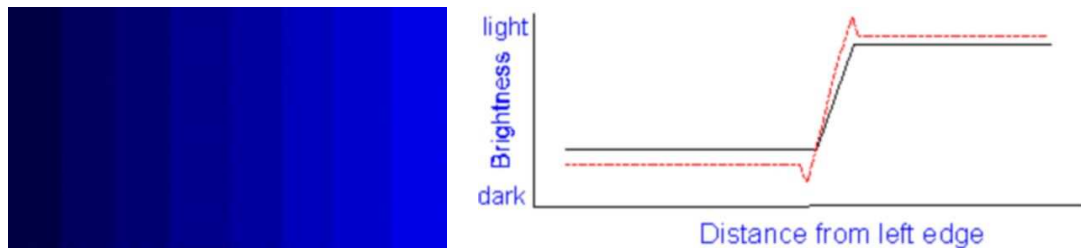


Figure 3.3: *Left: Mach Band Effect. Right: Schematic Explanation.*

The most common effect is called *mach bands*. The left picture of Figure 3.3 illustrates the effect. The image contains eight steps of the blue. Notice how the color in each of the eight steps of blue appears to change at the transition, being darker on the left and brighter on the right. But, the color is in reality the same for each step. The right picture illustrates the effect schematically. Whenever we are presented with a steep gradient as shown by the black line, we actually see the red line. This can be explained by the lateral inhibition phenomenon. Let us assume that the edge has brighter color on the right and darker color on the left. For the region just to the left of the edge, a large inhibitory response from the right brighter region makes it darker. On the other hand, the region just to the right of the edge receives lesser inhibition due to the dark surround giving the brighter region.

3.3.6 *Spatial Frequency Sensitivity*

The density of the sensors on the retina and their convergence on the ganglion cells also limit the human capability to detect spatial frequency. In fact, our eyes act as band pass filters passing frequencies between 2 – 60 cycles per degree of angle subtended to the eye. But, we can barely detect frequencies above 30 cycles per degree. So, for all practical purposes, the cut off frequency is often considered as 30 cycles per degree.

And as expected, this band becomes narrower and narrower as the brightness decreases. And in dark we are limited to very low resolution vision as mentioned earlier. In fact, it is interesting to note that through the evolution process different animals have developed eyes which acts as different band pass filters depending on their requirements. For example, a falcon needs to detect its prey from high up in the sky. So a falcon's eye can detect spatial frequencies between 5 – 80 cycles per degree.

3.3.7 Contrast Sensitivity Function

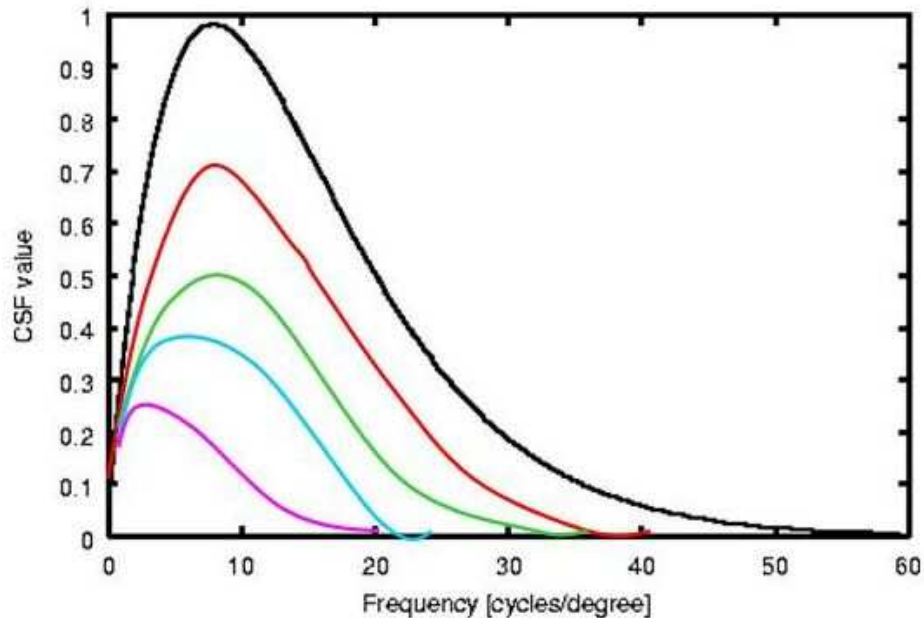


Figure 3.4: *The Contrast Sensitive Function for Human Eye.*

In fact, we need signals to have a minimum contrast to decipher their spatial frequency. This is called the *contrast threshold*. This threshold changes depending on the spatial frequency. The contrast sensitivity function is shown in Figure 3.4. Usually, the contrast sensitivity of humans increase with frequency till it reaches a peak and then starts to fall down being almost zero after 60 cycles per degree. This implies that the human visual system is not sensitive to smooth luminance changes. The sensitivity increases with more rapid changes and for very rapid changes the sensitivity again decreases.

However, the contrast sensitivity decreases with lower brightness. This means that we need more contrast to detect different spatial frequency at lower brightness. Also, as expected, the maximum spatial frequency we can detect reduces. And the frequency at which it reaches a peak keeps reducing with decreasing brightness. Note that at very low brightness the curve almost decreases monotonically.

Also, it has been showed that our contrast sensitivity is also dependent on the orientation of the signal. We are maximum sensitive to horizontal or vertical signals and the contrast sensitivity is lesser for other oblique angles.

3.4 Relationship to Tiled Displays

Now that we have introduced the different capabilities and limitations, here are a few instances of how we can use this knowledge while building tiled displays.

3.4.1 Resolution

Tiled displays are built with the goal of providing the users with a extremely high resolution display. Now the question is, how much resolution do we really need? Our knowledge of visual system (as presented in the preceding section) will answer this question easily.

Humans can see a maximum of 30 cycles/degree. Thus for a person at distance d ft from the screen, the distance of the screen that subtends an angle of one degree on eye is given by the product of the distance (in inches) and the angle (in radians), which is $12d\pi/180$ inches. To match the maximum human sensitivity, as per the Nyquist sampling condition, we should have 60 pixels in this dimension. Hence the required resolution r in pixels/inch should satisfy

$$r > \frac{60}{\frac{12d\pi}{180}} > \frac{286}{d}$$

The plot of d vs r is shown in Figure 3.5. Also, note that this is the minimum requirement for spatial frequency in horizontal and vertical directions. Our spatial frequency sensitivities are lower for oblique directions and hence we will require less resolution that given by Figure 3.5. So, Though theoretically, we may need infinite resolution (for $d = 0$), for all practical purposes, a maximum resolution of 500 – 600 pixels/inch should be sufficient.

3.4.2 Black Offset

Note that we found that we need higher contrast at lower brightness to detect different spatial frequency. Also note that with black offset, the contrast of the signal reduces more as the brightness of the signal decreases. So, perceptually black offset reduces contrast for the signals for which we would need more contrast.

3.4.3 Spatial Luminance Variation

From contrast sensitive function, we know that we are not very sensitive to gradual luminance variation. From this fact and the Weber law, a quantitative measure of the amount of spatial luminance variation we can tolerate has been determined [Lloyd02]. We can tolerate a luminance variation of

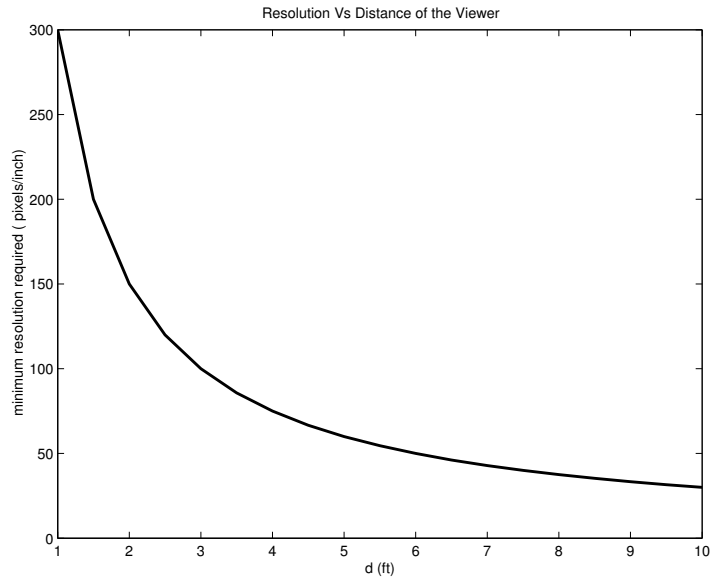


Figure 3.5: Left: This shows the plot of the distance of the viewer from the screen d vs the minimum resolution r required by a display

$\tau = 10 - 15\%$ per degree of the eye. Therefore, given a resolution of r pixels/inch and the viewer distance of d ft, we can tolerate a luminance variation of $\frac{\tau}{d \times \frac{\pi}{180} \times r}$ per pixel.

3.4.4 Visual Acuity

Due to the much higher concentration of the rods in the fovea than in the periphery, we have much higher visual acuity near the fovea than in the periphery. Thus, reducing the resolution in the peripheral visual field of a tracked user may simplify the image generation without any degradation in the perceived image quality, especially when the user is at a distance and the display covers a large field of view. In fact, this increased resolution in the fovea has the perception of increasing the overall contrast of the display and is called the *punch effect*. This effect is utilized in many CRT projectors. The resolution at the pixels of CRT projectors often degrade due to several optical effects. However, this being in the peripheral vision, goes unnoticed. But the punch effect thus created is used to the CRTs advantage.

3.4.5 Flicker

It has been shown that the flicker we can tolerate depends upon the brightness of the image. We are more sensitive to flicker at higher brightness, especially in a dark room settings. Hence, we need a higher refresh rates at higher brightness. In fact, this guides the refresh rate we need to have as our

displays become brighter and brighter. However, this is more relevant for emissive projection devices, such as CRTs.

These are a few ways we can use the limitations and capabilities of human visual system to build displays and optimize their performances.

CHAPTER 4

Color Variation in Multi-Projector Displays

The color of multi-projector displays shows significant spatial variation which can be very distracting, thus breaking the illusion of having a single display. The variation can be caused by device dependent reasons like *intra-projector color variation* (color variation within a single projector) and *inter-projector color variation* (color variation across different projectors) or by other device independent reasons like non-Lambertian and curved display surface, inter-reflection and so on [Majumder00, Stone1a, Stone1b]. Further, deliberate alignment of projectors in an overlapping fashion introduces significant luminance variation.

We define a simple parametric space to study the color variation of multi-projector displays. The parameters are space, time and input. Given a fixed input and time, the nature of the change of color over space characterizes spatial color variation characteristics. Similarly, given the same pixel location and input, the change in color with time defines temporal color variation characteristics. Finally, for the same pixel location and time, the color response with changing input defines input response characteristics. We analyze the intra and inter projector color variations for multi-projector displays and show that multi-projector displays are different from traditional displays in many ways and hence assumptions that can be safely made about other display devices cannot be made for these displays.

Next, we *identify* the different device dependent parameters of a projector that can cause color variation in a multi-projector display like position, orientation, zoom, lamp age and projector controls such as brightness, contrast and white balance. We *analyze the effects of the changes* in these parameters on the color variation and provide insights to the possible reasons for these variations. There has been some work on characterizing specifically the 3D color spaces of both LCD and DLP projectors [Stone1a, Stone1b]. Our study in this chapter complements this work.

From these analysis we make the *key observation* that the most significant cause of the spatial variation in color of a multi-projector display is the variation in luminance. Most tiled displays are made of multiple projectors of the same make and model that vary negligibly in chrominance.

However, before we delve deep into the study of the property of the color variation, we present

1. The details of the measurement process, instruments and other extraneous factors that may have an effect on our analysis.
2. Our notation for describing color and some properties of ideal displays based on this notation.

4.1 Measurement

As test projectors for our experiments, we used multiple Sharp, NEC, Nview, Proxima and Epson projectors (both LCD and DLP) and both front and back projection systems. We used at least 3 – 4 projectors of each model. The graphs and charts we present are only samples of the results achieved from different kinds of projectors. Since, similar results were achieved from different kinds of projectors consistently, these results are representative of general projector characteristics.

4.1.1 *Measuring Devices*

The goal of the process of measurement is to find the luminance and the chrominance properties at different points of the tiled display accurately. There are two options for the optical sensors that one might use for this purpose.

Spectroradiometer is an expensive precision-instrument that can measure any color projected by the projector accurately enabling us to work in a laboratory-calibrated device-independent 3D color space. But, it can measure only one point at a time at a very slow rate of about 1 – 20 seconds per measurement. Further, it would be difficult to measure the response of every pixel separately at a reasonable geometric accuracy. Thus, it is unsuitable for acquiring high resolution data.

A *color camera*, on the other hand, is relatively inexpensive and is suitable for acquiring high resolution data in a very short time. There are many existing algorithms to find the geometric correspondence between the camera coordinates and the projector coordinates assuring geometric accuracy of the data acquired. But, the limitations lie in its relative photometric inaccuracy.

With these options in hand, we used both types of sensors, but for different purposes. For point measurements, we used a precision spectroradiometer (Photo Research PR 715). But, for finding the

spatial color/luminance variation across a projector, where we need to measure the color at potentially every pixel of a projector, we use a high resolution digital camera. To reduce the photometric inaccuracies of the camera by a reasonable amount we use the following methods.

Using Camera as Reliable Measuring Device: The non-linearity of the camera is recovered using the algorithm presented in [Debevec97]. From this we generate a color look-up-table that linearizes the camera response. Every picture from the camera is linearized using this color look-up-table.

It is important that the camera does not introduce additional spatial variation than is already present on the display wall. Hence, the camera must produce flat fields when it is measuring a flat color. It is mentioned in [Debevec97] that most cameras satisfy this property at lower aperture settings, especially below $F8$. Our camera (Fujifilm MX 2900) showed a standard deviation of 2 – 3% for flat field images. These flat field images were generated by taking pictures of nearly-diffused planar surfaces illuminated by a studio light with a diffusion filter mounted on it.

To assure that a camera image is not under or over exposed we run simple under or over saturation tests. The differing exposures are accounted for by appropriate scaling factors [Debevec97].

Finally, to assure geometric accuracy of the measurements, we use a geometric calibration method [Hereld02] to find accurate camera to projector correspondence.

We cannot measure all the colors projected by the projector, if the 3D color space of the camera does not contain the space of the projector, thus restricting us to work in a device dependent 3D color space. However, we do not use the camera for any chrominance measurements, but only luminance measurements. So, this does not pose a problem.

4.1.2 Screen Material and View Dependency

For experiments on front projection systems we use a close to Lambertian screen that do not amplify the color variations. But the Jenmar screen we use for our back projection system is not Lambertian. Thus, the measuring devices are sensitive to viewing angles. In case of the spectroradiometer, we orient it perpendicular to the point that is being measured. But for the camera, the view dependency cannot be eliminated. However, we use the camera for qualitative analysis of the nature of the luminance variation in a single projector. Since we are not trying to generate an accurate quantitative model of the variation, the view dependency is not critical.

4.1.3 Ambient Light

We try to reduce ambient light seen by the sensors as much as possible by taking the readings in a dark room turning off all lights. When taking the measurement of a projector, we turn off all adjacent projectors. Further, we use black material to cover up the white walls of the room to avoid inter-reflected light.

4.2 Our Notation

There are several representations of color as presented in Appendix A. Please refer to this section for an in-depth treatise on color and its measurement. Based on this, we use the following notation of color for this thesis. A color K at a point is measured by the tuple (L, C) . $L = lum(K)$ is the *luminance* or amount of light falling at the point measured in cd/m^2 (as defined in Section A.1), and $C = chr(K)$ is the *chrominance* defined by the chromaticity coordinates tuple $C = (x, y)$ (as defined in section A.2.6).

4.2.1 Color Operators

Addition: The optical superposition of two colors $K_1 = (L_1, C_1)$ and $K_2 = (L_2, C_2)$ is defined as $K = (L, C) = K_1 \oplus K_2$, where

$$L = \sum_{i=1}^2 L_i; C = \frac{\sum_{i=1}^2 L_i C_i}{L}.$$

Note that \oplus is both commutative and associative. This is consistent with the definition in the previous section, since the proportion of each color is given by L_i/L .

Luminance Scaling: The luminance scaling of a color $K_1 = (L_1, C_1)$ by a scalar k is defined as $K = (L, C) = k \otimes K_1$, where

$$L = kL_1; C = C_1.$$

Note that \otimes does not change the chrominance of a color and distributes over \oplus .

Observation: If $K_1 = (L_1, C_1)$, $K_2 = (L_2, C_2)$ and $C_1 = C_2$ then the chrominance C of $K = K_1 \oplus K_2$ is the same as C_1 .

4.2.2 Ideal Displays

All displays produce color by using three primaries. These three colors (e.g. R,G,B) and the input paths for these primaries are called channels, $l \in \{r, g, b\}$. The input for each primary has a range from 0.0 to 1.0. Let the colors projected by the display for the input of 1.0 at each channel (and 0.0 in other two channels) be (L_R, x_R, y_R) , (L_G, x_G, y_G) and (L_B, x_B, y_B) respectively. The triangle formed by the chromaticity coordinates of these primaries is called the *color gamut* of the display. Thus, color gamut is independent of the luminance L .

As mentioned before, since the gamut of the display (the triangle made by the coordinates (x_R, y_R) , (x_G, y_G) and (x_B, y_B) in the chromaticity diagram) is always a subset of the CIE chromaticity space defined by the imaginary primaries, a real display can never produce all possible colors. Also, notice that the position of the three primaries in the chromaticity diagram is away from the boundary of the visual spectrum, which says that they are not monochromatic light. Each phosphor produces a band of wavelength and as a result produces a color that is less saturated than the monochromatic color of the same hue. However, the real primaries must be chosen such that they are *independent*. Independent means that none of the primaries can be reproduced by a combination of two other primaries. Or in other words, the three primaries cannot lie on a straight line in the chromaticity diagram.

Ideally, it is desirable to have a display where given the properties of the primaries, one can predict, using simple formulae, the properties of any color produced by the combination of the primaries. This becomes easy if the display satisfies the following properties.

1. *Channel Independence*: This assumes that the light projected from one channel is independent of the other two. Thus, this indicates that light from other channels should not interfere with the light projected from a channel.
2. *Channel Constancy*: This assumes that only luminance changes with changing channel inputs. For input $0.0 \leq r \leq 1.0$, the chromaticity coordinates (x_r, y_r) of r are constant at (x_R, y_R) and only the luminance L_r changes.
3. *Spatial Homogeneity*: The response of all the pixels of the display is identical for any input.
4. *Temporal Stability*: The response for any input at any pixel of the display does not change with time.

The property of optical superposition states that light falling at the same physical location from different sources adds up. The properties of channel constancy, channel independence, optical superposition along with the assumption that with an input of $(0, 0, 0)$ the display outputs zero light indicates that the color projected at a pixel is a linear combination of the color projected by the maximum values of the red, green and blue channels alone when the values of the other two channels are set to zero. Hence, for any input $c = (r, g, b)$, $0.0 \leq r, g, b \leq 1.0$, the luminance and chrominance of c is given by \oplus as

$$L_c = L_r + L_g + L_b$$

$$(x_c, y_c) = \frac{L_r}{L_c}(x_R, y_R) + \frac{L_g}{L_c}(x_G, y_G) + \frac{L_b}{L_c}(x_B, y_B).$$

This is referred to as the *linear combination property*.

Given the linear combination, the spatial homogeneity, and the temporal stability property, we can predict the color at any pixel at any input from the response of the primaries at any one pixel of the display. Most traditional display devices like CRT monitors satisfy these properties to a reasonable accuracy or the deviation from this ideal behavior is simple enough to be modeled by simple linear mathematical functions [D.H.Brainard89]. However, we will see in this chapter, a projector is not such an ideal device.

In the next few sections we study the intra and inter-projector color properties from the measurements taken using a spectroradiometer or a camera.

4.3 Intra-Projector Variation

In this section, we study the intra-projector variations. In the process we show that the projectors do not follow the desirable properties mentioned above.

4.3.1 Input Variation

One important consequence of a display to satisfy *channel independence* and *channel constancy* property is that the response for black (input of $(0, 0, 0)$) should have zero light. However in projectors, because of leakage light, some light is projected even for black. This is called the *black offset*. Hence the chromaticity for any channel at zero is the chromaticity of this achromatic black. As the inputs increase, the chromaticity reaches a constant value as it should for a device following channel constancy. This is demonstrated in Figure 4.1. The contours shown in Figure 4.2 shows how the gamut

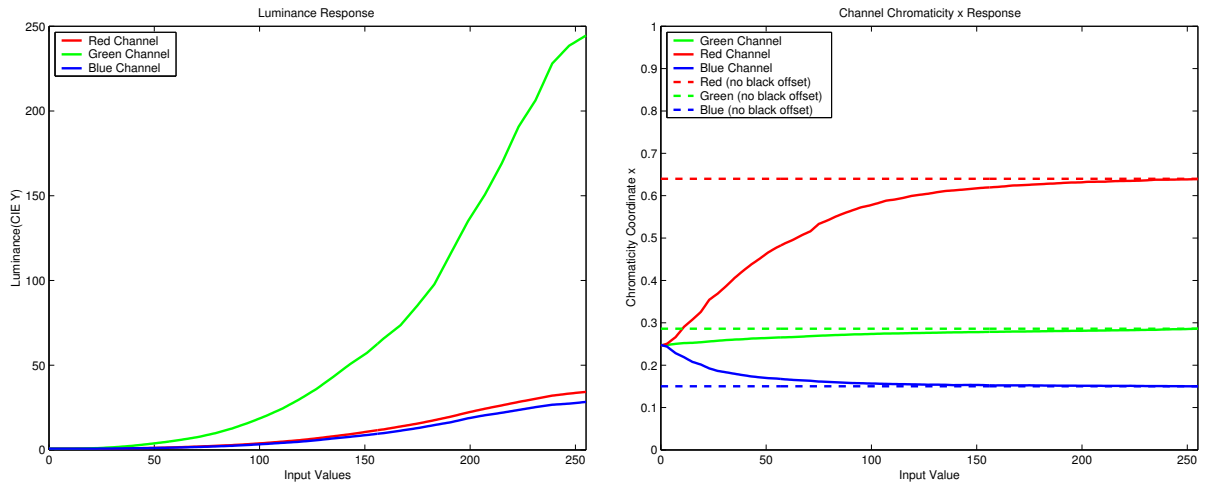


Figure 4.1: Left: Luminance Response of the three channels; Right: Chromaticity x for the three channels. The shape of the curves for chromaticity y are similar. The dotted lines show the chromaticity coordinates when the black offset was removed from all the readings.

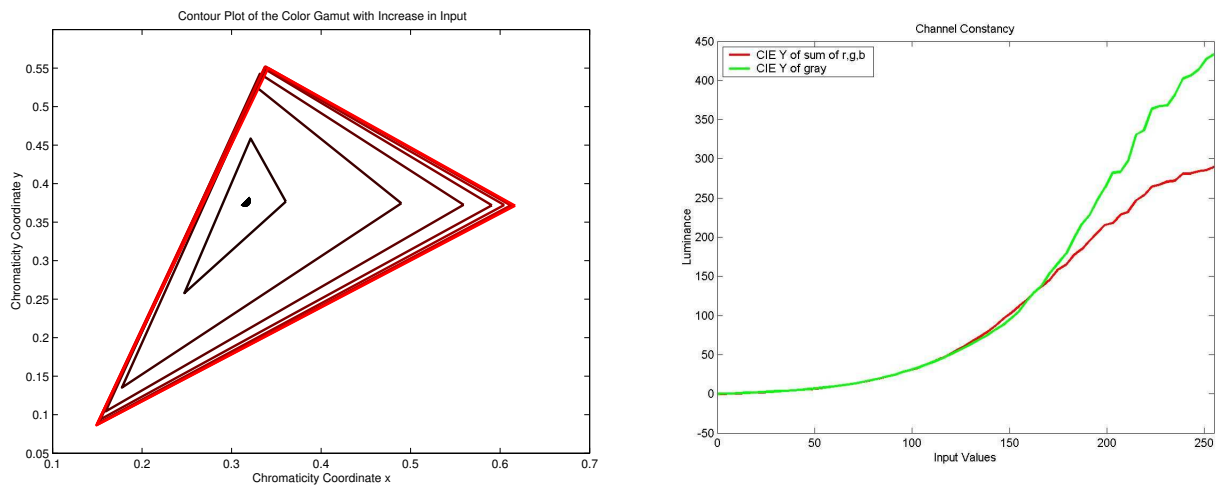


Figure 4.2: Left: Gamut Contour as the input changes from 0 to 255 at intervals of 32; Right: Channel Constancy of DLP projectors with white filter.

starts out as a single point for 0 in all the three channels and then attains the final red triangle at the highest input value. However, if this black offset is subtracted from the response of all inputs, the chromaticity coordinate curves for the three channels (shown with the dotted lines in right picture of Figure 4.1) will be constant [Stone1a, Stone1b].

From the various measurements we had from the spectroradiometer, we found that this black offset can be up to 2% of the maximum luminance projected per channel. However, this can deviate considerably across different projectors. We studied the black offset of fifteen same brand projectors with similar control settings. They showed a relative standard deviation of about 25%.

If the black offset is accounted for by the linear offset term, almost all projectors exhibit the linear combination property. However, some DLP projectors do not exhibit the linear combination property for the grays. We found that in DLP projectors with a four-segment color wheel that a clear filter element is used to enhance the contrast of grays beyond that achievable with a simple combination of red, green and blue filter channels. This difference is illustrated in Figure 4.2. The effect has been modeled in [Stone1a] by an additive gamut with an extrusion at the white point.

It has been shown before that the CRT monitors have a per channel non-linear luminance response which resembles a power function [Berns92b, Berns92a, D.H.Brainard89]. This assures a monotonic nature of the response. Unlike this, we found that projectors typically have S-shaped non-monotonic response as shown in Figure 4.1 and 4.6 (for two channels of a projector). The black offset is characteristic of projectors with light blocking technologies like liquid crystal device (LCD) or digital micro mirror (DMD). Projectors using cathode ray tube technology do not show the black offset problem to a perceptible extent. Following are some of the reasons for the black offset.

1. For projectors in 'driven to black' mode, the black offset can be easily controlled to be very low by increasing the applied voltage to the LCD. However, for projectors with 'driven to white' mode the amount of light leaking out for black cannot be controlled by increasing the voltage. Hence, these projectors can have high black offsets leading to poor contrast.
2. The Schlieren lens used in polymer dispersed liquid crystal (PDLC) devices often cannot separate the polarized and the unpolarized light well and can pass unpolarized light at black, thus reducing contrast.
3. In DMD devices, the light that is reflected by the mirrors in their off positions needs to be well absorbed. The elimination of this light is often not perfect. Further, interreflections may

happen off the mirrors. Further, light may also be reflected from the structures on which the micro-mirrors are mounted. All these may lead to large black offset and thus lower contrast.

4.3.2 Spatial Variation

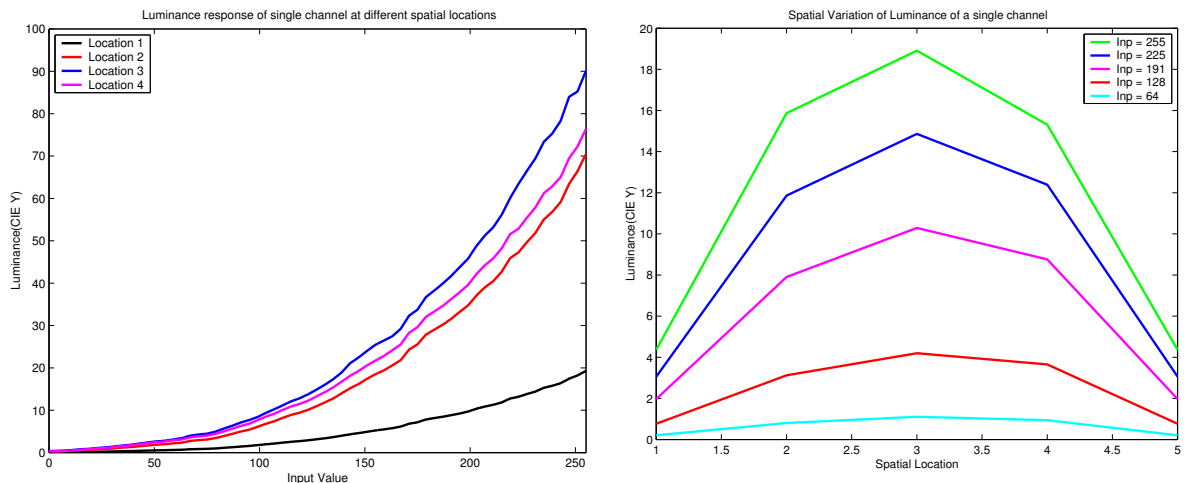


Figure 4.3: Left: Luminance Response of the red channel plotted against input at four different spatial locations; Right: Luminance Variation of different inputs of the red channel plotted against spatial location. The responses are similar for other channels.

Projectors are not spatially homogeneous either. Accurate luminance and chrominance readings were taken at five equally spaced locations on the projector diagonal using the spectroradiometer. We named these locations from 1 to 5 starting at the top left corner position. The luminance reaches a peak at the center (location 3) as seen in Figure 4.3. The luminance falls off at the fringes by a factor which may be as high as 80% of the peak luminance at the center for the rear projection systems, and about 50% for front projection system. This considerable fall-off in luminance indicates that having wide overlaps between projectors in a multi-projector display can help us to get a better overall dynamic range.

Further, the important thing to note here is that only the luminance changes spatially while the color gamut remains almost identical as shown in Figure 4.4. The gamut is measured from the chromaticity coordinates of the primaries at their highest intensities. We measured the input chromaticity response at different spatial locations and found that the gamut varies little spatially for the whole range of inputs. Figure 4.5 shows the spatial variation of the chromaticity coordinates of green to illustrate this. Note that the both the chromaticity coordinates x and y are spatially constant.

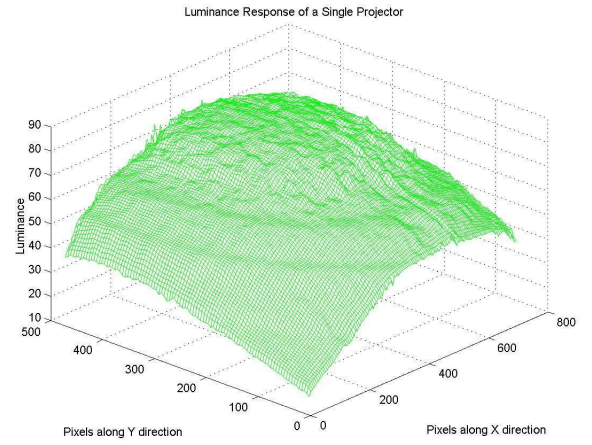
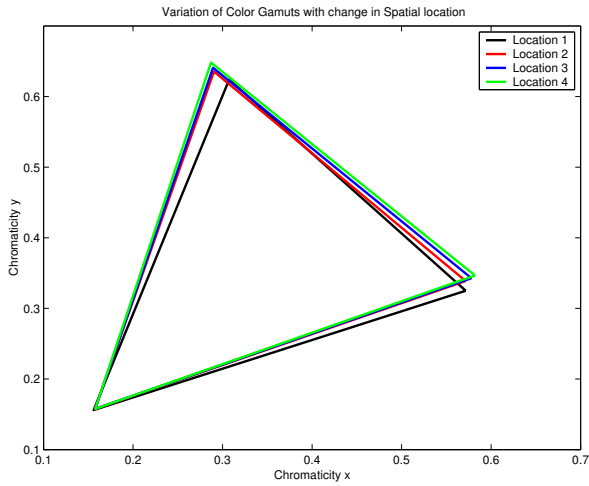


Figure 4.4: Left: Color gamut at four different spatial locations of the same projector; Right: Spatial variation in luminance of a single projector for input (1, 0, 0).

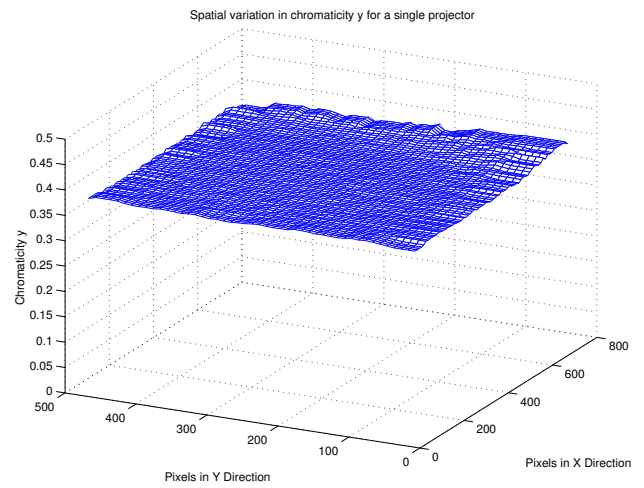
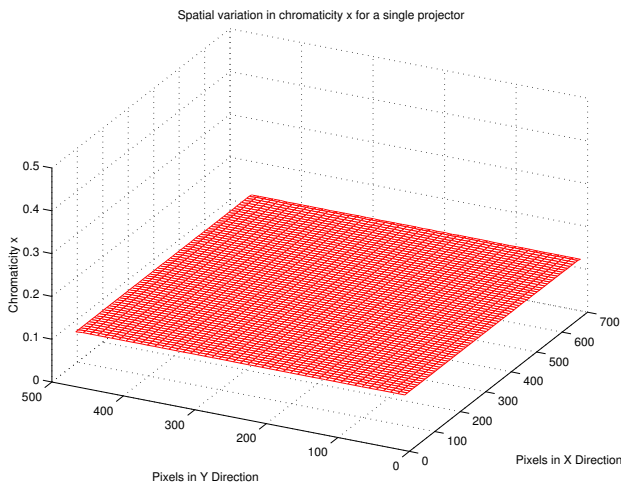


Figure 4.5: Spatial Variation in chromaticity coordinates x (left) and y (right) for maximum input of green in a single projector.

Given these observations from the spectroradiometer measurements, we used a camera to measure the intra-projector spatial luminance variation at a much higher resolution. The readings are taken by carefully aligning the camera perpendicular to the screen. The luminance response shows a peak somewhere near the center and then falls off radially towards the fringes in an asymmetric fashion. Finally, the pattern of this fall-off varies from projector to projector. Figure 4.4 shows the luminance variation across a single projector's field of view for input (1, 0, 0).

Another important observation is the normalized per channel non-linear luminance response remains constant spatially. This indicates that the shape of the luminance fall off is similar for all inputs of a channel. Hence, the shape of the non-linearity response does not change, but only the range changes.

1. *Physical reasons for luminance variation:* The spatial fall off in luminance in projectors can be due to following reasons which are not dependent on the projection technology [Stupp99].
 - (a) The spatial fall off also depends on the distance attenuation of light. This distance attenuation depends on the throw ratio of the projectors. The higher the throw ratio, the lower is the distance attenuation of light. Usually for rear projection systems, small throw ratio projectors are used to reduce the space required behind the screen. Hence, they often show higher luminance fall off at the fringes.
 - (b) The optical elements within the projector like the integrators and others result in a certain degree of vignetting or non-uniform field brightness.
 - (c) As illustrated in Section 4.4, non-orthogonal alignment of the projector with respect to the display surface produces both an optical distortion (keystoning) and a resultant gradient in flux density.
 - (d) The non-Lambertian nature of the display makes the luminance variation more acute. The asymmetry in the fall-off pattern gets pronounced with off-axis projection, as we will see in the following sections. This indicates that the orientation of the projector is partially responsible for this asymmetry.

The technology dependent spatial luminance fall off in CRT projectors may be due to the following reasons [Stupp99].

- (a) When the light is incident at larger angles of the face plate, total internal reflection can result in some light getting trapped in the glass and hence less light coming out of the system. This gives lower luminance at the fringes.
- (b) If the light collectors are flat, light is lost at the fringes. Usually, they are made convex at the expense of having more expensive optics to avoid this loss of light at the fringes

The technology dependent spatial luminance fall off in light valve projectors may be due to the following reasons.

- (a) The amount of light reflected by the glass substrate on which the filters are mounted is usually a function of angle of incidence. It is 4% at normal incidence and becoming 100% after the critical angle for total internal reflection. This changes the amount of light transmitted for both telecentric and non-telecentric systems thus leading to spatial luminance fall off at higher angles. This may cause the asymmetry in fall-off for non-telecentric systems. As a solution, often the gradient is built into the filter.
- (b) At very high temperature, the arc of some of the halide lamps can bow. This creates spatial luminance variation patterns.

2. *Physical reasons of chrominance variation:* The chrominance depends on the physical red, green and blue filters of the projectors which are (within manufacturing tolerances) independent of the spatial coordinates. Hence, the chrominance is also spatially almost constant. A few reasons for the small variations in chrominance and the color gamut are as follows [Stupp99].

- (a) The spectrum produced by the dichroic filters shift to the left with larger angles of incidence. Thus, if light strikes the filter in a non-telecentric manner, this can cause color gradient either in the horizontal or the vertical directions.
- (b) If the surface of the dichroic filter is not flat, the spectral characteristic of the filter differs spatially. This leads to color blotches.
- (c) Due to different spatial distribution of the doping halide atoms near the lamp arc, different emission spectra can occur at different lamp regions introducing color blotches.
- (d) Most lamps have emission lines. To get narrow band colors from these lamps, the filters need to be very accurate which is not practically feasible. Thus, the error in the accuracy leads to projectors of same brand and make having slightly different color gamuts.

In CRT projectors, the different orientation of the CRT guns lead to color shifts which needs to be corrected by lenticular or total internal reflection screens.

4.3.3 Temporal Variation

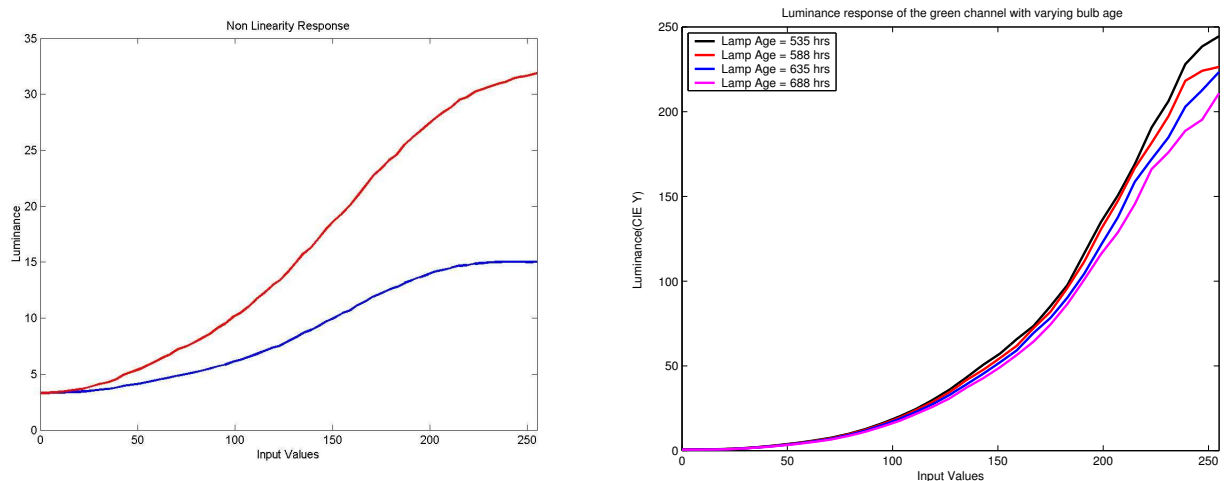


Figure 4.6: *Left: Per channel non-linear luminance response of red and blue channel; Right: Luminance Response of the green channel at four different bulb ages*

Finally, we find that the projectors are not temporally stable. The lamp in the projector ages with time and changes the color properties of the projector. Figure 4.6 shows a significant difference in luminance even within a short amount of time while the chrominance remains almost same. The luminance variation is due to the unpredictable temporal change in the position of the arc in the lamp. However, chrominance characteristics also drift a little after extensive use of about 800 – 900 hours. There is often a temporal chrominance shift in halide lamps. Since more than one type of atom is present for doping, sometimes this may interact at high temperature reducing the number of halide dopants present. These changes the emission spectrum of the lamp over time giving the slight drift in chrominance characteristics.

4.4 Projector Parameters that Change Color Properties

In this section, we identify the different projector parameters that can change the color properties of a projector, study the effects of varying these parameters on the color properties of a large area multi-projector display and provide insights for the possible reasons behind such effects.

4.4.1 Position

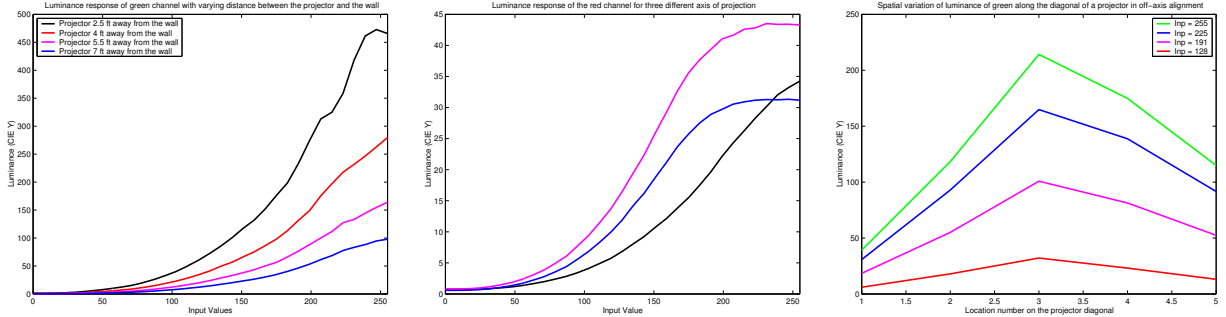


Figure 4.7: Left: Luminance Response of the green channel as the distance from the wall is varied along the axis of projection; Middle: Luminance Response of the red channel with varying axis of projection; Right: Luminance response of different inputs in the green channel plotted against the spatial location along the projector diagonal for oblique axis of projection.

Position is defined by the distance of the projector from the wall along the axis of projection and the alignment of the axis of projection with the planar display surface. We study the color properties with two sets of experiments. In one we keep the orientation constant while changing the distance from the wall and in the other we keep the distance constant while changing the orientation.

Distance form the Wall

Figure 4.7 shows the luminance response as we move the projector at different positions along its axis of projection. The chrominance remains constant. Further, the shape of the spatial variance of the luminance also remains the same as shown in Figure 4.3 and 4.4.

By moving the projector away from the wall, the projection area increases. Hence the amount of light falling per unit area changes, but the nature of the fall off does not change, as reflected in the observation. Thus, the total energy remains the same but the energy density changes with the distance from the center of the projector. Further, with the increase in distance, the projector’s throw ratio changes which can cause a change in luminance only.

Off-Axis or Orthogonal Projection

In this set of experiments, we kept the projector at the same distance from the wall while we rotated it about x , y , and z direction to have an off-axis projection at four orientations between orthogonal to angled axis of projection of 60 degrees. In this case also we found that the chrominance remains constant while the luminance response changes. Figure 4.7 shows the results. The nature of the spatial

variation is no longer symmetric as in the case of orthogonal position (Figure 4.3). Near the longer boundary of the key-stoned projection which is physically farther away from the projector, there is a higher drop in luminance.

As the orientation becomes more oblique, the luminance attenuation at the projector boundary further away from the screen increases, resulting in asymmetric fall-off. This is due to two reasons. First, the light from each pixel gets distributed over a larger area. Second, the angled surface receives less incident light due to the cosine effect. The results for vertical direction do not show a symmetry even for orthogonal projection due to offset projection.

In the above cases, since moving the projector around does not change the internal filters of the projector and their setup, the chrominance remains constant as expected.

4.4.2 Projector Controls

The projectors offer us various controls like zoom, brightness, contrast and white balance. Knowing how these controls affect the luminance and chrominance properties of the projector can help us decide the desirable settings for the projector controls that reduce variation within and across projectors. Thus, we can select the best possible dynamic range and color resolution offered by the device.

Zoom

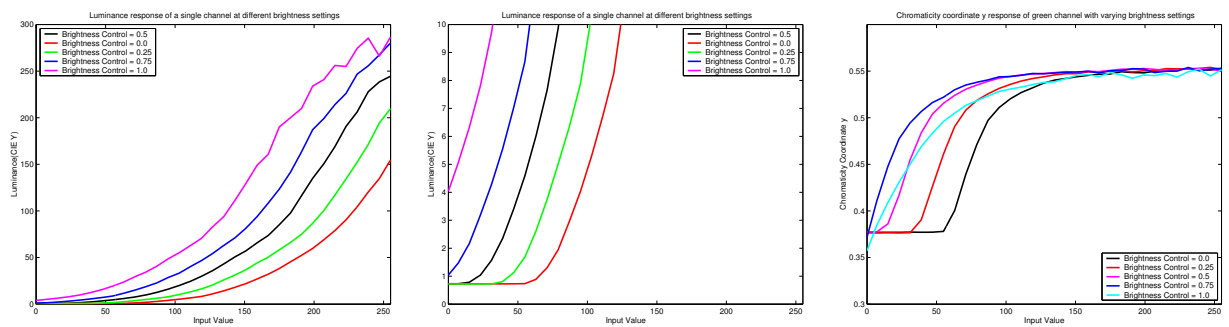


Figure 4.8: Left: Luminance Response of the green channel with varying brightness settings; Middle: Luminance Response of the green channel with varying brightness settings zoomed near the lower input range to show the change in the black offset; Right: Chrominance Response of the green channel with varying brightness settings.

We tested the projectors at four different zoom settings. Both luminance and chrominance remain constant with the change in zoom settings of the projector.

With the change in zoom, the amount of light for each pixel gets distributed over a different area. For a focused projector, it is distributed over a small area, while for an unfocused projector it is distributed over a larger area. However, the total area of projection remains the same and the total amount of photon energy falling in that area remains same. Hence the light per unit area remains unchanged, while the percentage of light that each unit area receives from the different pixels changes.

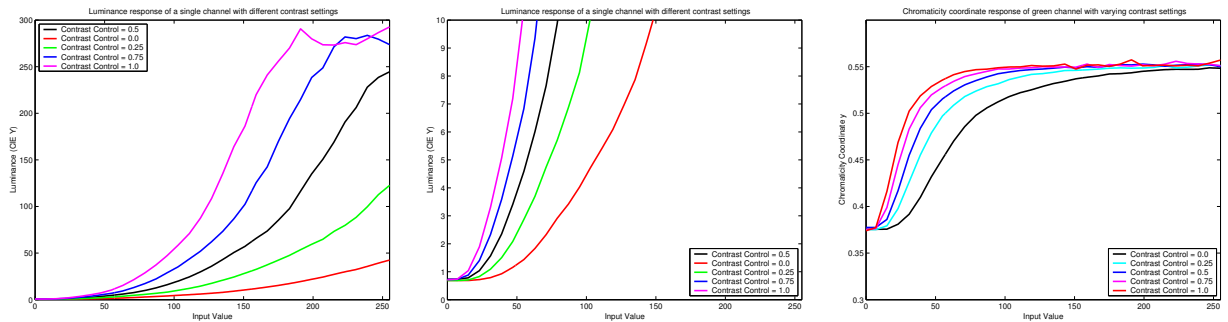


Figure 4.9: *Left: Luminance Response of the green channel with varying contrast settings; Middle: Luminance Response of the green channel with varying contrast settings zoomed near the lower luminance region to show that there is no change in the black offset; Right: Chrominance Response of the green channel with varying contrast settings.*

Brightness

Luminance and chrominance response is measured by putting the brightness control at 5 different positions. [Poynton96] mentions that usually the brightness control in displays change the black offset. However, in projectors, this control affects both the gain and black offset of the luminance response of *all the three channels similarly and simultaneously*. The results are illustrated in Figure 4.8. As the brightness is increased, both the black offset and the gain of the luminance increases. However, if the brightness is too low, the luminance response gets clipped at the lower input range. In these settings, since the luminance remains at the same level for many lower inputs, the chromaticity coordinates also remains constant. At very high brightness settings, we observed some non-monotonicity in the luminance response for the higher input range. As a consequence, the chromaticity coordinates also show some non-monotonicity at the higher brightness settings. Thus, it is ideal to have the brightness control set so that there is no clipping in the lower input range or non-monotonicity at higher input ranges. For example, in these illustrations, the ideal setting is between 0.5 and 0.75.

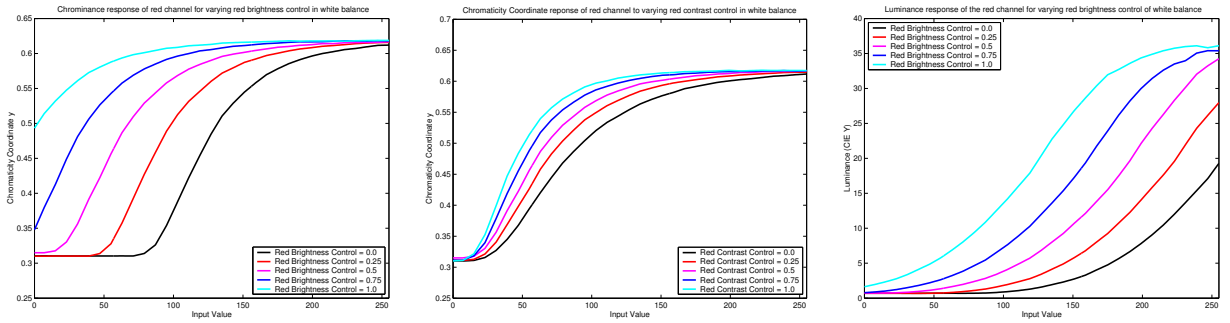


Figure 4.10: Left: Chrominance Response of the green channel with varying green brightness settings for white balance; Middle: Chrominance Response of the red channel with varying red contrast settings for white balancing; Right: Luminance Response of the red channel with varying red brightness settings in white balance.

Projector Brand and Model	Red		Green		Blue	
	x	y	x	y	x	y
Sharp XG-E3000U	0.62	0.32	0.33	0.62	0.14	0.07
NEC MT-1035	0.55	0.31	0.35	0.57	0.15	0.09
nView D700Z	0.54	0.34	0.28	0.58	0.16	0.07
Epson 715c	0.64	0.35	0.30	0.67	0.15	0.05
Proxima DX1	0.62	0.37	0.33	0.55	0.15	0.07
<i>Max Distance</i>	0.085		0.086		0.028	

Table 4.1: Chromaticity Coordinates of the primaries of different brands of projectors

Contrast

We perform similar experiments for the contrast control. This also affects *all the three channels similarly and simultaneously*. The results are illustrated in Figure 4.9. [Poynton96] mentions that usually the contrast control changes the gain of the luminance curve. We found the same effect with the projectors. As the gain increases, the luminance difference became significant enough at lower input ranges to push the chromaticity away from the gray chromaticity values towards the chromaticity coordinates of the respective primaries. However, the luminance response starts to show severe non-monotonicity at higher contrast settings, thus reducing the input range of monotonic behavior. So, contrast setting should be in the monotonic range to maximally use the available color resolution.

White Balance

The white balance usually has a brightness and contrast control for two of the three channels and the third channel acts as a reference and is fixed. We put these in five different settings for our readings. The luminance and the chrominance response changes exactly the same way as for the independent brightness and contrast controls, but the change affects *only one channel at a time* instead of affecting all of them similarly. Thus, it controls the proportion of the contribution from each channel to a color which in turn changes the white balance (Figure 4.10).

4.5 Inter-Projector Variation

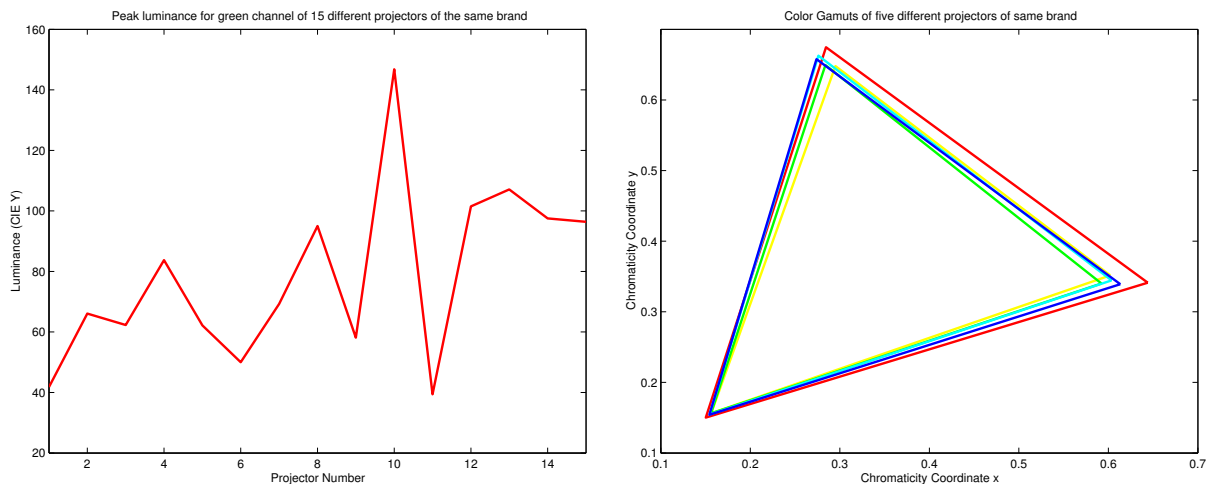


Figure 4.11: Left: Peak luminance of green channel for fifteen different projectors of the same model with same control settings; Right: Color gamut of 5 different projectors of the same model. Compare the large variation in luminance in Figure 4.11 with small variation in chrominance.

In this section we study how these properties of a projector vary across different projectors. Figure 4.11 shows the luminance and color gamut response for the maximum intensity of a single channel for different projectors of *same model* having exactly the same values for all the parameters defined in Section 4.4. There is nearly 66% variation in the luminance, while the variation in color gamut is relatively much smaller. This small variation is due to physical limitations in the accuracy of manufacturing identical optical elements like lens, bulbs and filters, even for same brand projectors.

Figure 4.12 also shows the high resolution chrominance response of a display wall made of four overlapping projectors of same model, projecting the same input at all pixels. Projectors of same brand usually use same brand bulb (which have similar white points) and similar filters justifying similarity

in the color gamut. However, this is not true for the grays of the DLP projectors that use the clear filter where the chrominance of grays differ significantly across different projectors due to large variation in this clear filter.

The color gamut across projectors of different brands differ more than same model projectors (Table 4.4.2). This is also illustrated in Figure 4.12. However, this is relatively much smaller when compared to the luminance variation.

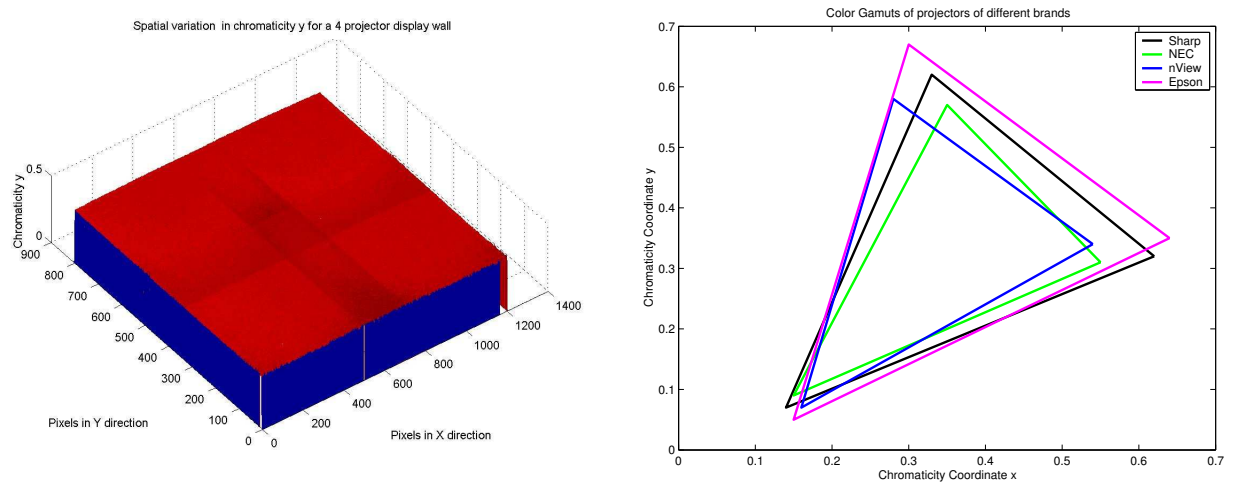


Figure 4.12: Left: Chrominance response of a display wall made of four overlapping projectors of same model; Right: Color gamut of projectors of different models.

4.6 Luminance Variation is the Primary Cause of Color Variation

The key observations from experiments and analysis of section 4.3, 4.4 and 4.5 can be summarized as

1. Within a single projector's field of view, luminance varies significantly while chrominance remains nearly constant.
2. Luminance variation is dominant across projectors of same model, but perceptually small chrominance variations also exist.
3. The variation in chrominance across projectors of different models is small when compared to the variation in luminance.
4. With the change in various projector parameters like brightness, contrast, zoom, distance and orientation, only luminance changes while chrominance remains constant.

CHAPTER 5

The Emineoptic Function

5.1 Definitions

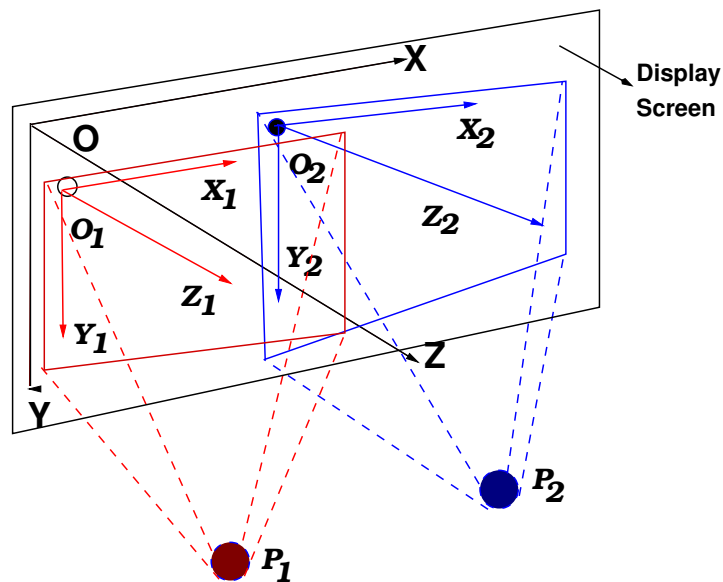


Figure 5.1: Projector and display coordinate space.

A *planar multi-projector display* is a display made of N projectors, projecting on a planar display screen. Each projector is denoted by P_j , $1 \leq j \leq N$. Figure 5.1 shows a simple two-projector display wall. The blue and red quadrilaterals show the areas of projection of P_1 and P_2 on the display screen.

A unified *display coordinate space* is defined by X , Y , and Z with origin O at the top left corner of the display plane. The *projector coordinate space* of a projector P_j is defined by X_j and Y_j on the display plane, Z_j , parallel to Z , with origin O_j at the top left corner of the projected area of P_j .

The coordinates of the display are denoted by (u, v) , and the coordinates of a projector P are denoted by (s, t) . These two coordinate pairs can be related by a *geometric warp*

$$(u, v) = G(s, t, p) \quad (5.1)$$

where $p = (p^x, p^y, p^z, \theta, \phi, \beta, f)$. Respectively, f , (p^x, p^y, p^z) and (θ, ϕ, β) are the focal length, position, and orientation of P in the display coordinate space. For all practical systems p does not change since projectors and screen do not move relative to each other. Hence, the dependency of G on p in Equation 5.1 is removed. Thus,

$$(u, v) = G(s, t) \quad (5.2)$$

A projector has three channels, $\{r, g, b\}$. In general, a channel is denoted by $l \in \{r, g, b\}$ and the corresponding input by $i_l \in \{i_r, i_g, i_b\}$, $0.0 \leq i_l \leq 1.0$.

Let the viewer be at $e = (e_x, e_y, e_z)$ in the display coordinate space. The BRDF of the screen is dependent on the display coordinates and the viewer location and is denoted by $\Lambda(u, v, e)$. We assume that the BRDF is independent of chrominance.

5.2 The Emineoptic Function

The *emineoptic function*, $E(u, v, i, e)$, for a multi-projector display is defined as the color reaching the viewer e from a display coordinate (u, v) when the input at that display coordinate is $i = (i_r, i_g, i_b)$.

5.2.1 Emineoptic Function for a Single Projector

Let us consider one projector coordinate (s, t) . Let $Q_l(s, t)$ be the maximum luminance that can be projected at that coordinate from channel l . For all inputs i_l , the luminance projected is a fraction of $Q_l(s, t)$ given by $h_l(s, t, i_l)$, $0.0 \leq h_l(s, t, i_l) \leq 1.0$. Let the chrominance at that coordinate for input i_l be $c_l(s, t, i_l)$. Thus, the color projected at this coordinate (s, t) for input i_l is given by

$$D_l(s, t, i_l) = (h_l(s, t, i_l)Q_l(s, t), c_l(s, t, i_l)) \quad (5.3)$$

$$= h_l(s, t, i_l) \otimes (Q_l(s, t), c_l(s, t, i_l)) \quad (5.4)$$

A projector satisfies the property of *channel constancy* by which $c_l(s, t, i_l)$ is independent of i_l . We call $c_l(s, t)$ the *channel chrominance* for the display coordinate (s, t) . Physically, c_l depends on the projector color filters and lamp characteristics. So,

$$D_l(s, t, i_l) = h_l(s, t, i_l) \otimes (Q_l(s, t), c_l(s, t)) \quad (5.5)$$

[Majumder02b] shows that h_l does not vary with (s, t) . So, it is denoted by $h_l(i_l)$, the *transfer function* for channel l . So,

$$D_l(s, t, i_l) = h_l(i_l) \otimes (Q_l(s, t), c_l(s, t)) \quad (5.6)$$

Note that h_l is similar to the gamma function in other displays. In projectors, this function cannot be expressed by a power (γ) function and hence we prefer to call it the *transfer function* for channel l . Further, h_l should satisfy the following two properties: $\min_{i_l} h_l(i_l) = 0$ and $\max_{i_l} h_l(i_l) = 1$.

Ideally, the channels of a projector are independent of each other and the color projected at (s, t) for input $i = (i_r, i_g, i_b)$, $T(s, t, i)$ is given by $D_r(s, t, i_r) \oplus D_g(s, t, i_g) \oplus D_b(s, t, i_b)$

However, in practice, some extra leakage light is projected at all times, in addition to the light projected from input i . This light is called the *black offset*. We represent this by $(B(s, t), c_B)$, where $B(s, t)$ is the spatially varying luminance component called the *black luminance function* and c_B is the chrominance. Thus, the light projected by a projector is

$$T(s, t, i) = D_r \oplus D_g \oplus D_b \oplus (B(s, t), c_B(s, t)). \quad (5.7)$$

Finally, for a viewer at e , the emineoptic function $E(u, v, i, e)$ for a single projector is

$$E(u, v, i, e) = \Lambda(u, v, e) \otimes T(s, t, i), \quad (5.8)$$

where $(u, v) = G(s, t)$.¹

5.2.2 Emineoptic Function for a Multi-Projector Display

Let N_P denote the set of projectors overlapping at (u, v) . The emineoptic function $E(u, v, i, e)$ for the tiled display is

$$E(u, v, i, e) = \oplus_{j \in N_P} E_j(u, v, i, e). \quad (5.9)$$

We assume a Lambertian screen for which Equation 5.9 becomes independent of e and is reduced to

$$E(u, v, i) = \oplus_{j \in N_P} T_j(s_j, t_j, i). \quad (5.10)$$

5.3 Relationship with Color Variation

Now, that we have described the emineoptic function, let us see how this models the different types of color variation (described in details in Chapter 4) in multi-projector displays.

¹When p is not assumed to be static, G , Q_l and B are also dependent on p .

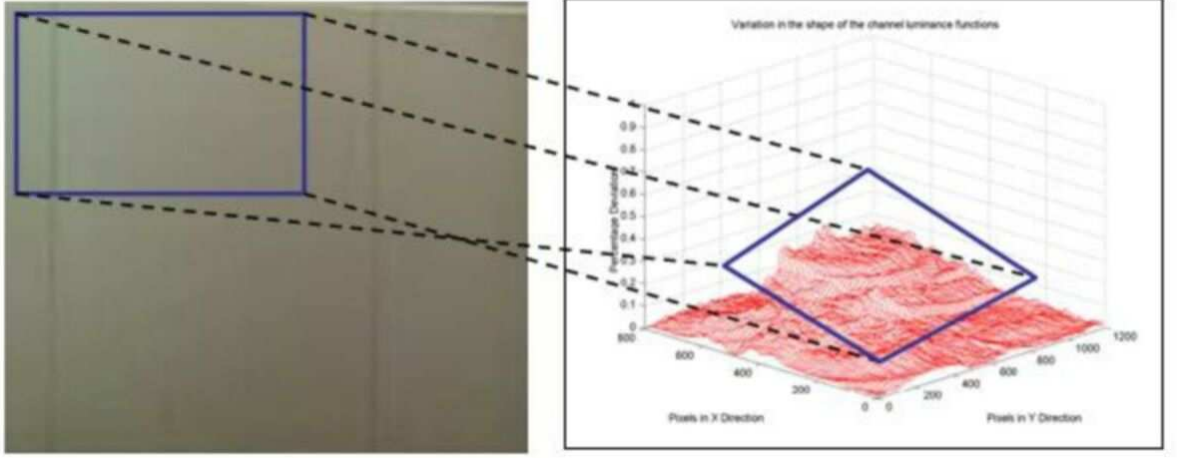


Figure 5.2: Left: Color blotches on a single projector. Right: Corresponding percentage deviation in the shape of the blue and green channel luminance functions.

Intra-Projector Variation

The intra projector luminance variation is due to the fact that the luminance function Q_l for each channel l for each projector is not flat as shown in Figure 4.4.

The chrominance variation, though less significant, is more complicated to model. The color blotches within a single projector are modeled as follows.

1. First, c_l varies spatially. Though it is *nearly* constant, as shown in Figure 4.5, it is *not exactly* constant. However, note that sometimes this variation is almost negligible and often cannot explain the color blotches that are still seen in the projectors.
2. The second reason became evident from the emineoptic function. Let the normalized luminance function for each channel be \bar{Q}_l and the maximum luminance for the channel be

$$M_l = \max_{\forall s,t} (Q_l(s, t)).$$

Note that the parameter M_l is not dependent on the spatial coordinates. Therefore,

$$Q_l(s, t) = M_l \bar{Q}_l(s, t)$$

Let us assume that c_l is constant over space and cannot cause the color botches. From the definition of color operators in Section 4.2.1, the chrominance for an input $i = (i_r, i_g, i_b)$, c_i , is given by

$$c_i = \sum_{l \in \{r,g,b\}} \frac{c_l M_l \bar{Q}_l h_l(i_l)}{\sum_{l \in \{r,g,b\}} M_l \bar{Q}_l h_l(i_l)} \quad (5.11)$$

Now, if \bar{Q}_l is the same for all the three channels, Equation 5.11 becomes

$$c_i = \sum_{l \in \{r,g,b\}} \frac{c_l M_l h_l(i_l)}{\sum_{l \in \{r,g,b\}} M_l h_l(i_l)}$$

where every term is independent of spatial coordinates. Hence, the chrominance does not vary spatially.

If \bar{Q}_l is different for each channel, i.e. the shape of the spatial variation in luminance for each channel is different, the three primaries combine in different proportions at different projector coordinates and we see color blotches. The hue of the color blotches depends on the amount of deviation in each channel. Thus, if the shape of the luminance function across the different channels can be made to be identical, some of the color blotches problem can be eliminated.

We verified this in some of the projectors where the channel chrominance was very close to constant. We found the variation in \bar{Q}_l across different channels to be a maximum of 20%. And the visible color blotches coincided with the sites of larger deviation. An example of this is illustrated in Figure 5.2.

Inter-Projector Variation

The inter-projector luminance variation is modeled by two parameters, the input transfer function h_l and the shapes of the luminance functions. These are projector dependent and hence different for different projectors.

The variation in color across different projectors is due to two factors again.

1. First, the relative luminance of the primaries with respect to each other can be found by the ratio M_l for each channel with the other. This ratio can vary from projector to projector. This means that the proportions of red, green and blue to generate a color would differ from one projector to another giving different chrominance, as illustrated in Figure 4. This proportion can be changed using the white balance control of the projectors.
2. Second, this variation can also be due to a difference in c_l across projectors. This means that the color gamut varies from projector to projector.

Overlap Regions

The color variation in the overlap region is modeled by the fact that the cardinality of N_P ($|N_P|$) is not the same at every display coordinate. The luminance and chrominance in the overlap region

can be found by using the addition color operator (presented in Section 4.2.1) on the luminance and chrominance from each of the $|N_P|$ projectors. The luminance from different projectors will add up to generate higher luminance in the overlap region. Also, if the channel chrominance of the contributing projectors are different, the overlap region will show a different chrominance than the non overlap region.

5.4 Model Verification

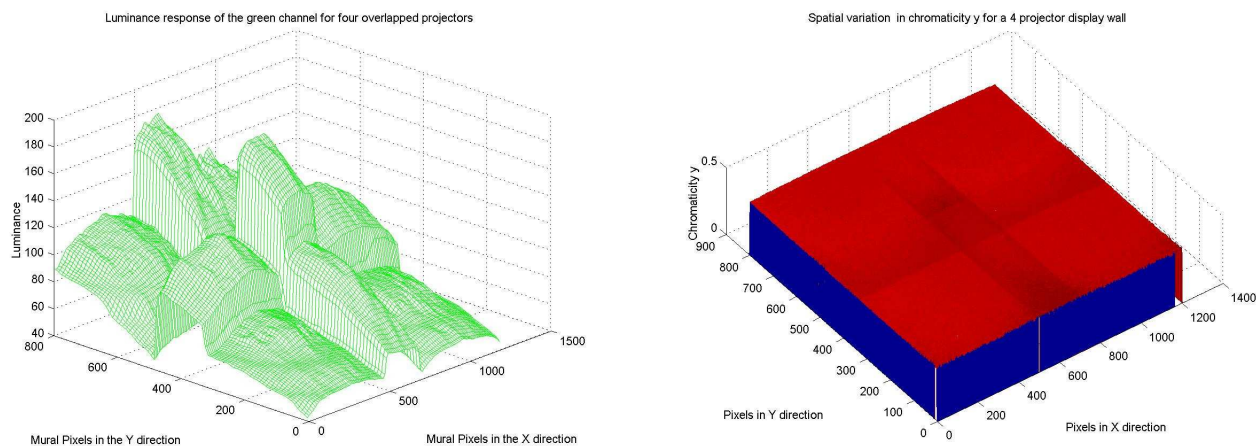


Figure 5.3: Reconstructed luminance (left) and chrominance y (right), measured from a camera image, for the emineoptic function at input $(1, 1, 0)$ of a four projector tiled display.

In this section, we present a brief verification of the emineoptic function. We use two methods to verify the model.

First, we project i at all display coordinates and *measure* the luminance using a camera. Next we *compute* the luminance for the same input i using Equation 5.10 from the estimated projector parameters h_l , Q_l , and B . We find this to be close to the measured response. Quantitatively, the measured response deviated from the computed response by 2 – 3%.

The chrominance cannot be verified in a similar way because the camera and the spectroradiometer have different 3D color spaces. So, instead of verifying the absolute value of the chrominance, we verify a property of the chrominance response. [Majumder02a, Majumder02b] show that c_l is close to identical for same model of projector. Our display is made of projectors of same brand and model. So, the chrominance response of the tiled display reconstructed from Equation 5.10 should not vary spatially. To verify this, we project input i at all display coordinates and *measure*

the chrominance using a camera. We found both the chromaticity coordinates to be flat as expected (Figure 5.3).

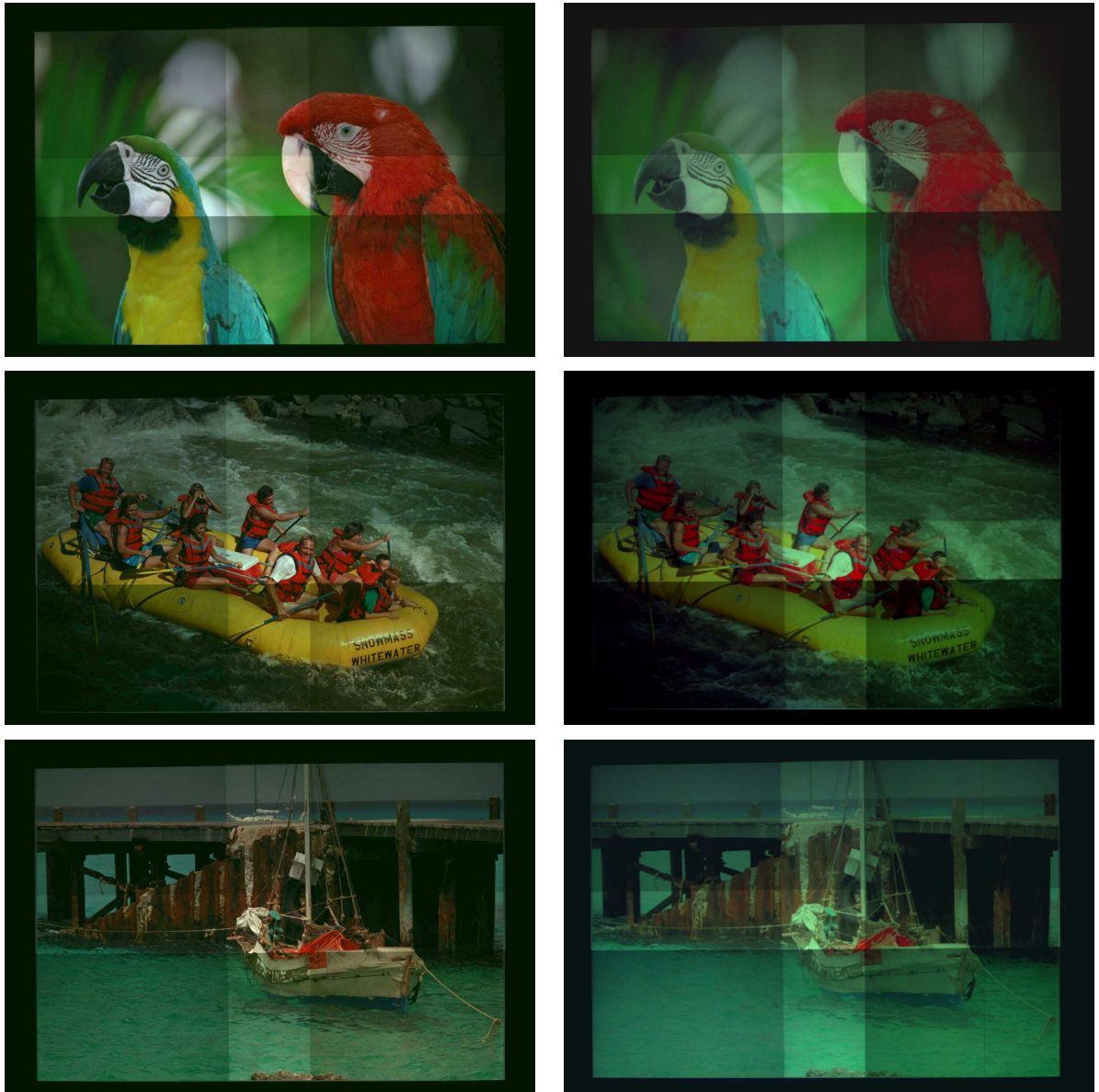


Figure 5.4: A 2×2 array of four projectors. Left Column: *Predicted Response*. Right Column: *Real Response*.

The second way to validate our model is to use the following experiment. First, we use a physical sensor (a camera) to capture the image of the physical display. The image is converted from the camera coordinate space to the display coordinate space using the geometric correspondence information generated by the geometric calibration method. The image thus generated is called the *actual response*.

Next, we reconstruct the model parameters for the tiled display. Then we use these parameters and the emineoptic function to *predict* the response of a hypothetical sensor when a test image is put up on this display. This is called the *predicted response*. This hypothetical sensor is also modeled using the emineoptic function.

Figure 5.4 shows the predicted and the real response for a set of test images. The hypothetical sensor being an ideal device, is assumed to have spatially invariant channel luminance, chrominance and the transfer functions and no black offset. However, it is often difficult, if not impossible, to simulate the parameters of the hypothetical sensor, especially the chrominance, to be exactly similar to the physical camera used. Thus, the actual and the predicted response may not be identical. The thing to note here is the similarity in response. For example, the bottom right projector has a more severe radial fall off than the others and is similar for both the actual and predicted response. Or, the bottom right projector has a lower brightness than the others that is predicted from the model correctly.

CHAPTER 6

A Framework for Achieving Color Seamlessness

In this chapter, we design a comprehensive framework for achieving color seamlessness and define color seamlessness formally. Finally, we show that this framework is unifying and can explain all the existing methods directed towards achieving color seamlessness.

6.1 The Framework

The framework to achieve any color correction for multi-projector displays consists of three steps.

1. **Reconstruction of the Emineoptic Function:** To correct for the color variation, we need to first capture the color variation across the multi projector display. This calls for the reconstruction of the emineoptic function for the particular display at hand. Thus, in this step, some sensors are used to reconstruct $E(u, v, i, e)$ of the display. The accuracy and speed of the reconstruction depends on the sensors being used.
2. **Modification of the Emineoptic Function:** Now, the reconstructed emineoptic function E has color seams. Hence, to achieve a display that has no seams, this E needs to be modified to E' , the *desired emineoptic function*. The modification is based on some goals that would control the quality of the seamlessness achieved. This step is thus called *modification*.
3. **Reprojection of the Desired Emineoptic Function:** Finally, we need to realize the desired emineoptic function, E' , on the display. This is called *reprojection*. This is achieved by manipulating one or more parameters of the emineoptic function, on the choice of which depends the interactivity and the performance of the correction.

6.2 Color Seamlessness

Several methods strive to correct for the color variation, but there is no formal definition of the goal that should be achieved in such corrections. In this section, we define a new and practical goal for color seamlessness.

Absolute Uniformity: An obvious goal of color seamlessness is to achieve absolute uniformity. The desired display E' is absolutely uniform if the color reaching the viewer e from *any* two display coordinates (u_1, v_1) and (u_2, v_2) , are equal.

$$\forall i, E'(u_1, v_1, i, e) = E'(u_2, v_2, i, e) \quad (6.1)$$

The goal of absolute uniformity *requires* the display quality to match the worst pixel on the display. This leads to compression in contrast, also called dynamic range, and hence poor display quality, as illustrated in Figure 1.7.

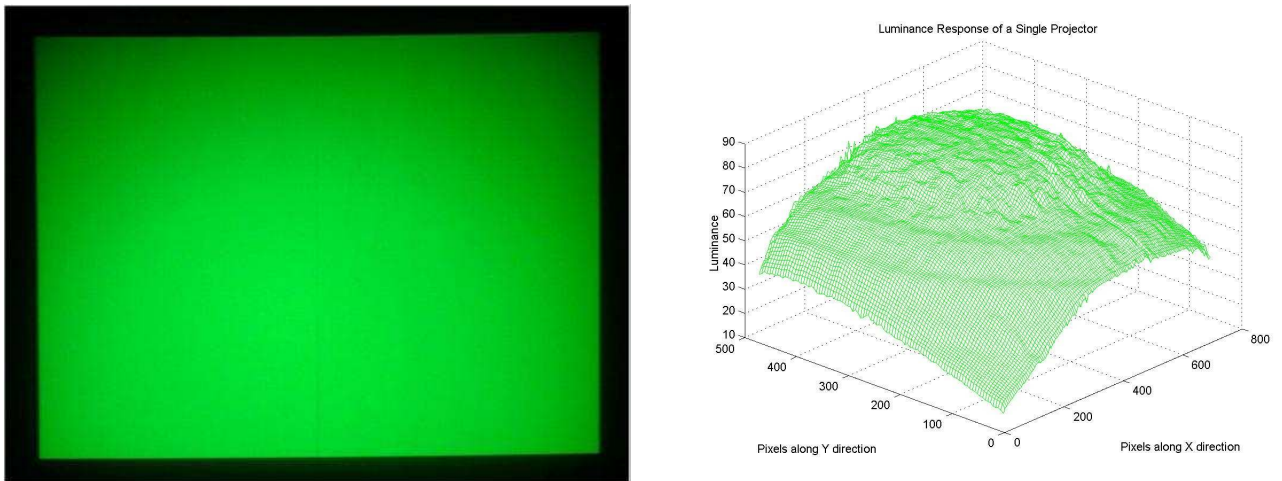


Figure 6.1: Left: A flat green image displayed on a single-projector display. Right: The luminance response for the left image. Note that it is not actually flat.

Perceptual Uniformity: The idea behind color seamlessness is to make a multi-projector display behave like a single projector. First, let us analyze the behavior of a single projector. Figure 6.1 shows a flat green image projected by a projector and its luminance variation. The non-flat luminance surface shows that a typical single-projector display is *not* photometrically uniform. But humans perceive them as uniform. So, we believe that it is sufficient for a multi-projector display to create a *perception* of being uniform.

Formally, the desired display is *perceptually uniform* if the color reaching the viewer e from any two display coordinates (u_1, v_1) and (u_2, v_2) differ within a certain visibly imperceptible threshold. That is,

$$\forall i, E'(u_1, v_1, i, e) - E'(u_2, v_2, i, e) \leq \Delta, \quad (6.2)$$

where Δ is a function that depends on parameters like distance between display coordinates, distance of viewer, angle of the viewing direction with respect to the display wall at the display coordinates, human perception capabilities and even the task to be accomplished by the user. Note that absolute color uniformity is a special case of perceptual uniformity where $\Delta = 0, \forall (u_1, v_1), (u_2, v_2)$.

Display Quality: High dynamic range, brightness, and wide color gamuts are essential for good image quality [Debevec97, Larson01]. Similarly, high lumens rating (high brightness), low black offsets (high contrast), and saturated colors (wide color gamut) are essential for good display quality. However, note that the criterion of perceptual uniformity alone which generates the desired display E' satisfying Equation 6.2 may not ensure a good display quality. For example, absolute photometric uniformity, which implies perceptual photometric uniformity, does not ensure good display quality.

Another important point to note is that the projector vendors usually design projectors which have the necessary capacity to achieve high display quality when used individually. Thus, the display with color variations which is formed by these projectors denoted by E exhibit high display quality in most places. Thus, if we impose an additional constraint that E' differs minimally from E , we can assure that these high display qualities are retained as much as possible. This can be expressed by the minimizing the sum of the distances between E and E' at every (u, v) . Thus,

$$\forall i, \text{ minimize } \sum |E(u, v, i, e) - E'(u, v, i, e)| \quad (6.3)$$

Color Seamlessness: Hence, color seamlessness is an optimization problem where the goal is to generate an E' that has maximal imperceptible color variation and minimum distance from the reconstructed E . In other words, the problem of achieving color seamlessness is an optimization problem where the goal is to *achieve perceptual uniformity while maximizing the display quality*.

6.3 Unifying Previous Work

In this section we explain all the existing methods using the framework proposed framework. This helps us to compare and contrast different existing methods within the framework of the emineoptic function.

6.3.1 *Manual Manipulation of Projector Controls*

The most common method used to achieve color correction in tiled displays made of abutting projectors, is to change the control settings of contrast, brightness, white balance manually. Figure 1.6 shows an example.

Reconstruction: In this method, the sensor used to reconstruct the emineoptic function is the human eye or a camera.

Modification: The goal here is to achieve perceptual uniformity in an informal sense.

Reprojection: The reprojection is done by manipulating the projector controls which means modifying the projector parameters of channel transfer function, h_l , and the maximum of channel luminance function, Q_l , given by $M_l = \max_{\forall(s,t)} Q_l$.

Shortcomings: Manipulation of controls cannot nullify the effect of the spatially varying luminance function, Q_l , and retains the seams across the projector boundaries as shown in Figure 1.6. Also, being manual, it is not scalable.

6.3.2 *Gamut Matching*

[Stone1a, Stone1b, Majumder00] try to match the color space or luminance across different projectors by linear transformations of color spaces and luminance responses.

Reconstruction: The emineoptic function is sampled at very few display coordinates (u, v) , usually at the center of each projector. A radiometer is used to estimate the channel chrominance, c_l , and the channel transfer function, h_l .

Modification: The goal is to achieve photometric uniformity by making the maximum of the channel luminance functions, M_l , and the channel chrominance, c_l , identical for all projectors.

Reprojection: For reprojection, the input parameter i is manipulated by linear transforms.

Shortcomings: Due to sparsity of sampling this method also cannot reconstruct the spatially varying luminance function, Q_l , and hence cannot achieve photometric uniformity. Further, we have not seen robust methods that can find the common color space of different projectors which would make [Bern03, Stone1a, Stone1b] scalable.

6.3.3 *Using the same lamp for all projectors*

Some methods [Pailthorpe01] use a common lamp for all projectors.

Reconstruction: Here there is no reconstruction step.

Modification: The goal is to equalize the maximum of the channel luminance functions, M_l , and the channel chrominance, c_l , for all projectors.

Reprojection: The reprojection is done by changing the parameter M_l directly by using a common lamp.

Shortcomings: This solution also does not address Q_l or h_l and addresses only the color variation contributed by the projector lamp. However, as mentioned in the previous chapters, this is not the sole cause of the color variation problem. Also, the use of a common lamp is not scalable and can be used for systems having not more than nine projector. Beyond this, the power of the common lamp required to produce a sufficiently bright display becomes prohibitive in terms of efficiency in performance and problems of thermal taxation that needs to be addressed. Further, this often involves a significant amount of skilled labor and cost.

6.3.4 Blending

Blending or feathering techniques attempt to blend the higher brightness in the overlap regions by weighing the contribution from each projector in the overlap region by a function. When done in software [Raskar98], this function can be carefully designed function to be a linear or cosine ramp. It can also be done optically using physical masks [Li00] or by modifying the analog signals to the projectors [Chen01]. Figure 1.6 shows some results.

Reconstruction: Here there is no reconstruction process.

Modification: The goal, though not formally defined, aims at achieving a smooth transition from the brighter overlap region to the dimmer non-overlap regions. This would achieve some kind of perceptual uniformity if the tiled display is made of identical projectors with linear h_l . Even if some estimate of h_l is used in some methods [Yang01], it is impossible to get identical projectors to produce a entirely seamless display.

Reprojection in Software Blending: In software blending [Raskar98] the reprojection is done by changing the input i is to $i' = \alpha_j(u, v, s_j, t_j) \times i$ where α is a function of the relative positions of projector and display coordinates such that $\sum_{j=1}^n \alpha_j = 1.0$ and $0.0 \leq \alpha_j \leq 1.0$. So, E is given by

$$E(u, v, i) = \oplus_{j \in N_P} T_j(s_j, t_j, \alpha_j \times i). \quad (6.4)$$

Reprojection in Other Types of Blending: In blending achieved both optically [Li00] or by manipulating the analog signal [Chen01], the reprojection is done by changing the function T_j itself at (u, v) given by

$$E(u, v, i) = \oplus_{j \in N_P} \alpha_j \times T_j(s_j, t_j, i). \quad (6.5)$$

Ideally, $\alpha_j \leq 1.0$ and $\sum_{j=1}^n \alpha_j = 1.0$.

Shortcomings: First, blending only addresses the overlap and does not address Q_l . Further, software blending often assumes a linear h_l which is not true in practice. Hence we see bands in the overlap regions as shown in Figure 1.6. In optical blending, the color transition brought into effect by the physical metal masks is often not a controlled smooth transition and does not assure the condition $\sum_{j=1}^n \alpha_j = 1.0$.

6.3.5 Luminance Matching

[Majumder02a], tries to match the luminance response at every display coordinate. This is different than absolute uniformity since this does not address chrominance but only luminance. So, we call this achieving photometric (luminance) uniformity instead of absolute color uniformity.

Reconstruction: This is probably the only existing method that makes an effort to reconstruct E in a rigorous manner using a digital camera.

Modification: The goal is formally defined as one of achieving photometric uniformity. Under the assumption that c_l is constant for all projectors, the method makes $lum(E)$ in Equation 5.8 identical at every (u, v) .

Reprojection: The reprojection is done by manipulating the input i at every pixel (s, t) of every projector differently.

Shortcomings: The results shown in Figure 1.7 suffers from the typical shortcomings of photometric uniformity (only in luminance) yielding low dynamic range images as mentioned in Section 6.2. Further, the sampling of E in (u, v) is limited by the camera resolution making this method unscalable.

CHAPTER 7

An Algorithm to Achieve Photometric Seamlessness

In this chapter, we describe an algorithm to generate perceptually seamless high quality displays. In this algorithm we address only the luminance variation across multi-projector display. This still yields good results due to two reasons.

1. Most displays are made of projectors of the same model. As shown in Chapter 4, the luminance variation in these displays is much more significant than chrominance variation which is almost negligible.
2. Humans are at least an order of magnitude more sensitive to variation in luminance than in chrominance [Goldstein01, Valois90].

Our method is automatic and scalable, and addresses the luminance variation within a single projector, across different projectors and in the overlapping regions in a unified manner. Further, the correction to achieve seamlessness is implemented in real time using commodity graphics hardware. Since we address only luminance variation, we say that our algorithm achieves photometric seamlessness.

Our algorithm follows three steps. First, it *reconstructs* the emineoptic function efficiently. It uses a photometer and a digital camera as sensor for this purpose. Then, it *modifies* the emineoptic function using a constrained gradient-based luminance smoothing algorithm. Finally, we *reproject* the modified function by changing *only* the input i at every display coordinate (u, v) . Further, the reprojection can be achieved in real time by using commodity graphics hardware. In this chapter we present the theory behind the reconstruction, modification and reprojection and show how these can be directly derived from the emineoptic function. The practical implementation using different sensors are described in details in Chapter 8.

7.1 Reconstruction

First we present an overview of the theory of reconstruction and then we describe the process in details.

7.1.1 Reconstruction Overview

The brief overview of the reconstruction process describes the sampling philosophy, sensors, accuracy of reconstruction, and the geometric warp we use for reconstruction.

Geometric Calibration

To reconstruct the emineoptic function, we require a geometric warp G that relates the projector coordinates (s, t) with the display coordinates (u, v) (Refer to Chapter 5). Most geometric calibration methods use a camera as the sensor and define the relationship between the projector coordinates (s, t) and the display coordinates (u, v) through the camera coordinates, which we denote by (x, y) . We use one such method [Hereld02] for our purpose. Note that any image taken by the camera to reconstruct the emineoptic function needs to be taken from the same position and orientation as the geometric calibration. We refer the reader to [Majumder02a] for a detailed treatise on using such geometric warps to extract the luminance and chrominance response from camera images.

Sampling the Emineoptic Function

The emineoptic function $E(u, v, i)$ defines the light reaching the viewer from display coordinates (u, v) for input i . To sample the emineoptic function densely in the spatial domain (u, v) , one can use a high-resolution digital camera. To sample it densely in the input domain, assuming that each i_l takes 2^8 discrete values, one needs to use $O(2^{24})$ images. This indicates an impractically large amount of data.

To reduce this data requirement, we use the properties of model parameters. For example, in Equation 5.7, since $h_l(i_l)$ does not depend on the spatial coordinates, we need to sample it at any one projector coordinate. $Q_l(s, t)$ and $B(s, t)$ need to be sampled densely only in the spatial domain and not in the input domain. Further, with the black offset removed, the response of each channel of the projector is independent of each other. Thus, we need just four (one for each channel and one for the black), high resolution camera images per projector, in addition to $O(2^8)$ single valued measurements to estimate $h_l(i_l)$.

In essence, we use a small set of measurements of the emineoptic function to *estimate* all the model parameters. Then, we use these estimated parameters to *compute* the complete emineoptic function. In addition to alleviating the data storage problem, estimating model parameters also helps in easy modification of the emineoptic function by modifying the model parameters appropriately and independently to achieve the desired photometric seamlessness.

Sensors and Accuracy

For accuracy and speed, we use a photometer and a camera together. The challenge in measuring h_l with a camera is to design an automatic method that can change the dynamic range of the camera appropriately to capture images of varying brightness. Since h_l change very little temporally [Majumder02b], we use a slower photometer (1 – 20 seconds per measurement) to estimate h_l more accurately at infrequent time intervals (usually once in 9 – 12 months). On the other hand, Q_l and B depend on spatial coordinates demanding geometrically accurate high-resolution measurements. Since Q_l and B are luminance measurements, a device dependent 3D color space like that of a camera does not pose a limitation. Finally, since these parameters change even with a small change in the position and orientation of the projectors, they need frequent and fast estimation. Hence a camera is a suitable device to reconstruct these luminance parameters. The issue of camera resolution with respect to the display resolution is addressed in Chapter 8.

7.1.2 Reconstruction Process

Now, we describe the reconstruction process in detail. First we estimate the model parameters for each projector individually and then reconstruct the emineoptic function for the whole display.

Estimating Model Parameters for a Single Projector

We describe the process to estimate $h_r(i_r)$, $Q_r(s, t)$ for channel r , and $B(s, t)$, for a single projector (Equations 5.6 and 5.7). The parameters for channels g and b are estimated analogously.

Transfer Function (h_l): By definition, $h_l(i_l)$ is the ratio of the luminance projected for i_l to the maximum luminance projected from channel l , *when black offset is zero*. But due to the presence of the black offset, we need to subtract the black offset from every measurement of luminance and then compute $h_l(i_l)$. It is derived as follows.

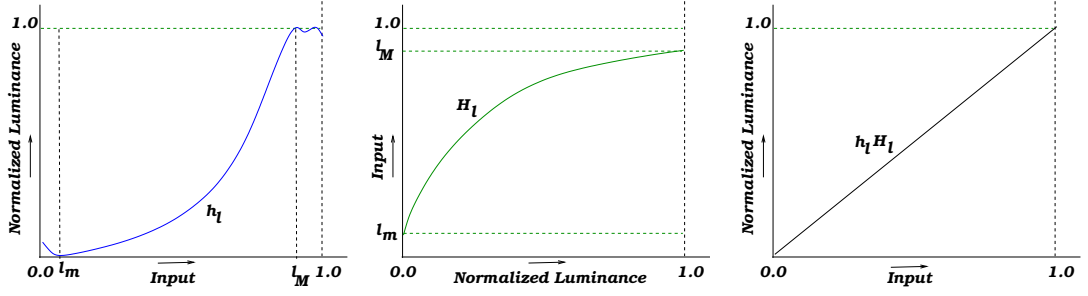


Figure 7.1: Left: Projector channel input transfer function; Middle: Projector channel linearization function; Right: Composition of the channel input transfer function and the channel linearization function.

Since, $h_l(i_l)$ does not depend on (s, t) , we drop these parameters for simplicity. For the same reason, we can use a photometer to take the luminance measurements from a single projector coordinate. Let the input be $(i_r, 0, 0)$. From Equation 5.7, the photometer measures $lum(T(i_r, 0, 0))$. Thus, from Equations 5.7 and 5.6,

$$lum(T(i_r, 0, 0)) = h_r(i_r)Q_r + h_g(0)Q_g + h_b(0)Q_b + B. \quad (7.1)$$

Let $lum(T(i_r, 0, 0))$ be minimum at $i_r = r_m$ and maximum at $i_r = r_M$ as shown in Figure 7.1 (In general, for a channel l , these two inputs are defined as l_m and l_M). Unlike the case of ideal devices, for projectors, often $lum(T(i_r, 0, 0))$ is non-monotonic, i.e. $r_m \neq 0$ and $r_M \neq 1$. But, by definition, $h_r(r_m) = 0$ and $h_r(r_M) = 1$. So, to find h_r from $lum(T(i_r, 0, 0))$, we need to normalize it in the input range between 0.0 and 1.0. This is derived from Equation 7.1 as,

$$\begin{aligned} lum(T(r_m, 0, 0)) &= h_g(0)Q_g + h_b(0)Q_b + B \\ lum(T(r_M, 0, 0)) &= Q_r(s, t) + h_g(0)Q_g + h_b(0)Q_b + B \\ &= Q_r(s, t) + lum(T(r_m, 0, 0)) \end{aligned}$$

Thus, h_r can then be found from Equation 7.1 as

$$h_r(i_r) = \frac{lum(T(i_r, 0, 0)) - lum(T(r_m, 0, 0))}{lum(T(r_M, 0, 0)) - lum(T(r_m, 0, 0))}. \quad (7.2)$$

We measure and compute h_r for $O(2^8)$ input values to sample the whole input space.

Luminance Functions (Q_l, B): We use a digital camera to reconstruct $Q_r(s, t)$ and $B(s, t)$. Note that, since $h_l(i_l)$ is the same for every coordinate (s, t) , the maximum and minimum luminance for each channel l are projected for the same inputs, l_m and l_M respectively, where $h_l(l_m) = 0$ and $h_l(l_M) = 1$.

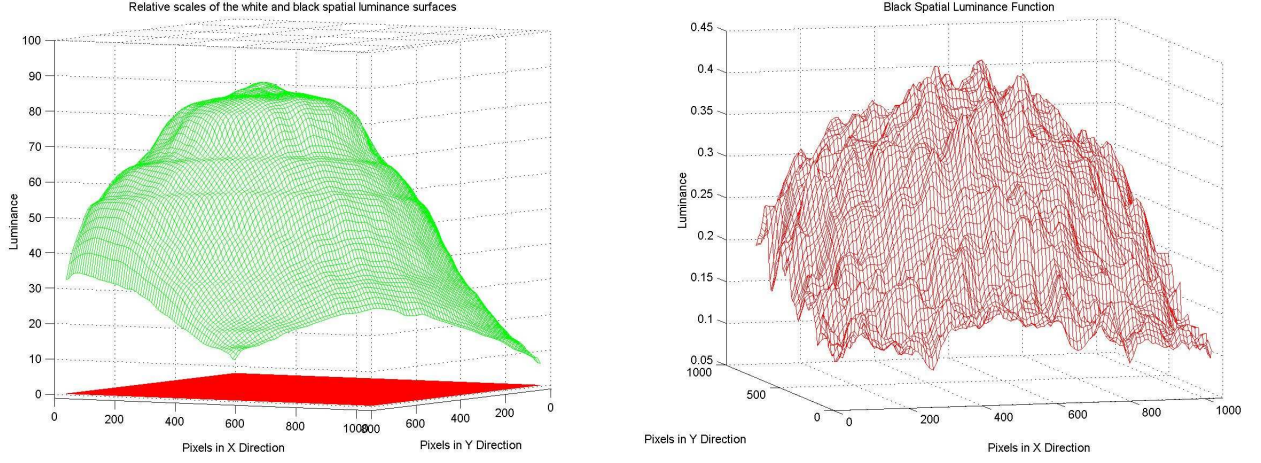


Figure 7.2: Left: The maximum luminance function for green channel and the black luminance function for a single projector. This figure gives an idea about their relative scales. Left: Zoomed in view of the black luminance surface.

Let $i_m = (r_m, g_m, b_m)$. For input i_m at all the display coordinates, the measured luminance of the display $lum(T(s, t, i_m))$ is the black offset $B(s, t)$. This can be derived from Equation 5.7 by substituting $h_l(l_m) = 0$,

$$lum(T(s, t, i_m)) = B(s, t). \quad (7.3)$$

Let us now compute $Q_r(s, t)$. Let $i_M = (r_M, g_m, b_m)$. The measured luminance projected at all the projector coordinates for input i_M is derived from Equation 5.7 as,

$$lum(T(s, t, i_M)) = W_r(s, t) = Q_r(s, t) + B(s, t). \quad (7.4)$$

Intuitively, W_l gives the maximum luminance response for a channel l (W for “white”). So we call $W_r(s, t)$ the *maximum luminance function* for channel r . From Equation 7.4,

$$Q_r(s, t) = W_r(s, t) - B(s, t). \quad (7.5)$$

Thus estimating h_l , c_l , Q_l and B for every projector, we can reconstruct $T(s, t, i)$ from Equation 5.7.

Reconstructing Emineoptic Function of the Display

Once we compute $T_j(s_j, t_j, i)$ for each projector P_j , we then reconstruct $E(u, v, i)$ using Equation 5.10. E thus generated for an input $i = (1, 1, 0)$ is shown in Figure 5.3.

7.2 Modification

The next step is to modify the reconstructed E to a *desired* E' that achieves color seamlessness. In this section we find such an E' . Since most display walls are made up of same model projectors, we assume that c_l is identical for all projectors [Majumder02b], and hence, $chr(E(u, v, i))$ is spatially invariant. Only $lum(E(u, v, i))$ varies spatially and we describe how we modify $lum(E(u, v, i))$ to achieve photometric seamlessness.

7.2.1 Choosing a Common Display Transfer Function

The transfer function $h_l(i_l)$ of a display with high contrast and intensity resolution should satisfy the following three conditions: $h_l(0) = 0$, $h_l(1) = 1$ and $h_l(i_l)$ is monotonic. For most projectors, $h_l(i_l)$ may not satisfy these properties. For example, $l_m \neq 0$ and $l_M \neq 1$. So, we *choose* a *common display transfer function* for each channel of all projectors, denoted by h'_l that satisfies the above properties.

With the common display transfer function h'_l (same for all projectors), Equation 5.10 becomes

$$lum(E(u, v, i)) = \sum_{l \in \{r, g, b\}} \left(h'_l(i_l) \sum_{j \in N_P} Q_{l_j} \right) + \sum_{j \in N_P} B_j. \quad (7.6)$$

From Equation 7.5,

$$lum(E(u, v, i)) = \sum_{l \in \{r, g, b\}} \left(h'_l(i_l) \sum_{j \in N_P} (W_{l_j} - B_j) \right) + \sum_{j \in N_P} B_j \quad (7.7)$$

where W_{l_j} and B_j are luminance functions of projector P_j .

7.2.2 Modifying Display Luminance Functions

In Equation 7.7, let $\mathcal{W}_l = \sum_{j \in N_P} W_{l_j}$ be called the *maximum display luminance function* for channel l and $\mathcal{B} = \sum_{j \in N_P} B_j$ be called the *black display luminance function*. While W_l and B are the luminance functions for a single projector, \mathcal{W}_l and \mathcal{B} are the luminance functions for the whole display. Thus Equation 7.7 becomes,

$$lum(E(u, v, i)) = \left(\sum_{l \in \{r, g, b\}} h'_l(i_l) (\mathcal{W}_l(u, v) - \mathcal{B}(u, v)) \right) + \mathcal{B}(u, v) \quad (7.8)$$

Note that the above equation for the emineoptic function of the *whole display* is identical to that of a single projector whose transfer function is h'_l and the luminance functions are \mathcal{W}_l and \mathcal{B} . Thus, by

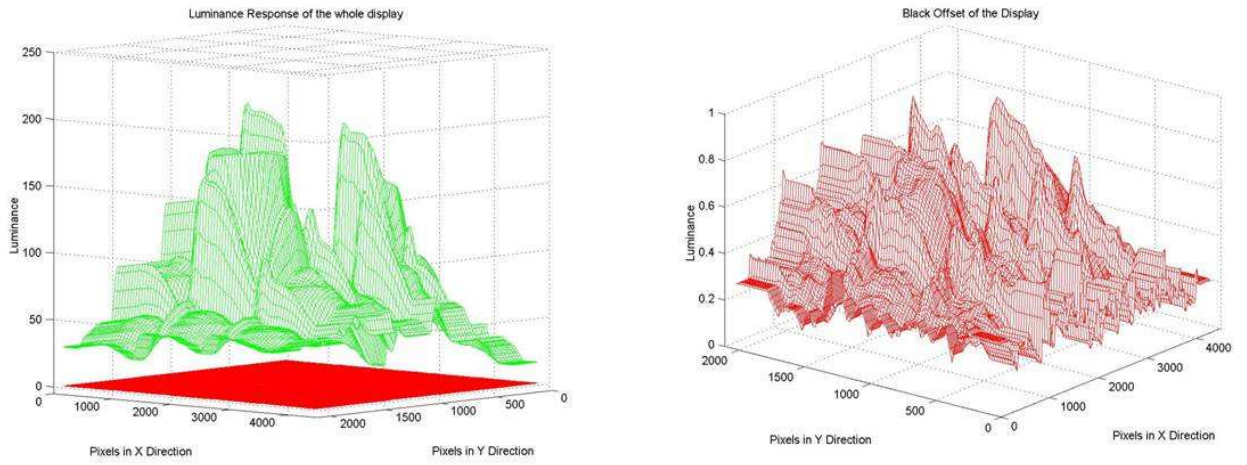


Figure 7.3: Left: The maximum luminance function for green channel and the black luminance function for a display made of 5×3 array of fifteen projectors. This figure gives an idea about their relative scales. Right: A zoomed in view of the black luminance surface for the whole display .

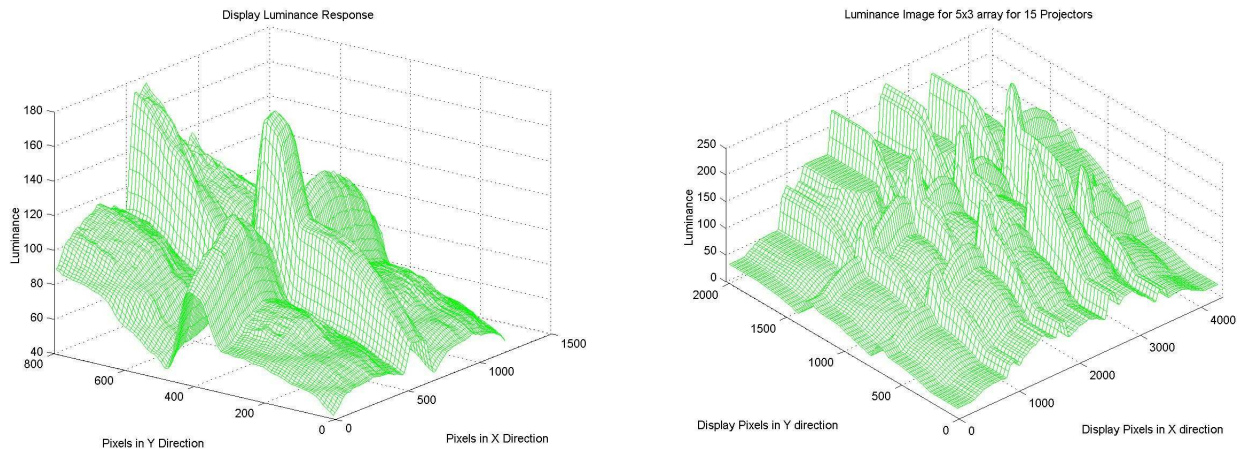


Figure 7.4: Reconstructed display luminance function of green channel for a 2×2 array of projectors (left) and 3×5 array of projectors (right). The high luminance regions correspond to the overlap regions across different projectors.

matching the input transfer functions, we have made the multi-projector display identical to a single projector display. Figure 7.3 shows the luminance functions for the whole display. Compare this with Figure 7.2 which illustrates the single projector case. But note that, unlike a single projector display, \mathcal{W}_l and \mathcal{B} of the multi-projector display have sharp discontinuities which result in perceivable edges. As an additional illustration, Figure 7.4 shows \mathcal{W}_g for a four and fifteen projector display.

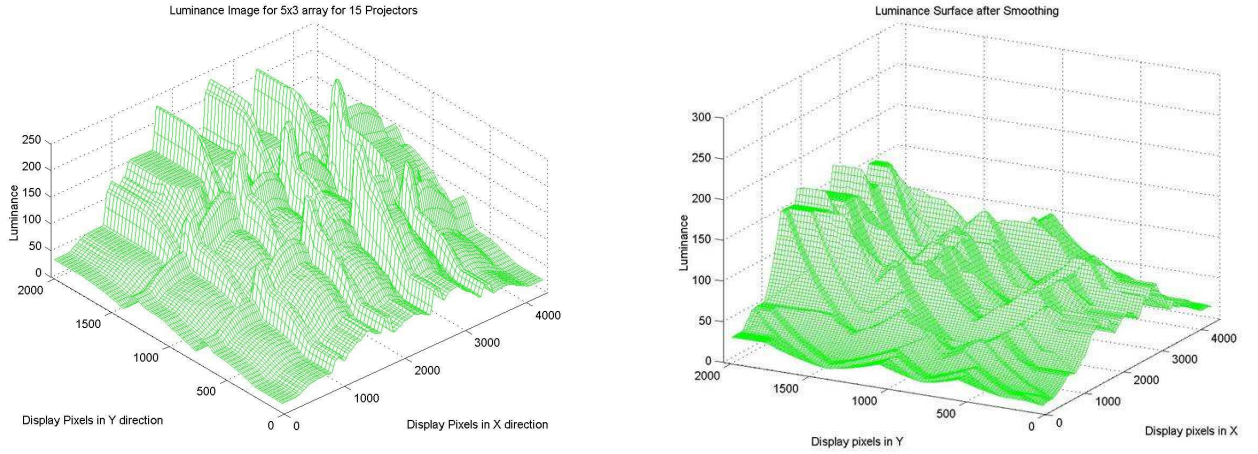


Figure 7.5: Left: Reconstructed display luminance function of green channel for a 3×5 array of projectors Right: Smooth display function for green channel achieved by applying the smoothing algorithm on the display luminance function in the left figure.

So, we modify $\mathcal{W}_l(u, v)$ and $\mathcal{B}(u, v)$ by smoothing them to $\mathcal{W}'_l(u, v)$ and $\mathcal{B}'(u, v)$ respectively to remove the perceptible discontinuities. At the same time, the modification is designed in such a way that $\mathcal{W}'_l(u, v)$ and $\mathcal{B}'(u, v)$ are as close to $\mathcal{W}_l(u, v)$ and $\mathcal{B}(u, v)$ as possible to maintain the original high dynamic range. We call the method to achieve this smoothing as the *constrained gradient-based smoothing* and is explained in detail in the following section. The $\mathcal{W}'_l(u, v)$ thus generated is called the *smooth maximum display luminance function* for channel l and $\mathcal{B}'(u, v)$ is called the *smooth black display luminance function*. Figure 7.5 shows $\mathcal{W}'_g(u, v)$ for a fifteen-projector display. Figure 7.9 shows the smoothing with different smoothing parameters.

The luminance of the *modified desired emineoptic function* $E'(u, v, i)$ thus generated is

$$lum(E'(u, v, i)) = \left(\sum_{l \in \{r, g, b\}} h'_l(i_l) (\mathcal{W}'_l(u, v) - \mathcal{B}'(u, v)) \right) + \mathcal{B}'(u, v) \quad (7.9)$$

When each of $\mathcal{W}'_l(u, v)$ and $\mathcal{B}'(u, v)$ is smooth, $lum(E'(u, v, i))$ is also smooth and satisfies Inequality 6.2 to achieve photometric seamlessness.

7.2.3 Constrained Gradient Based Smoothing

In this section we present the constrained gradient based smoothing algorithm that is used to modify $\mathcal{W}_l(u, v)$ to $\mathcal{W}'_l(u, v)$. Since the variation in $\mathcal{B}(u, v)$ is almost negligible when compared to the scale of $\mathcal{W}_l(u, v)$, we approximate $\mathcal{B}'(u, v)$ by $\mathcal{B}'(u, v) = \max_{\forall u, v} \mathcal{B}(u, v)$ since this is the minimum luminance that can be achieved at all display coordinates.

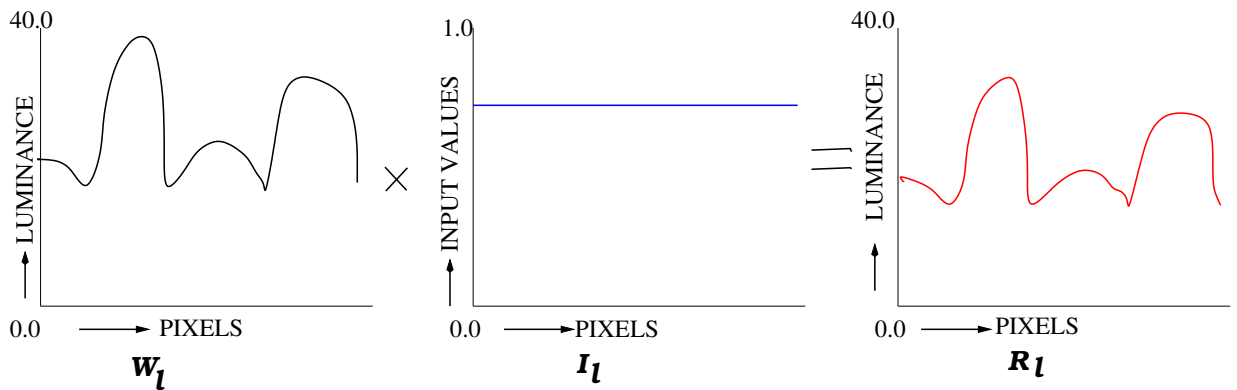


Figure 7.6: The problem: The left figure shows the reconstructed maximum luminance function, the middle figure shows the image to be displayed and the right figure shows the image seen by the viewer. Note that this image is distorted by the luminance variation of the display.

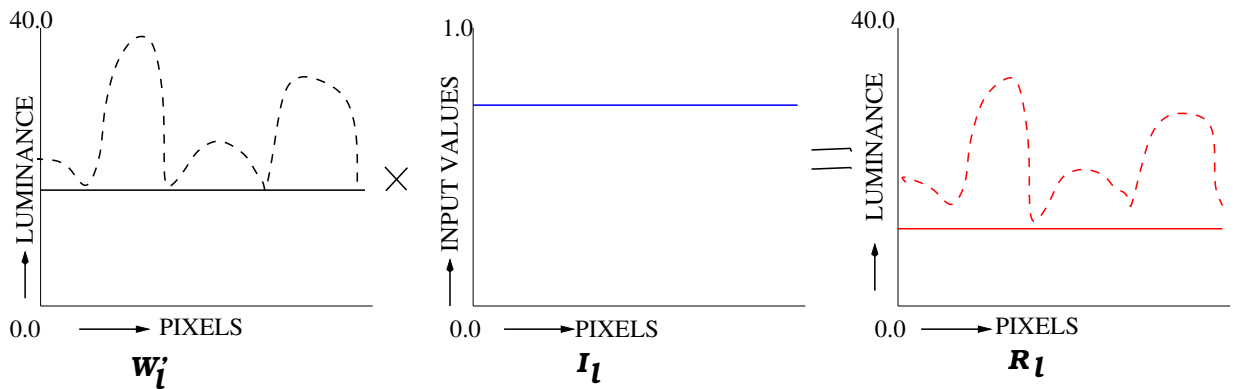


Figure 7.7: Photometric uniformity: The left figure shows the modified luminance function, and the right shows the image seen by the viewer. Note that the image seen by the viewer though similar to image to be displayed, it has significant reduction in dynamic range.

The Problem

For simplicity of explanation, we assume $\mathcal{B}(u, v)$ to be zero in this section. Let an image $I_l(u, v)$, whose value at every display coordinate (u, v) is i_l be projected on the display wall. As per Equation

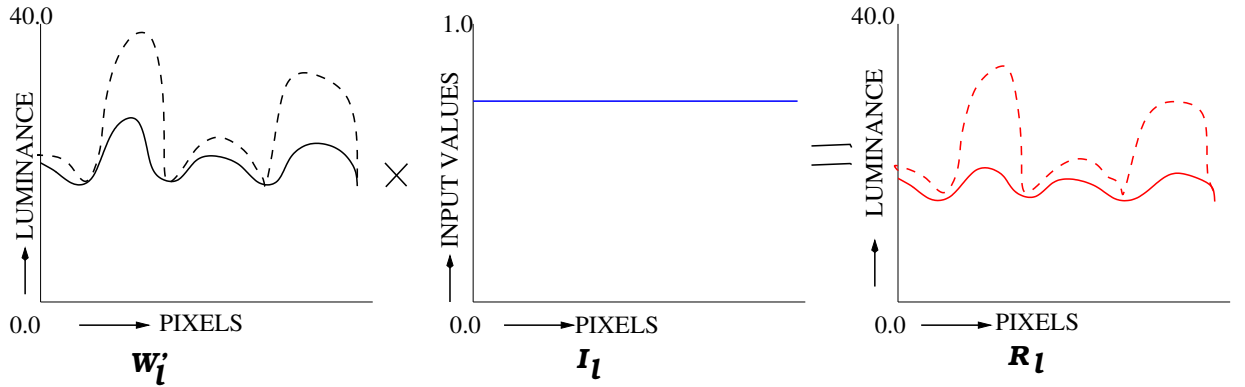


Figure 7.8: Optimization problem: The display luminance response is modified to achieve perceptual uniformity with minimal loss in display quality.

7.8, the resulting image $R_l(u, v)$ is given by multiplication of $\mathcal{W}_l(u, v)$ and $I_l(u, v)$, as shown in Figure 7.6 (For illustration purposes, we use a one dimensional \mathcal{W}_l and I_l). Note that the image projected by the display $I_l(u, v)$ and the result observed by the viewer $R_l(u, v)$ are different and the difference is dictated by the variation in $\mathcal{W}_l(u, v)$.

To make $R_l(u, v)$ similar to $I_l(u, v)$, we can modify $\mathcal{W}_l(u, v)$ to be a constant function, $\mathcal{W}'_l(u, v)$, as shown in Figure 7.7. This, by definition, is a photometrically uniform display [Majumder02a], but leads to *poor utilization of display capabilities* and *significant reduction in dynamic range*.

Optimization Problem

To avoid this, as mentioned in Section 6.2, we pose the problem of achieving seamlessness as an *optimization problem* where we aim to find a $\mathcal{W}'_l(u, v)$ that *minimizes the discontinuities* to assure *perceptual uniformity* while *maximizing the utilization of display capabilities* to assure *high display quality*, as shown in Figure 7.8. Perception studies have found that humans are most sensitive to significant luminance discontinuities and insensitive to smooth changes [Chorley81, Goldstein01, Valois88, Lloyd02]. When I_l is displayed on such a $\mathcal{W}'_l(u, v)$, the difference between $R_l(u, v)$ and $I_l(u, v)$, though measurably present, is imperceptible to a human observer.

Formally, $\mathcal{W}'_l(u, v)$ is defined by the following optimization constraints.

Capability Constraint: This constraint ensures that \mathcal{W}'_l never goes beyond the display capability of \mathcal{W}_l .

$$\mathcal{W}'_l \leq \mathcal{W}_l. \quad (7.10)$$

Perceptual Uniformity Constraint: This constraint assures that \mathcal{W}'_l has a smooth variation imperceptible to humans.

$$\frac{\partial \mathcal{W}'_l}{\partial x} \leq \frac{1}{\lambda} \times \mathcal{W}'_l. \quad (7.11)$$

where λ is the *smoothing parameter* and $\frac{\partial \mathcal{W}'_l}{\partial x}$ is the gradient of \mathcal{W}'_l along any direction x . Compare Inequality 7.11 with Inequality 6.2. Our empirical results show that the luminance responses of most single projector displays satisfy Inequality 7.11.

Display Quality Optimization Function: The above two constraints can yield many feasible \mathcal{W}'_l . To assure minimum loss in display quality we choose the \mathcal{W}'_l that is the closest to \mathcal{W} , i.e. the \mathcal{W}'_l that *minimizes* $\mathcal{W}_l - \mathcal{W}'_l$.

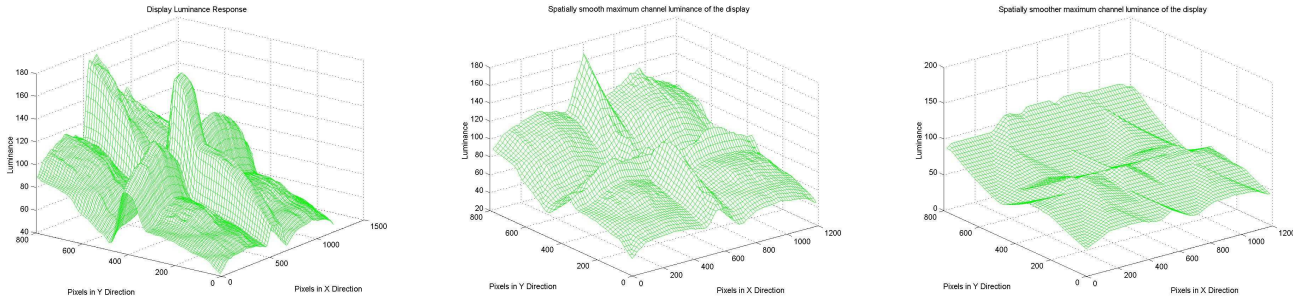


Figure 7.9: This shows the smooth luminance surface for different smoothing parameters. *Left:* Reconstructed display luminance function of green channel for a 2×2 array of projectors *Middle:* Smooth display function for green channel achieved by applying the smoothing algorithm on the display luminance function with $\lambda = 400$. *Right:* Smoothing applied with a higher smoothing parameter of $\lambda = 800$ to generate a smoother display surface.

Linear Programming Formulation

We show that the above optimization constraints and objective can be expressed as linear functions. Therefore, it can be solved optimally using *linear programming* in linear time.

Equations 7.10 and 7.11 assume both $\mathcal{W}_l(u, v)$ and $\mathcal{W}'_l(u, v)$ to be continuous functions. In practice, the sampled discrete version of these functions are denoted by $w[u][v]$ and $w'[u][v]$ respectively. The constraints and the objective functions can be described on $w[u][v]$ and $w'[u][v]$ as follows.

Capability Constraint: This can be expressed as

$$w'[u][v] < w[u][v], \quad \forall u, v.$$

Perceptual Uniformity Constraint: For each of the eight neighbors (u', v') of a pixel (u, v) , where $u' \in \{u - 1, u, u + 1\}$ and $v' \in \{v - 1, v, v + 1\}$, the gradient when expressed using a linear filter produces the linear constraint

$$\frac{|w'[u][v] - w'[u'][v']|}{\sqrt{|u - u'|^2 + |v - v'|^2}} \leq \frac{1}{\lambda} w'[u][v], \quad \forall u, v, u', v'.$$

Display Quality Optimization Function: If $L_w \times H_w$ is the size of the display, the objective function becomes

$$\text{maximize } \sum_{u=1}^{H_w} \sum_{v=1}^{L_w} w'[u][v].$$

Alternative Optimal Algorithm

We have developed an iterative algorithm that achieves the same result.

Initialize

0. $minval = \min_{\forall i, j} (d[i][j]);$
1. **forall** $(i, j), d'[i][j] = minval; \text{endfor};$
2. $knot_points = \{(i, j) | d'[i][j] = d[i][j]\};$
3. $free_points = \{(i, j) | (i, j) \notin knot_points\};$
4. $absolute_static = \phi;$
5. **forall** $(i, j), dist[i][j] = d[i][j] - d'[i][j]; \text{endfor};$

Repeat

6. $mindist = \min_{\forall (i, j) \in free_points} dist[i][j]$
7. $minallowance = MAXINT;$
8. **forall** $(i, j) \in knot_points$
9. $neighbor = \{(k, l) | k \in \{i - 1, i, i + 1\}, l \in \{j - 1, j, j + 1\}\}$
10. **forall** $(e, f) \in neighbor$
11. **if** $(e, f) \in free_points$ **then**
12. $delta = (1 + w) * d'[i][j] - d'[e][f]$
13. **endif**
14. $minallowance = \min(delta, minallowance)$

```

15.   endfor
16. endfor
17. distance_to_be_moved = min(minallowance, mindist);
18. forall  $(i, j) \in \textit{free\_points}$ ,
19.    $d'[i][j] = d'[i][j] + \textit{distance\_to\_be\_moved}$ ;
20.    $\textit{dist}[i][j] = \textit{dist}[i][j] - \textit{distance\_to\_be\_moved}$ ;
21. endfor
22. forall  $(i, j) \in \textit{free\_points}$ ,
23.   if  $\textit{dist}[i][j] = 0$  then
24.      $\textit{knot\_points} = \textit{knot\_points} \cup (i, j)$ ;
25.      $\textit{free\_points} = \textit{free\_points} - (i, j)$ ;
26.   endif

27. forall  $(i, j) \in \textit{knot\_points}$ 
28.    $\textit{neighbor} = \{(k, l) | k \in \{i - 1, i, i + 1\}, l \in \{j - 1, j, j + 1\}\}$ 
29.   forall  $(e, f) \in \textit{neighbor}$ 
30.     if  $(e, f) \in \textit{free\_points}$  then
31.        $\textit{delta} = (1 + w) * d'[i][j] - d'[e][f]$ 
31.     endif
32.     if  $\textit{delta} = 0$  then
33.        $\textit{knot\_points} = \textit{knot\_points} \cup (e, f)$ ;
34.        $\textit{free\_points} = \textit{free\_points} - (e, f)$ ;
35.     endif
36.   endfor
37. endfor

38. forall  $(i, j) \in \textit{knot\_points}$ 
39.    $\textit{neighbor} = \{(k, l) | k \in \{i - 1, i, i + 1\}, l \in \{j - 1, j, j + 1\}\}$ 
40.   if  $\textit{neighbor} \subset (\textit{knot\_points} \cup \textit{absolutely\_static})$  then
41.      $\textit{absolute\_static} = \textit{absolute\_static} \cup (i, j)$ ;
42.      $\textit{knot\_points} = \textit{knot\_points} - (i, j)$ ;

```

43. **endfor**

44. **Until** $knot_points = free_points = \phi$

At any iteration, the points in d' can be free, knot or absolutely static. Initially all the points are free. At the first step, all the points of d' that touches d are set as knot points. Every time a point in d' reaches d or cannot go up any further based on the gradient constraint, it becomes a knot and cannot move any further up. If all the eight neighbors of a knot are also knots, then the knot is made an absolutely static point after which no computation is also applied to it.

In each iteration, we move up the free points by a fixed amount. This value is decided in such a way that d' does not violate any of the constraints. Then we find which free points which have become knots and the knots which have become absolutely static and proceed with our next iteration. The algorithm ends when all the points have become absolutely static.

Lines 0 – 5 initializes d' and the sets $knotpoints$, $free_points$ and $absolutely_static$. The data structure $dist$ records the distance of d' from the corresponding point in d . Lines 6 – 43 describes each iteration. In line 6 we find the minimum distance of any free point in d' from its corresponding point in d designated by $mindist$. This satisfies the capability constraint. In lines 8 – 15 we find the minimum distance a free point in d' can be lifted up while maintaining the gradient constrained designated by $minallowance$. In line 17 – 21 we push all the free points in d' up by the minimum of $mindist$ and $minallowance$. In line 22 – 26 we find the new knots based on the capability constraint. In lines 27 – 37 we find the new knots based on the gradient constraint. In lines 38 – 43 we find the knots which becomes absolutely static. Then we repeat the iterations until all the points are absolutely static.

7.3 Reprojection

The goal of reprojection is to achieve the modified emineoptic function $E'(u, v, i)$ given by Equation 7.9. We have modified \mathcal{W}_l and \mathcal{B} and also the transfer function h_l for each projector. However, these parameters cannot be changed with the precision required to achieve the modified emineoptic function. Hence, we do not modify the model parameters and achieve the desired response accurately by changing only the input i_l at every projector coordinate.

7.3.1 Retaining Actual Luminance Functions

To achieve the desired response in Equation 7.9 we modify the input $i_l(u, v)$ in Equation 7.8 to $i'_l(u, v)$ such that

$$\left(\sum_{l \in \{r, g, b\}} h'_l(i'_l) (\mathcal{W}_l - \mathcal{B}) \right) + \mathcal{B} = \left(\sum_{l \in \{r, g, b\}} h'_l(i_l) (\mathcal{W}'_l - \mathcal{B}') \right) + \mathcal{B}' \quad (7.12)$$

The i'_l that satisfies the above equation is

$$h'_l(i'_l(u, v)) = h'_l(i_l(u, v)) \mathcal{S}_l(u, v) + \mathcal{O}_l(u, v), \quad (7.13)$$

where

$$\mathcal{S}_l(u, v) = \frac{\mathcal{W}'_l(u, v) - \mathcal{B}'(u, v)}{\mathcal{W}_l(u, v) - \mathcal{B}(u, v)}; \quad \mathcal{O}_l(u, v) = \frac{\mathcal{B}'(u, v) - \mathcal{B}(u, v)}{3(\mathcal{W}_l(u, v) - \mathcal{B}(u, v))} \quad (7.14)$$

The *scaling map* \mathcal{S}_l , and the *offset map* \mathcal{O}_l are called the *display smoothing maps* for channel l .

From these display smoothing maps, we generate the *projector smoothing maps*, $S_{l_j}(s_j, t_j)$ and $O_{l_j}(s_j, t_j)$ for channel l of projector P_j as,

$$S_{l_j}(s_j, t_j) = \mathcal{S}_l(G_j(s_j, t_j)); \quad O_{l_j}(s_j, t_j) = \mathcal{O}_l(G_j(s_j, t_j))$$

where $(u, v) = G_j(s_j, t_j)$ (Refer to Section 5). Note that it can be proved that the above computation of S_{l_j} and O_{l_j} is correct, and we should not compute them based on the luminance contribution of individual projectors.

Using these projector smoothing maps, the modified input i'_l of projector P_j at coordinate (s_j, t_j) has to be computed such that

$$h'_l(i'_l(s_j, t_j)) = h'_l(i_l(s_j, t_j)) S_{l_j}(s_j, t_j) + O_{l_j}(s_j, t_j) \quad (7.15)$$

7.3.2 Retaining Actual Transfer Function

The goal of this section is to find the input $\bar{i}(s_j, t_j)$ that would make

$$h_{l_j}(\bar{i}(s_j, t_j)) = h'_l(i'_l(s_j, t_j)). \quad (7.16)$$

For that, let us first assume a hypothetical function A_{l_j} that transforms the projector channel input transfer function h_{l_j} of projector P_j to the common display transfer function h'_l .

$$h'_l(i'_l) = h_{l_j}(A_{l_j}(i'_l)) \quad (7.17)$$

Thus, comparing Equation 7.16 and 7.17, we find,

$$\bar{i}(s_j, t_j) = A_{l_j}(i'_l) \quad (7.18)$$

So, the goal of this section is to find A_{l_j} .

Towards that end, I introduce the function

$$H_{l_j} = A_{l_j} h'_l{}^{-1} \quad (7.19)$$

Note that the composition of $h_{l_j}(H_{l_j})$ is an identity function.

$$H_{l_j} = h_{l_j}^{-1} \quad (7.20)$$

Thus, in effect, the H_{l_j} is inverse of the projector channel input transfer function and can be directly computed from h_{l_j} for every projector. We call H_{l_j} , the *projector channel linearization function* for channel l of projector P_j . This is illustrated in Figure 7.1.

The next thing to note is that the composition of the projector channel linearization function, H_{l_j} , and the common display transfer function, h'_l , gives us the hypothetical function A_{l_j} for each projector.

$$A_{l_j} = H_{l_j} h'_l \quad (7.21)$$

Thus, from Equation 7.18 and 7.21, we now find

$$\bar{i}_l(s_j, t_j) = H_{l_j}(h'_l(i_l(s_j, t_j))S_{l_j}(s_j, t_j) + O_{l_j}(s_j, t_j)) \quad (7.22)$$

Intuitively, Equation 7.22 can be explained as follows. Smoothing maps assume inputs designed for linear devices. The function h'_l converts an input generated for a non-linear device to an input for a linear device. Finally, they need to be converted back to inputs suitable for the non-linear projectors. The projector specific H_{l_j} achieves this conversion.

Thus, all the modifications we make to achieve a seamless E' is brought into effect by only changing the input $i_l(s_j, t_j)$ to be projected by each channel l of each projector P_j at its coordinates (s_j, t_j) .

7.4 Chrominance

The algorithm just presented solves the restricted problem of achieving photometric seamlessness across multi-projector displays. However, the chrominance variation across such displays, though

much insignificant when compared to the magnitude of the luminance variation problem, is not entirely non-existent. So, in future, we need to address the chrominance variation problem, we need to reconstruct the chrominance functions. So, here we briefly explain how to reconstruct the chrominance functions.

Reconstructing Channel Chrominance (c_l): Similarly, measuring the chrominance of any input i_R should ideally give c_r . But, due to the black offset, this is not true. We measure the chrominance $chr(T(s, t, (r_M, 0, 0)))$. From Equation 5.7 and from the definition of \oplus , we know that

$$chr(T(s, t, (r_M, 0, 0))) = \frac{c_r Q_r(s, t) + c_B B(s, t)}{Q_r(s, t) + B(s, t)}. \quad (7.23)$$

We can compute c_r from this equation because all other parameters are known.

7.5 Enhancements to Address Chrominance

However, note that chrominance is by definition dependent on the luminance (Refer to Section 4.2). Thus handling the chrominance variation is not a mere extension of the algorithm to achieve photometric (luminance) seamlessness. Instead, including chrominance while maintaining both perceptual uniformity and high display quality can be shown to be a five dimensional optimization problem. Further, since luminance is well quantified in the perceptual literature, it is relatively easy to design quantitative objective functions for such an optimization. This becomes increasingly difficult when chrominance is involved.

In the current algorithm, we have only corrected for the perceptual luminance variations. It has been shown in Chapter 4, that many of the chrominance blotches are manifestation of luminance variations which has not addressed in our algorithm. From the limitations of the human vision and the results achieved from our algorithm to achieve photometric seamlessness (presented in Chapter 8), it is evident that correcting for the luminance variation problem can take us a long way towards achieving perceptually uniform high quality displays. Thus, it is worth while to augment the current algorithm with other kinds of luminance corrections in future and quantify the amount of perceptual seamlessness that can be achieved by addressing the luminance alone.

CHAPTER 8

System

In this chapter we will describe the implementation of the algorithm presented in the preceding section in details. This system was implemented and demonstrated on three different multi-projector display walls at Argonne National Laboratory (a 5×3 array of fifteen projectors, a 3×2 array of six projectors and a 2×2 array of four projectors).

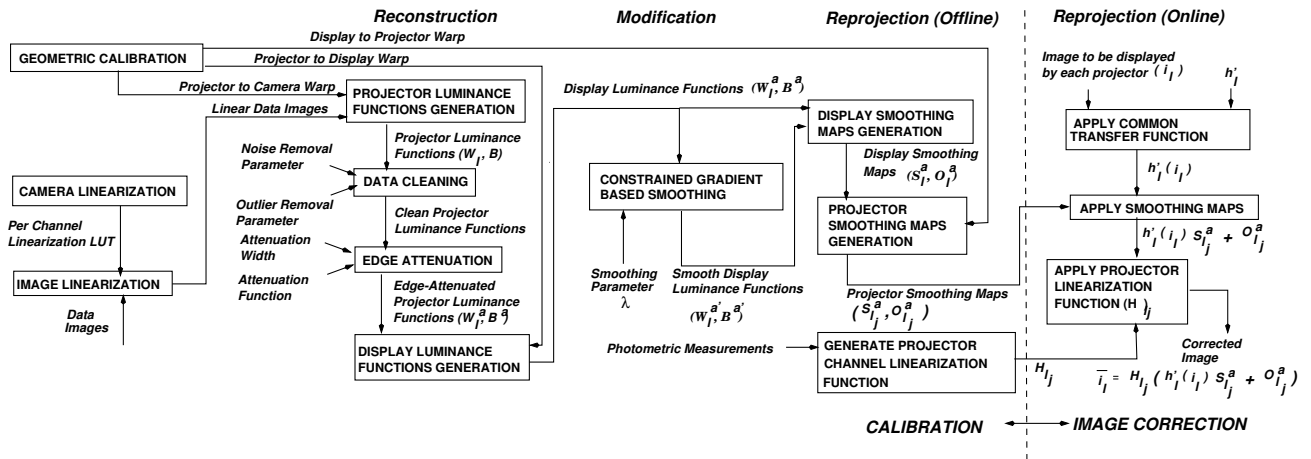


Figure 8.1: System pipeline

The system pipeline is illustrated in Figure 8.1. The reconstruction, modification and part of the reprojection are done off-line. These comprise the *calibration* step. The output of this step is the projector smoothing maps and the channel linearization function. These are then used in the *image correction* step to correct any image projected on the display. This image correction step can be implemented in real-time using commodity graphics hardware. Both the calibration and the real time image correction steps are discussed below.

8.1 Calibration

Let us now see the details of the calibration procedure.

8.1.1 Geometric Calibration

First, we perform a geometric calibration procedure that defines the geometric relationships between the projector pixels (s_j, t_j) , camera pixels (x, y) and the display pixels (u, v) . This geometric calibration procedure uses the static camera to take pictures of some known static patterns put up on the display. By processing these pictures, the geometric calibration procedure defines two warps : $G_{P_j \rightarrow C}(s_j, t_j)$ which maps a pixel (s_j, t_j) of projector P_j to the camera pixel (x, y) , and $G_{C \rightarrow D}(x, y)$ which maps a camera pixel (x, y) to a display pixel (u, v) . The concatenation of these two warps defines $G_{P_j \rightarrow D}(s_j, t_j)$ which maps a projector pixel (s_j, t_j) directly to display pixel (u, v) . These three warps give us the geometric information we need to find the luminance functions of each projector.

Several geometric calibration algorithms have been designed in the past [Yang01, Raskar99b, Raskar99a]. Any geometric calibration algorithm that can define accurately the two warps $G_{P_j \rightarrow C}$ and $G_{C \rightarrow D}$ can be used for our method. For our implementation, we use a geometric calibration procedure that defines two *cubic non-linear* warps $G_{P_j \rightarrow C}$ and $G_{C \rightarrow D}$. These non-linear warps include the radial distortion correction for both the camera and the projectors. This warp can be implemented in real time on traditional graphics pipeline using texture mapping. The details of this algorithm are available in [Hereld02].

8.1.2 Measuring Channel Intensity Response of Camera

First, we reconstruct the non-linear intensity transfer function for each channel of the camera using the algorithm of [Debevec97]. This is then used to linearize per channel response of every camera image. This is shown as the *camera linearization* step in Figure 8.1.

8.1.3 Measuring Channel Transfer Function of Projector

As mentioned in Chapter 4, the projector input channel transfer function does not vary spatially. Hence, we use a narrow field of view photometer to measure the per channel non-linear luminance response at the center of every projector. From this we find the channel linearization function H_{l_j}

for each channel of each projector which is represented by a LUT that would linearize this luminance response. This is used for all coordinates of the projector.

8.1.4 Data Capture for Measuring the Luminance Functions

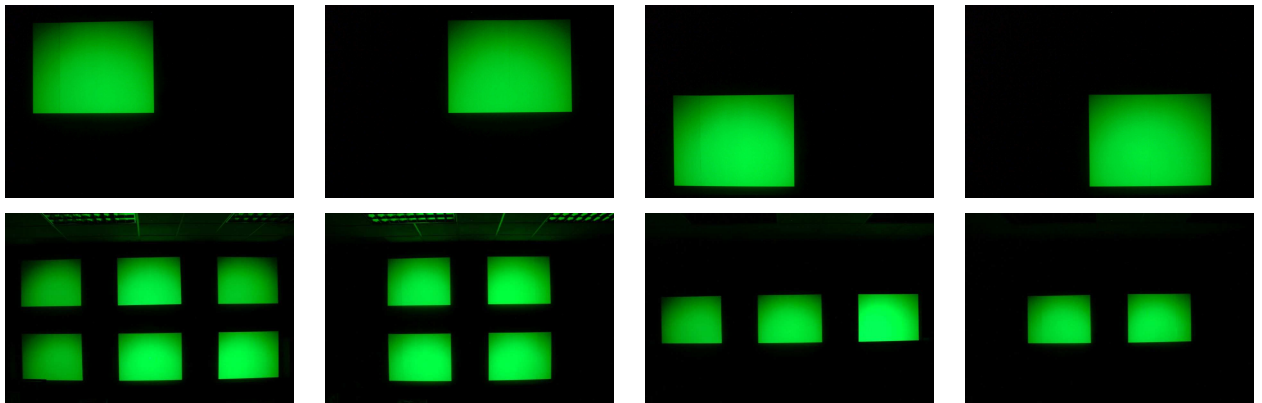


Figure 8.2: To compute the maximum display luminance surface for green channel, we need only four pictures. Top: Pictures taken for a display made of a 2×2 array of 4 projectors. Bottom: The pictures taken for a display made of a 3×5 array of 15 projectors.

To reconstruct the spatially varying luminance functions we use a high resolution digital camera. The camera is set at a point from where the whole display is covered in the camera’s field of view. Then we take a set of images of the multi-projector display for the geometric calibration. Then keeping the camera in the same location, we capture the images to reconstruct the luminance functions. To reduce the number of camera images required to reconstruct the projector luminance functions, measurements from multiple non-overlapping projectors are captured in the same image. Figure 8.2 shows the camera images used to compute W_g for all projectors in two of our display configurations. (Similar images, but at different exposure, are taken to reconstruct B .) Following example from [Debevec97], we relate the images of different exposures by a scale factor. This scale factor is determined by dividing the exposure to which the image is transformed by the exposure at which the image was captured.

8.1.5 Measuring Projector Luminance Functions

Reconstruction

Next we generate the luminance functions for every projector P_j . For this, we first linearize the camera images and then transform the RGB data to luminance using standard RGB to XYZ transformations. Next we apply the geometric warp $G_{P_j \rightarrow C}$ on every projector pixel (s_j, t_j) and transform it to the

camera coordinate space and read the luminance at that transformed pixel from the luminance of the camera images using bilinear interpolation.

Cleaning Up Measured Data

The projector luminance functions thus generated have noise and outliers due to hot spots in the projectors and/or the camera and the nature of the screen material. The noise is removed by a Weiner filter and the outliers, by a median filter. The user-provided kernels for these filters are referred to as the *outlier removal* and the *noise removal* parameters respectively in Figure 8.1. The kernel of the filters is chosen by studying the frequency of the outliers and the natures of the noise in the reconstructed luminance functions.

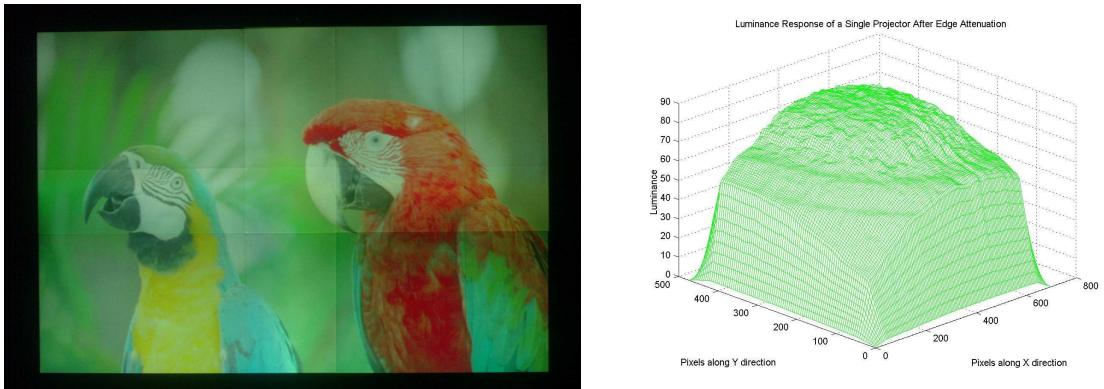


Figure 8.3: Left: Result with no edge attenuation. Right: Edge attenuation of the maximum luminance function of a single projector.

Edge Attenuation

The projector smoothing maps generated in the reprojection stage usually show a sharp discontinuity at the projector boundaries where the transition from overlap to non-overlap region occurs. Geometric misregistration of this edge, even by one pixel, creates an edge artifact as shown in Figure 8.3. To increase the robustness of our method against such misregistrations, we introduce an *edge attenuation* process. By this process, we attenuate the luminance of a few pixels at the boundary of projector luminance functions (W_{l_j} and B_j) using a cosine or a linear function. The edge attenuation is done completely in software and does not involve any new measurement or change in the reconstruction process. So, the attenuation width can be set to any value less than the width of the overlap region.

Note that, we just need an approximate knowledge of the overlap width available and not the exact correspondence between projectors in the overlap region.

Let the edge attenuation function be $F_j(s_j, t_j)$. The edge-attenuated *projector* luminance functions are given by

$$W_{l_j}^a = W_{l_j} \times F_j; B_j^a = B_j \times F_j$$

The edge-attenuated *display* luminance functions \mathcal{W}_l^a and \mathcal{B}^a are generated from $W_{l_j}^a$ and B_j^a using Equation 7.7 and 7.8. These edge-attenuated smooth display luminance functions, $\mathcal{W}_l^{a'}$ and $\mathcal{B}^{a'}$, are generated from \mathcal{W}_l^a and \mathcal{B}^a using the constrained gradient-based luminance smoothing. The pictures in Figure 7.4 include this edge attenuation.

8.1.6 Display Luminance Surface Generation

Once we have the projector luminance functions for every projector P_j , we find the contribution of every projector at (u, v) by the inverse warp of $G_{P_j \rightarrow D}$ denoted by $G_{D \rightarrow P_j}(u, v)$ and add them up.

8.1.7 Smoothing Map Generation

To account for the edge attenuation, the display smoothing maps are generated from the display luminance functions by

$$\mathcal{S}_l^a(u, v) = \frac{\mathcal{W}_l^{a'} - \mathcal{B}^{a'}}{\mathcal{W}_l^a - \mathcal{B}^a}; \mathcal{O}_l^a(u, v) = \frac{\mathcal{B}^{a'} - \mathcal{B}^a}{3(\mathcal{W}_l^a - \mathcal{B}^a)} \quad (8.1)$$

$\mathcal{S}_l^a(u, v)$ is called the *attenuation map* since it is used to scale the input in the reprojection step and conceptually achieves the attenuation of reconstructed luminance function to the smooth luminance function. $\mathcal{O}_l^a(u, v)$ is called the *offset map* since it is added to the scaled input in the reprojection step and is conceptually used to correct for the black offset.

8.1.8 Projector Smoothing Map Generation

Finally, the *projector* smoothing maps should be generated as follows.

$$S_{l_j}^a = \mathcal{S}_l^a(G_j(s_j, t_j))F_j; O_{l_j}^a = \mathcal{O}_l^a(G_j(s_j, t_j))F_j \quad (8.2)$$

Figure 8.4 shows the scaling map thus generated for the whole display and one projector.

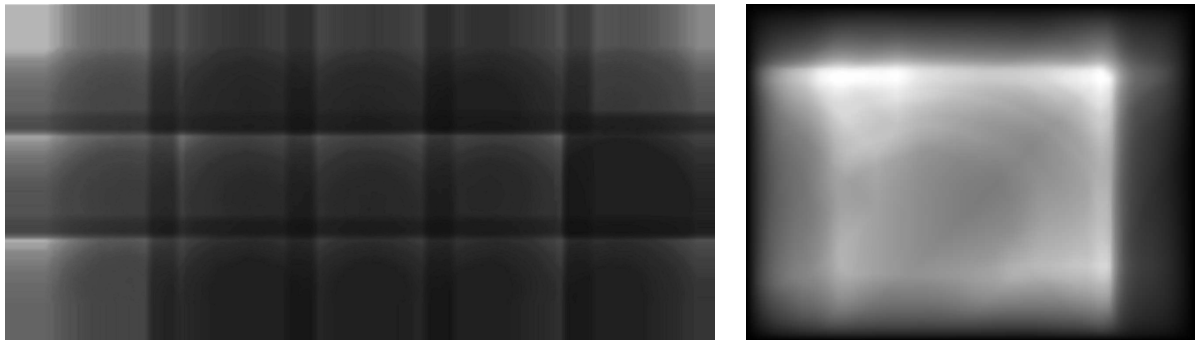


Figure 8.4: Left: Display attenuation map for a 3×5 projector array. Right: The projector attenuation map for one projector.

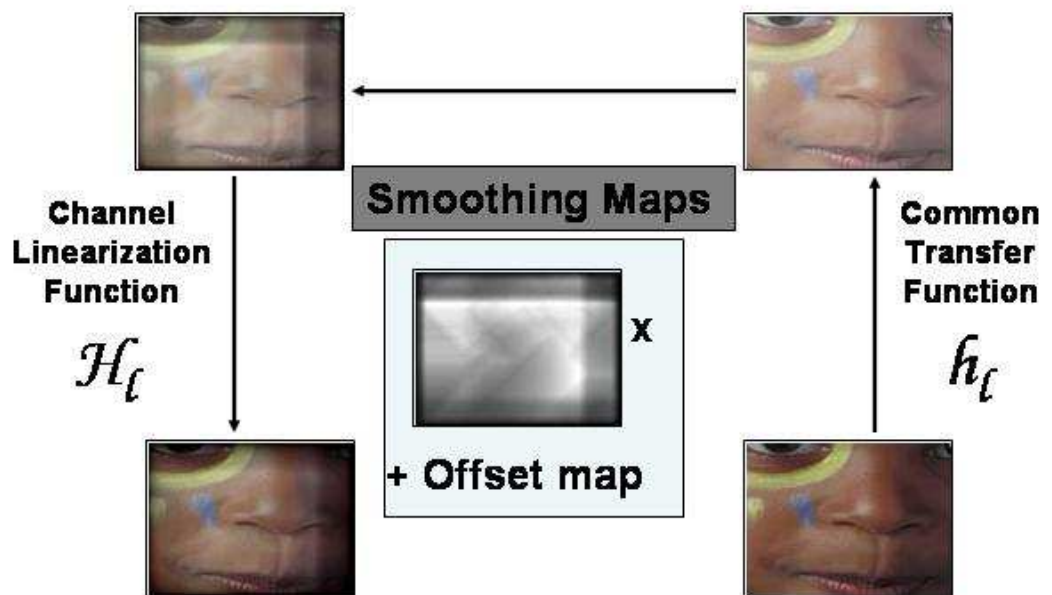


Figure 8.5: Image Correction Pipeline.

8.1.9 Image Correction

The smoothing maps generated by Equation 8.2 in the calibration step is used to correct any image projected on the display using Equation 7.22. In Equation 7.22, we know all the parameters in the right hand side of the equation except $h'_i(i_l)$. This can be any arbitrary monotonic function such that $h'_i(0) = 0$ and $h'_i(1) = 1$. In our implementation we use $h'_i(i_l) = i_l^2$ which produces a pleasing appearance in the test imagery.

Real-time Implementation

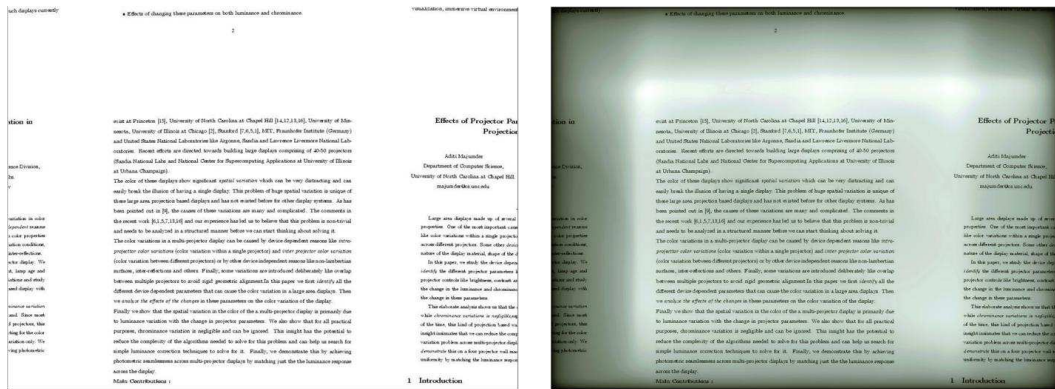


Figure 8.6: Left: Image from a single projector before correction. Right: Image after correction. Note that the boundaries of the corrected image which overlaps with other projectors are darker to compensate for the higher brightness in the overlap region.

We achieve the image correction in real time using *pixels shaders* in commodity graphics hardware to do per pixel color correction. *Multi-texturing* is used for applying h'_i and the smoothing maps. Due to unavailability of 1D look up tables, the channel linearization function H_{l_j} is applied using dependent 2D texture look-ups. Figure 8.6 illustrates the effect of applying this correction to the image from a single projector. Figure 8.5 shows the pipeline of the image correction.

8.2 Results

We have applied our algorithm to display walls of different sizes. Figure 8.7 shows the digital photographs of our results on a 2×3 array of six projectors, 3×5 array of fifteen projectors, and a 2×2 array of four projectors. Figure 8.8 compares the results of our method with one that achieves photometric uniformity.

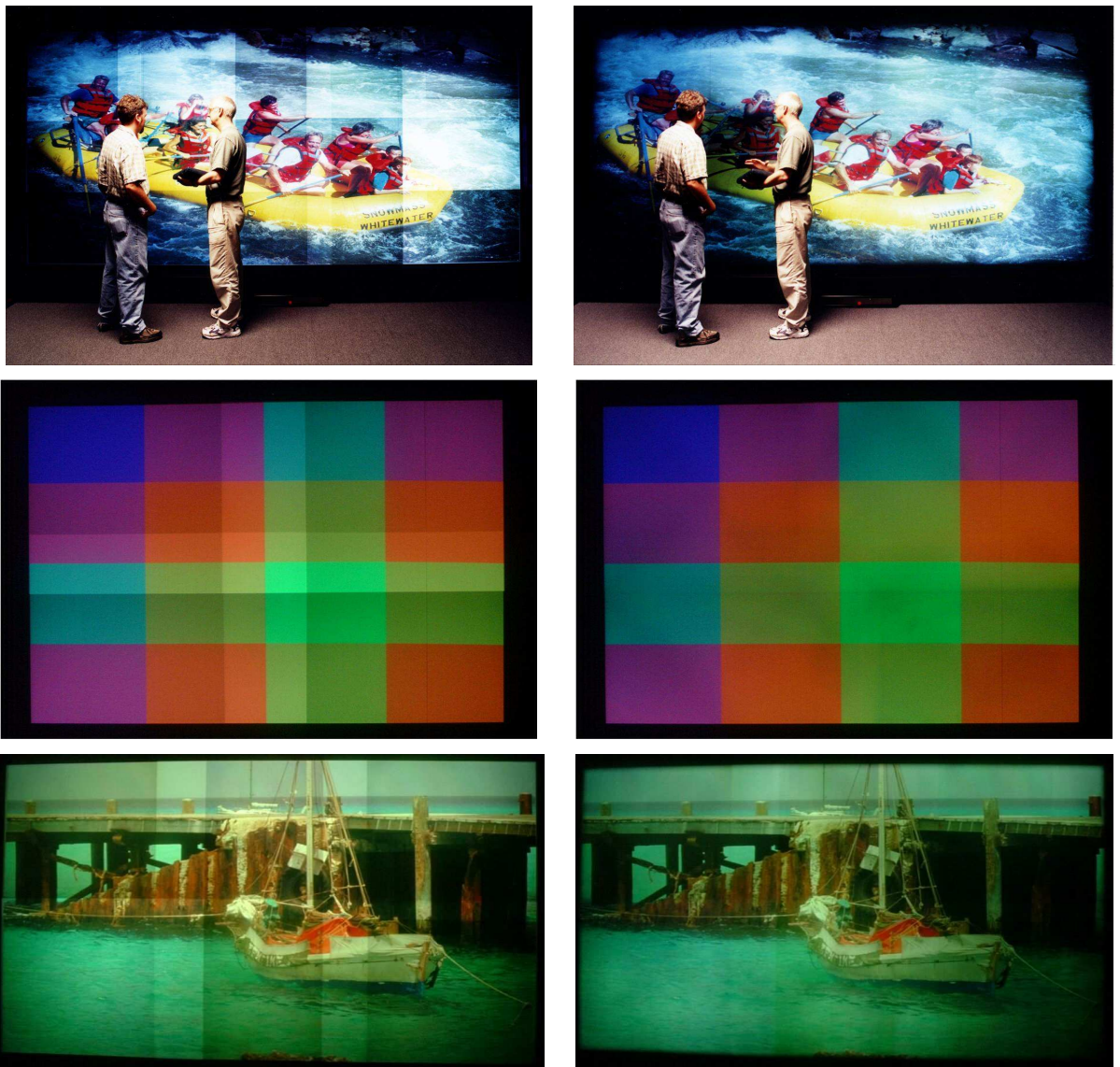


Figure 8.7: Digital photographs of actual displays made of 3×5 , 2×2 and 2×3 array of projectors. Left: Before correction. Right: After constrained gradient based luminance smoothing.



Figure 8.8: Digital photographs of a fifteen projector tiled display. Left: Before any correction. Middle: After photometric uniformity. Right: After constrained gradient based luminance smoothing.

In the printout of this paper or on a small display monitor, since the results are shown as a scaled down image, the threshold for detecting the color non-uniformity is lower than when the same results are projected in the actual 10×6 feet display.

8.3 Smoothing Parameter



Figure 8.9: Digital Photograph of a fifteen projector tiled display. Left: Before any correction. Middle: Results with smoothing parameter of $\lambda = 400$. Right: Results with smoothing parameter of $\lambda = 800$.

Humans can tolerate about 1 – 15% variation in luminance per degree of visual angle [Lloyd02, Chorley81]. Let us denote this threshold with τ . The parameter λ defines the *per pixel* relative luminance variation that a human being can tolerate and can be estimated from the expected perpendicular distance d of the user from the wall and the resolution r of the display in pixels per unit distance.

$$\lambda = \frac{d \times \frac{\pi}{180} \times r}{\tau} \quad (8.3)$$

The camera position used to calibrate the wall may be a safe estimate of the user position and r can be found from the physical measurements of the size of the wall. For example, for our fifteen projector wall of size 10×6 feet and resolution 4500×2000 , the number of pixels per inch is approximately 30. We assume that the user is about 6 feet away from the wall, and then applying the above equation and τ of 10%, we find that w is approximately 400.

With a decrease in the smoothing parameter, the surface becomes less smooth perceptually, but the average dynamic range of the display increases. Figure 8.9 shows an example.

However, one important thing to note here is that the tolerance threshold depends on the image content. For example, when watching a movie with high frequency image content, the tolerance threshold is higher, the highest being 15%. But for a desktop or slide presentation environment, which involves mostly flat colors, the threshold is much lower. Thus, the ideal smoothing parameter not

only depends on the display resolution and the distance of the viewer from the display, but also on the specific image content.

8.4 Scalability

When dealing with very high resolution walls, the limited camera resolution can affect the scalability of our algorithm. We present here a scalable version of our algorithm where we *change only the method for reconstructing the display luminance function*. We reconstruct the luminance surface for parts of the display at a time and then stitch them together to generate the luminance surface for the whole display.

Figure 8.10 illustrates the procedure for a display wall made up of four projectors. First, we place the camera at position A when camera's field of view sees the whole display (four projectors) and run a geometric calibration algorithm. The geometric warps from this process are denoted by G_A .

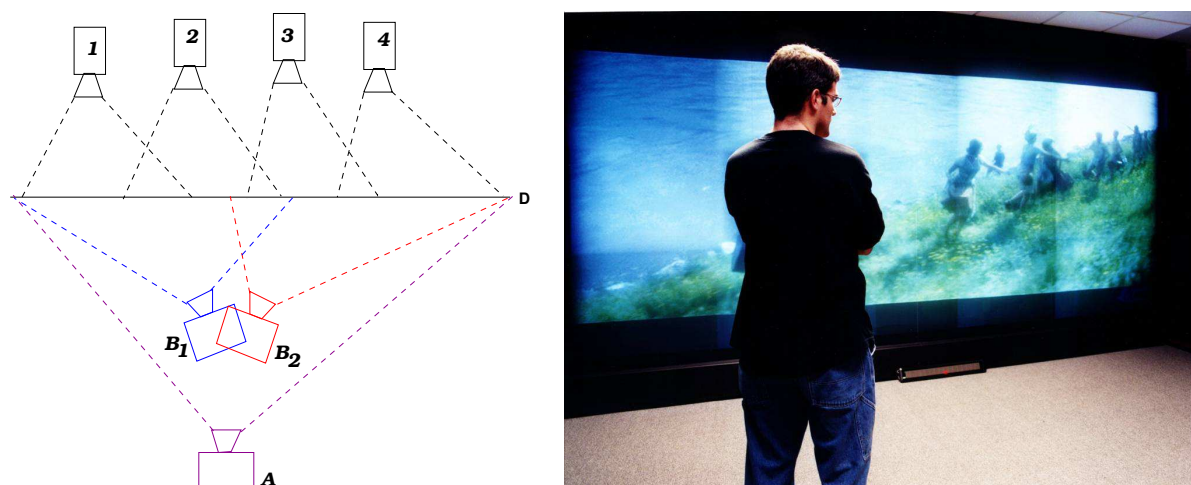


Figure 8.10: Left: The camera and projector set up for our scalable algorithm; Right: Seams visible when the display is viewed from oblique angles due to non-Lambertian characteristics of the display surface.

Next we move the camera to B and/or change the zoom to get higher resolution views of parts of the display. We rotate the camera to see different parts of the display. For example, in Figure 8.10, the camera sees projectors P_1 and P_2 from B_1 and projectors P_3 and P_4 from B_2 . We perform our geometric calibration from the orientations, B_1 and B_2 and let the corresponding geometric warps be G_{B_1} and G_{B_2} respectively.

We also take the pictures for our color correction (similar to Figure 8.2) from B_1 and B_2 . We reconstruct W_l^a for P_1 and P_2 from the pictures taken from B_1 using G_{B_1} and for P_3 and P_4 from the pictures taken from B_2 using G_{B_2} . We stitch these *projector* luminance functions using the common geometric warp G_A to generate the *display* luminance functions. The rest of the process remains exactly the same. Please note that we find the luminance response from location B only. Figure 8.11 illustrates the result.



Figure 8.11: Digital photograph of eight projector tiled display showing the result of our scalable algorithm. The display luminance function for the left and right four projector configurations are reconstructed from two different orientations. The display luminance surface for the eight projectors is stitched from these. Left: Before correction. Right: After correction.

8.5 Other Issues

8.5.1 Black Offset

Typically, B^a is less than 0.4% of W_l^a and has negligible effect on the smoothing maps. We implemented an alternate version of our system assuming a black offset of zero. Except for a slight increase in the dynamic range, the results were very similar to those produced by our implementation without this assumption. We did not see a great improvement in blacks due to large quantization errors near the black region of the inputs. Further, the software edge attenuation, discussed in Section 8.1.5, cannot achieve the required feathering for the blacks. Thus, black images still show faint seams. This can only be alleviated by some physical or optical edge attenuation that can truly feather the light projected for black.

8.5.2 View Dependency

Since the screens of the systems we used to demonstrate our algorithm are non-Lambertian, our correction is accurate from the position of the camera. However, the result looks seamless for an

wide range of viewing angle and distances from the wall. However, the result looks seamless for an wide angle of 120 – 150 degrees and shows some seams when viewed extremely oblique angles as shown in Figure 8.10.

8.5.3 *White Balance*

Our method generates per-pixel attenuation map for each channel. Since each channel may get attenuated differently, the grays may not be retained as grays when transformed by the these attenuation maps. This may lead to faint color blotches in the results. Hence, we use the maps generated for the green channel for all channels. Since the nature of luminance variation is similar across the three channels, the small inaccuracies introduced by this do not show any visible artifacts.

8.5.4 *Dynamic Range*

It is important for the brightness of each projector to be well within the dynamic range of the camera. This can be verified by simple under or over saturation tests of the camera images. In display walls made of many projectors there may be large brightness variation across projectors. In such cases, the camera exposure should be adjusted to accommodate for this variation. This change in exposure should be taken into account by appropriate scaling factors while generating the luminance surface [Debevec97]. Using the same exposure for all projectors leads to contouring artifacts as seen in a few results.

8.5.5 *Accuracy of Geometric Calibration*

Our display had pixels about $2.5mm$ in size. A misalignment of even a couple of pixels in the reconstructed luminance response can cause perceived discontinuities without the edge attenuation. The edge attenuation alleviates the situation and we can tolerate greater errors of about 5 – 6 pixels in the display space.

CHAPTER 9

Evaluation Metrics

In the preceding chapters we have presented an algorithm to achieve photometric seamlessness in multi-projector displays. Our results in the Chapter 8 show that we have achieved seamless displays that produce high quality images. But, we need to quantify how good this display is to compare our method with other existing methods, or even the results of our own method when different performance parameters are used. In this chapter we present such an evaluation metric that can quantify the quality of the photometric seamlessness achieved.

There has been many work in the past on quantifying image quality by designing some perceptual error metric [Lubin95, Daly93, Pattanaik98, Ramasubramanian99, Ferwerda97]. These metrics have been used in the graphics and vision community to compare image quality, especially for image synthesis and compression techniques. Most of these techniques compare images against a golden reference. For example, for compression techniques the golden reference is an uncompressed image against which images compressed using different compression techniques can be compared. For image synthesis, an image generated using some physically-based model like global illumination is used as a golden reference and images generated by other techniques are compared with this golden reference.

The problem we face while using such an algorithm to evaluate the results from our algorithm is the *lack of such a golden reference*. The digital image that we are projecting on the display should be our golden reference. But when we put it on the display (both corrected and uncorrected) and capture a digital image of the projected imagery using a camera, we have already gone through two different color spaces, one of the projectors and the other of the cameras. Thus, it does not make sense to compare the digital photograph of the projected imagery with the original digital image to find the difference. So, I designed a new metric to compare the luminance properties of the display before and after correction.

9.1 Goal

The basic approach of our algorithm has been to achieve perceptually smooth luminance variation while maximizing the mean dynamic range of the display. Note that the uncorrected display has the maximum mean dynamic range. Any correction would only reduce the mean dynamic range of the display. But this uncorrected display is significantly different from the original digital image just because of the difference in appearance caused due to the luminance variation of the display. The other extreme is a display that is photometrically uniform. This is similar in appearance to the original digital image but significantly different than it in dynamic range. The ideal solution lies somewhere in between these two. Further, note that to compare the results, we need to use some sensor to capture the display properties. A digital camera is a general and reasonable sensor to use for this purpose. When comparing the results captured by this sensor with the original digital input, we should find a way to extract reasonable information about the appearance of the display being insensitive to the camera and projector's color spaces.

Thus, following are the requirements of our error metric. First, we should find a way to bring the original digital image and the digital images of the photographs within a common reference frame so that they can be compared. Second, the error metric that we design should capture the optimization nature of the problem. Third, this metric should be able indicate how the dynamic range, brightness and general appearance of the image is affected by the correction. Fourth, it should be able to make reasonable judgments going beyond the different color spaces of the original, projected and the recaptured image. We designed a metric to evaluate the appearance of the images from the uncorrected and corrected displays that satisfies all these requirements.

9.2 Overview

Let the original digital image that we put up on the display be called the *reference image* R . We would like to compare this image with the image projected on the display which has either been left uncorrected or has been corrected using different algorithms.

9.2.1 Capturing Data

For this purpose, we use a digital camera. We run our geometric calibration algorithm with the camera at location A . Then keeping the camera in the same location, we take the images of the display when

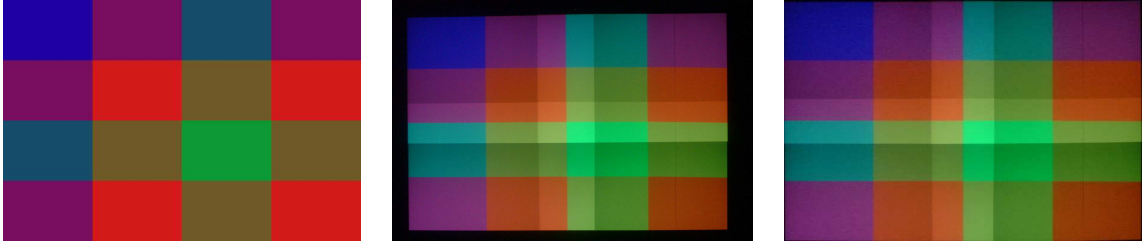


Figure 9.1: *Left: Reference image. Middle: Result image. Right: The recaptured image corresponding to the result image in the middle.*

R is projected on it. This image taken by the camera is called the *result image* and is denoted by O_C . Next we use the geometric transformations to convert this image O_C into the display coordinate space. This is called *recaptured image* and is denoted by O . Note that O and R now have the same resolution and are geometrically comparable pixel by pixel. Figure 9.1 illustrates this.

Note that we may have more than one recaptured image if we are trying to compare different algorithms. Thus, for generality we denote each of these by O_i . Note that all these result images for the corresponding recaptured images should be captured with the same camera settings to be comparable. However, note that the R and the O_i s are still in different color space and hence still not directly comparable photometrically. Figure 9.2 shows a reference image and more than one recaptured images when we are trying to compare different algorithms. In this particular example, we have the reference image, the recaptured image for uncorrected display (O_1) and the recaptured image for the display with photometric seamlessness (O_2) achieved by the algorithm in Chapter 7 using a smoothing parameter of 400.

9.2.2 Photometric Comparability

The next step is to make these reference and the recaptured images comparable photometrically. For this, we first find the mean value of all the pixels for R and O_i . This gives the overall *brightness* of the images and is denoted by B_R and B_{O_i} respectively. This mean can give us a way to compare the overall brightness of the different geometric images.

Next, we find the vector deviation of each pixel value from the corresponding mean B of the image. The images thus generated from R and O_i are called R^D and O_i^D . Next, for each channel, we compress the range of O_i^D and R^D within the maximum and minimum of all values of O_i^D s and R^D generating R^M and O_i^M respectively. This translates the range of each image around the same mean and compresses the range in the same reference space thus helping us to compare similar quantities

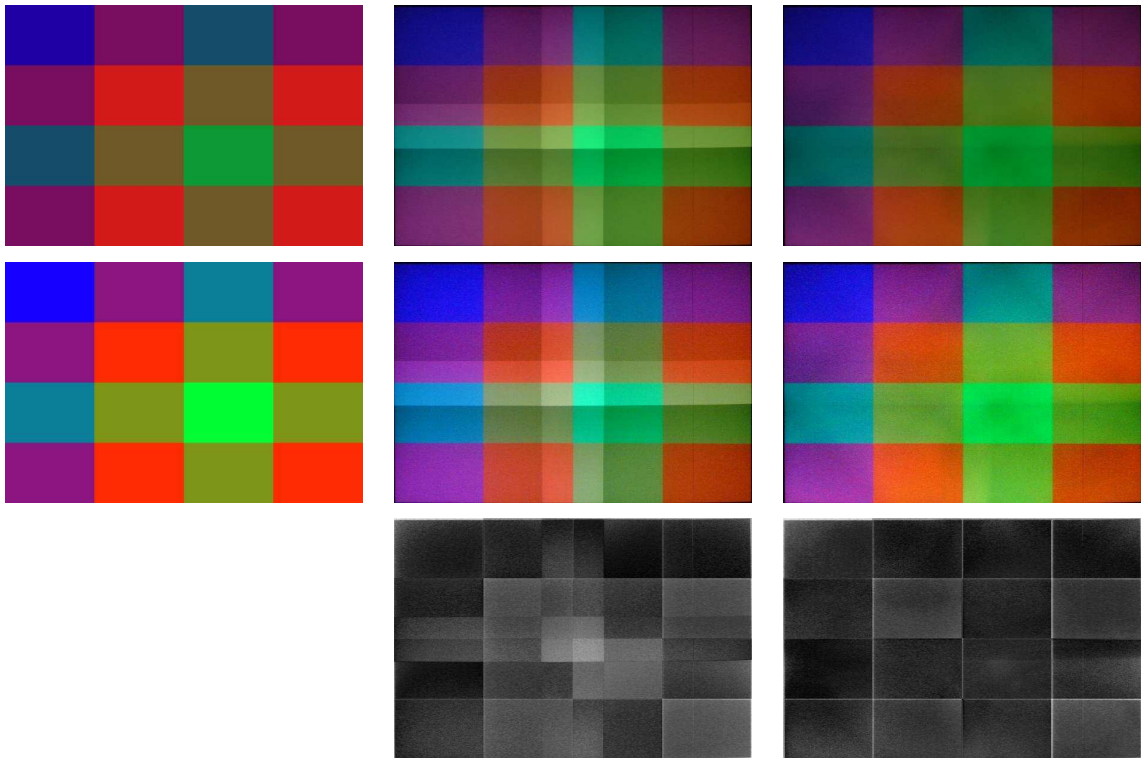


Figure 9.2: *Top Row: Left: Reference image. Middle: Recaptured image for uncorrected display. Right: Recaptured image with a photometrically seamlessness display. Middle Row: Left: Comparable reference image. Middle: Comparable recaptured image for uncorrected display. Right: Comparable recaptured image for photometrically seamless display. Bottom Row: Middle: Error of the comparable recaptured image for uncorrected display from the comparable reference image. Right: Error of the comparable recaptured image for photometrically seamless display from the comparable reference image.*

even if the reference image R does not have the same overall brightness of the recaptured images O_i . This kind of change can be caused due to changes in the exposure of the camera. R_M is called the *comparable reference image* and O_i^M s are called the *comparable recaptured images*. The second row of Figure 9.2 illustrates these for the reference and recaptured images in the first row of the same figure. The difference between the maximum and minimum for each channel of images R^M and O_i^M define their respective *dynamic range* vector DR .

9.2.3 Error Images Generation

Next we generate the error image E_i representing the error between comparable recaptured images O_i^M and comparable reference image R_M by finding the normalized pixel-wise Euclidian distance between R^M and O_i^M . This is illustrated in Figure 9.2. The sum and mean of E_i gives the *total* and the *mean* error of O_i from R denoted by TE_i and ME_i respectively.

9.2.4 Error Metric

The brightness (B), dynamic range (DR) and error images (E) comprise our error metric. Note that there may not be any physical O_i that can exactly resemble R . The method only brings R and O_i s in a similar reference frame in terms of per channel intensity values but can not do so for more physical parameters like color gamut or luminance. Hence, the evaluation lies in the fact whether the errors are reduced by applying a correction method rather than errors disappearing altogether.

9.2.5 Evaluation Results

Figure 9.3 shows the reference image R and the recaptured images that we want to compare. In this case, they are images taken before correcting O_1 , after matching the display response at every pixel O_2 and then after smoothing it with $w = 400$ O_3 . Figure 9.3 also shows the error images E_1 , E_2 and E_3 . Table 9.2.5 shows the values of the various metric. Note that, the brightness and dynamic range of the results of smoothing is higher than those of matching. The total and mean error and the percentage of extra edge pixels are also reduced more with smoothing as expected.

Figure 9.4 and Table 9.2.5 show the same for a flat white reference image. Here you notice how the camera color gamut can change the color appearance of the images.

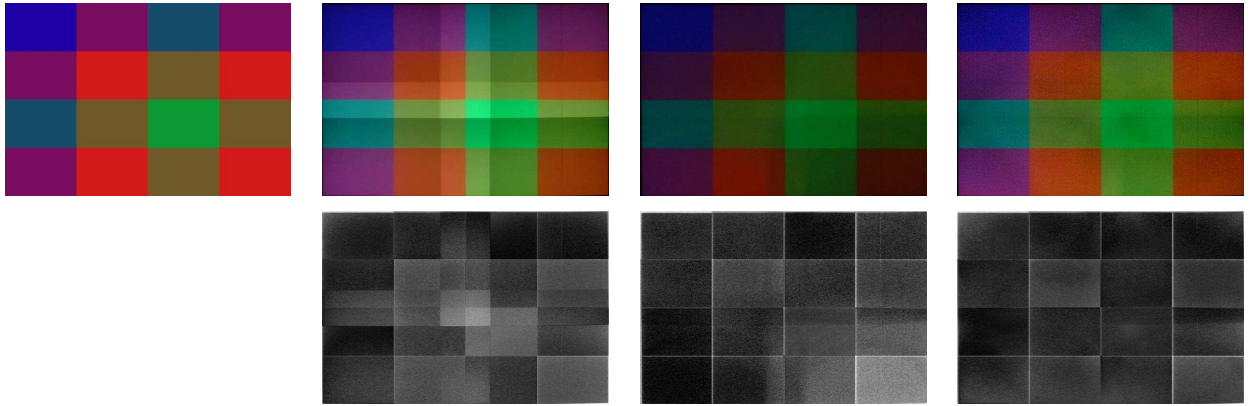


Figure 9.3: Top Row from left: (1) The reference image R . (2) Recaptured image before correction (O_1) (3) Recaptured image after photometric uniformity (O_2). (4) Recaptured image after achieving photometric seamlessness with smoothing parameter 400 (O_3). Bottom Row from left: (2) Error image for uncorrected display (E_1). (3) Error image for photometric uniformity (E_2). (4) Error image for photometric seamlessness with smoothing parameter 200. (E_3).

Img	Brightness _{<i>i</i>}	Dynamic Range _{<i>i</i>}	Total Error _{<i>i</i>}	Mean Error _{<i>i</i>}
R	(115, 51, 66)	(197, 154, 136)	NA	NA
O_1	(88, 83, 67)	(209, 240, 159)	60962	0.25
O_2	(41, 39, 30)	(121, 137, 111)	56223	0.23
O_3	(75, 67, 51)	(174, 168, 155)	45766	0.18

Table 9.1: Results for the images shown in Figure 9.3

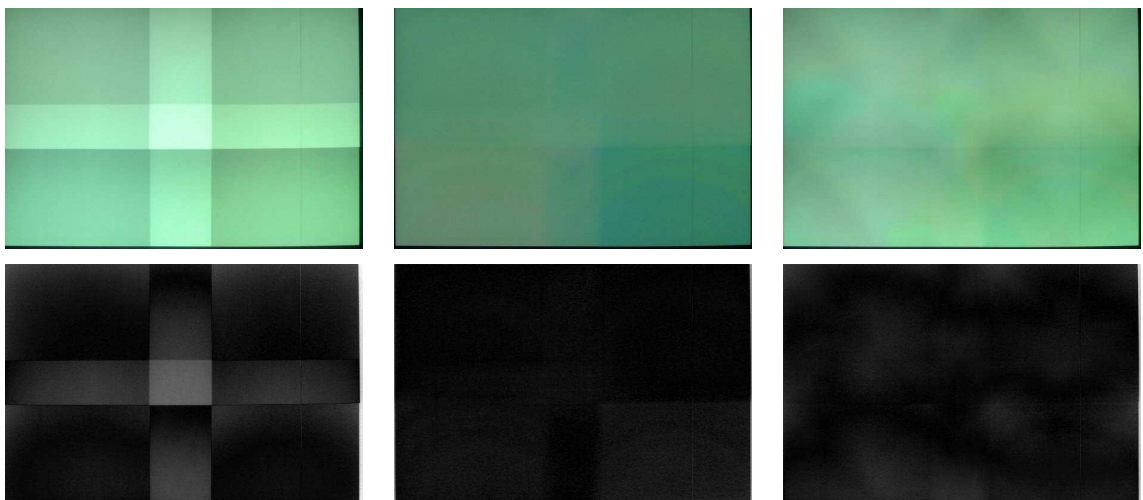


Figure 9.4: Top Row from Left: (1) Recaptured image with uncorrected display (O_1) (2) Recaptured image after photometric uniformity (O_2). (3) Recaptured image after photometric seamlessness with smoothing parameter 400 (O_3). Bottom Row from left: (4) E_1 . (5) E_2 . (6) E_3 .

Img	Brightness _i	Dynamic Range _i	Total Error _i	Mean Error _i
R	(255, 255, 255)	(0, 0, 0)	NA	NA
O_1	(135, 204, 160)	(60, 90, 70)	30049	0.12
O_2	(76, 135, 105)	(30, 20, 20)	14214	0.06
O_3	(117, 182, 137)	(40, 60, 50)	13887	0.05

Table 9.2: Results for the images shown in Figure 9.4

Img	Brightness _i	Dynamic Range _i	Total Error _i	Mean Error _i
R	(125, 115, 81)	(236, 223, 231)	NA	NA
O_1	(106, 117, 66)	(248, 227, 241)	251577	0.26
O_2	(68, 92, 46)	(206, 227, 201)	160942	0.16
O_3	(63, 85, 42)	(195, 227, 172)	146448	0.14

Table 9.3: Results for the images shown in Figure 9.5

Table 9.2.5 shows the results for images in Figure 9.5 where O_1 is the image before correction, O_2 is the image after smoothing with parameter 400 and O_3 is the image after smoothing with parameter 800. The corresponding recaptured and error images are shown in Figure 9.5.

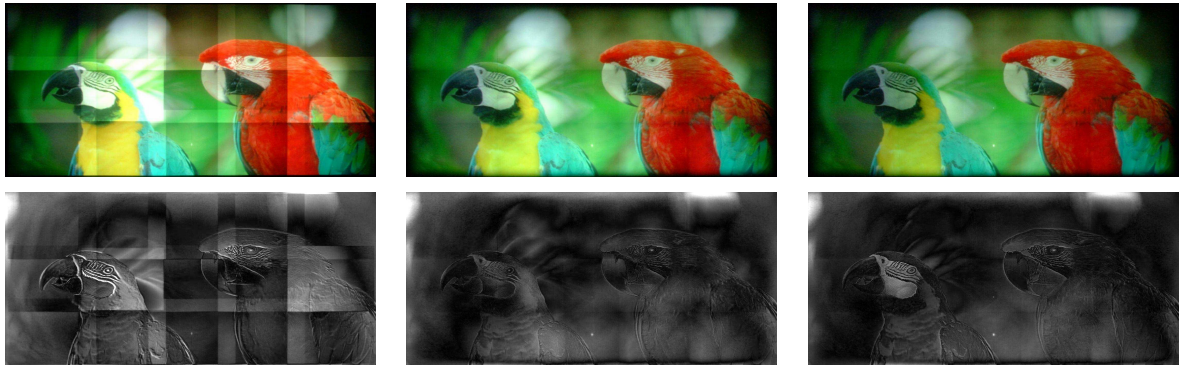


Figure 9.5: Top Row from Left: (1) Recaptured image with uncorrected display (O_1) (2) Recaptured image after photometric seamlessness with smoothing parameter 400 (O_2). (3) Recaptured image after photometric seamlessness with smoothing parameter 800 (O_3). Bottom Row from left: (4) E_1 . (5) E_2 . (6) E_3 .

From the above results, it is clear that the error TE and ME is high with an uncorrected display and becomes smaller with the increase in smoothing parameter. In this phase, the error is due to the presence of sharp luminance variation which leads to a change in appearance. At some

point the error reaches a minimum, after which it increases with increase in smoothing parameter. This is the reason that the error is more when the smoothing parameter is infinity (photometrically uniform display) than when it is 400 or 800. In this phase, the error is due to the compression in the dynamic range which also leads to a change in appearance. Thus, in all cases the error signifies change in photometric appearance, but for different reasons. In Section 8.3, it was mentioned that the ideal smoothing parameter depends on the image content. The smoothing parameter for which the minimum error is achieved signifies the ideal smoothing parameter for the specific image. This is illustrated in Figure 9.6.

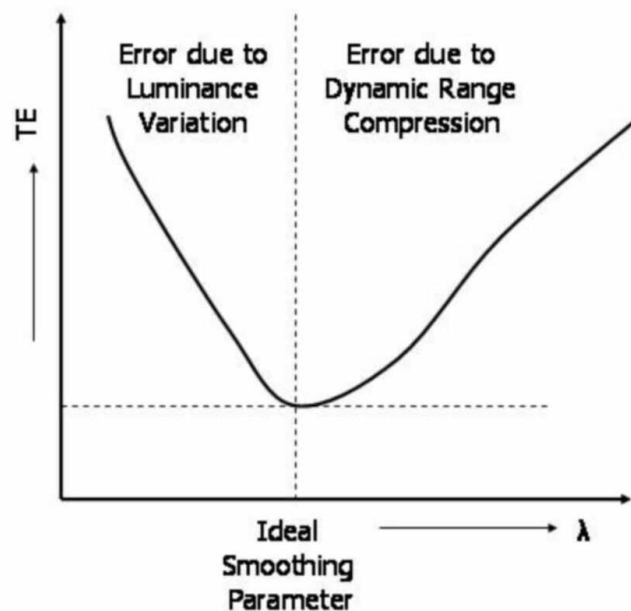


Figure 9.6: *Error vs Smoothing Parameter.*

CHAPTER 10

Conclusion

This dissertation makes an effort to study the color variation in multi-projector displays in a comprehensive fashion. Several empirical studies were conducted with many contemporary off-the-shelf projector devices. It is evident from the several studies in Chapter 4 that some part of the problem can be alleviated by designing projectors that would have lower black offsets, higher contrasts and lesser spatial variations in color. However, [Stupp99] shows that such improvements would make projectors much more expensive thus making such tiled displays cost prohibitive defeating the very purpose of the making such displays common place.

Instead, to make such displays easy to realize, my work introduces a general comprehensive framework of the *emineoptic function* that models the color projected on planar multi-projector displays and can act as a fundamental guide to study *color variation issues* for such displays. The general formal definition of color seamlessness can help define different kinds of goals based on application requirement, user ability and display property. These two together can be used to design novel algorithms. Last but not the least, I demonstrate how to optimize the emineoptic function to design a practical, working system that achieves seamless high quality multi-projector displays at interactive rates.

We believe that our work presents the first fundamental tool required to address the problem of color variation in multi-projector displays in a structured fashion. However, there are many specific issues that can be identified within this framework and needs to be solved. For example, we need to design practical algorithms for displays varying in chrominance also. We need to address the issue of non-Lambertian surfaces. In many applications, we need to have a system that continuously adjusts its photometric correction while in use to successively improve the response and automatically adapt to system changes (e.g. small geometric changes or changes in lamp characteristics due to aging). Last but not the least, several features and improvements in the projectors can be made to

realize such displays easily and flexibly. First, it is desirable to have standard digital computer and network interfaces in the projectors to easily interface them with the driving computers. Second, embedded systems accessible by internal and external software applications should be provided in the projectors that can be used to achieve different kinds of geometric and photometric corrections, tile reconfigurations and other feedback corrections interactively. Such advanced projectors along with more advanced methods designed from such models as the emineoptic function would make highly flexible perceptually seamless tiled displays commonplace in the near future.

APPENDIX A

Color and Measurement

A.1 Color

Color is the perception created in a sensor by a spectrum of light S . The spectrum S is a function of wavelength, λ . $S(\lambda)$ gives the amount of light of wavelength λ present in the spectrum. As humans, the sensor we are interested in is the human eye.

Monochromatic color ideally refers to light of a single wavelength. This is very difficult to achieve physically. It is known that the color sensations reported by an observer with normal color vision vary as a function of wavelength of the light stimulus. This holds true for any wavelength in the range of $400 - 650nm$. The sensations reported by the observers exposed to the various wavelengths are known as *hues*. In 1976, Murch and Ball performed an experiment. Subjects were asked to identify the colors of light made of very narrow wavelength band ($10nm$), covering the whole visual spectrum. The observers were asked to characterize each stimulus with four numbers corresponding to the amount of blue, green, yellow and red perceived to be present in that particular target. The results of the study showed that the human perception is insensitive to wavelengths of less than $400nm$ and above $650nm$. So $400 - 650nm$ is called the *visual spectrum* of light. In $450 - 480nm$, the predominant sensation was that of blue. Green has a fairly broad band from $500 - 550nm$. Yellow was concentrated in a narrow band of $570 - 590nm$. Wavelengths above $610nm$ were characterized as red. Another important observation was, that most of the colors were characterized with more than two categories. For example a $500nm$ stimulus was given an average rating of 6.3 green, 2.2 blue, 0.8 yellow and 0.1 red. The best or purest colors - defined as the maximum value estimated for one color category and minimum value for the other three categories - indicated pure blue at about $470nm$, pure green at about $505nm$ and pure red at about $575nm$. This is illustrated in Figure A.1.



Figure A.1: The color spectrum of light for different wavelength

Achromatic color can occur only when the amount of light emitted or reflected by an object does not vary as a function of the wavelength. In other words, equal amount of all wavelengths are present in the spectrum of this light.

Objects in the visual environment that reflect or emit distributions of wavelength in unequal amounts are said to be chromatic. That means the spectrum of a *chromatic color* has different amounts of different wavelengths of light.

A color has two attributes associated with it, namely *luminance* and *chrominance*. Chrominance is has two components, *hue* and *saturation*.

1. **Luminance:** This is the amount of light/energy in the color and is measured by cd/m^2 . This has a direct relationship with the perceived brightness of a color.

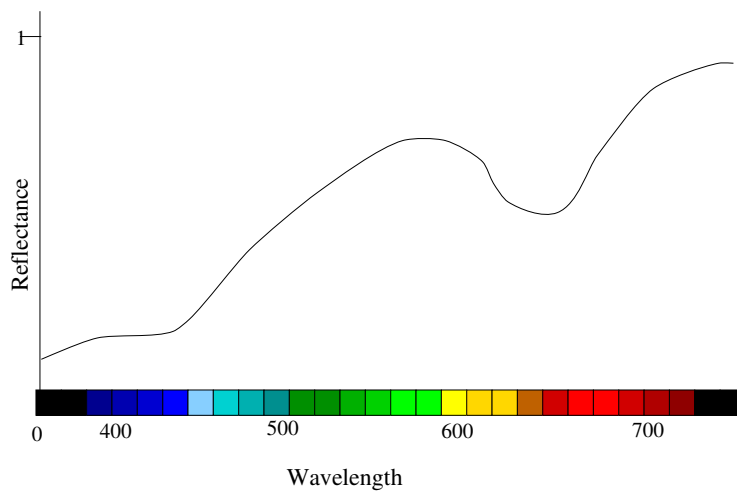


Figure A.2: Spectrum of a red color

2. **Hue:** The hue is decided by the relative amounts of the different wavelengths present in a color. For example, a spectrum as in Figure A.2 would have a red hue since it has more of the red wavelengths than the others.
3. **Saturation:** A pure monochromatic light is seldom encountered in the real world. However, if a very narrow band of wavelength is taken, an observer will be able to identify a dominant hue.

As the band is increased, this dominant hue remains the same, but, it becomes less distinct or clear. It is said that the *hue is less saturated*.

Thus, saturation depends upon the relative dominance of pure hue in a color sample.

- (a) Saturation decreases if the band of wavelengths in a color is increased.
- (b) It also decreases if the amount of neutral color added to the pure hue is increased

A.2 Measuring Color

In order deal with color and understand it, we next see how do we measure color. The techniques of measuring color comprise the science of *colorimetry*.

A.2.1 Light Sources

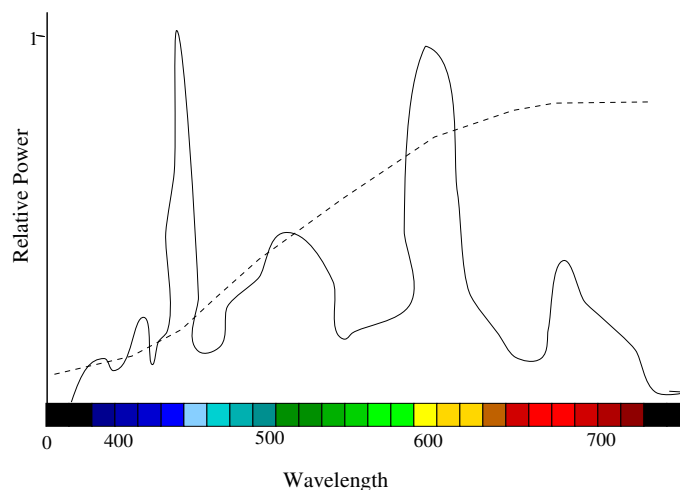


Figure A.3: Comparison of the relative power distributions for spectral power distribution of a fluorescent (solid line) and a tungsten (dotted line) light sources

The *spectral power distribution of a source* is the power of its electro-magnetic radiation as a function of wavelength. Spectral power distribution can vary greatly for different sources of light as shown in Figure A.3. However note that the in the figure the power values are expressed in terms of relative power, not absolute. Such expression is sufficient for most purposes.

Measuring the color characteristics of a light source means to measure this spectral power distribution of the light source.

A.2.2 Objects

When light reaches an object, some of it gets absorbed, and the rest is transmitted and reflected. The amount of light that is reflected and transmitted generally varies at different wavelengths. This variation is described in terms of *spectral reflectance* or *spectral transmittance* properties. *Spectral reflectance(transmittance) of an object* describe the fraction of the incident power reflected (transmitted) by the object, as a function of the wavelength. For example, the spectrum shown in Figure A.2 is the spectral reflectance of a red Cortland apple.

A.2.3 Color Stimuli

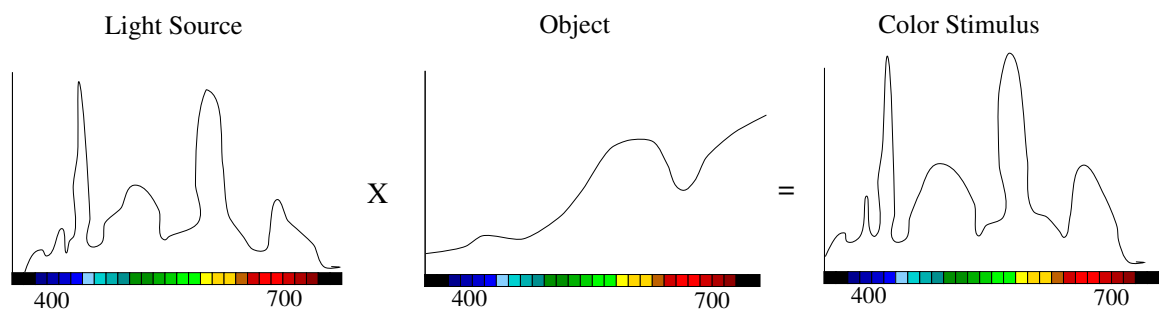


Figure A.4: Calculation of the spectral power distribution of a Cortland apple illuminated with fluorescent light

The *spectral power distribution of a color stimulus* is the product of the spectral power distribution of the light source and the spectral reflectance distribution of the object. The color stimulus is the result of the light that has been reflected from or transmitted through various objects. In Figure A.4 we show the color stimulus resulting by illuminating a Cortland apple with a fluorescent light.

The important thing to note here is that the color of any object is not *invariant*, nor is it solely dependent on the reflectance properties of the object. An object may be made to look of color by changing the light source with which it is illuminated.

A.2.4 Human Color Vision

Human color vision derives from the response of three photo-receptors contained in the retina of the eye, called ρ , γ and β . Each of these photo-receptors responds differently to the varying wavelengths of light. The approximate *spectral sensitivities* of these photo-receptors, or, in other words, their relative sensitivity to light as the function of its wavelength is shown in Figure A.5.

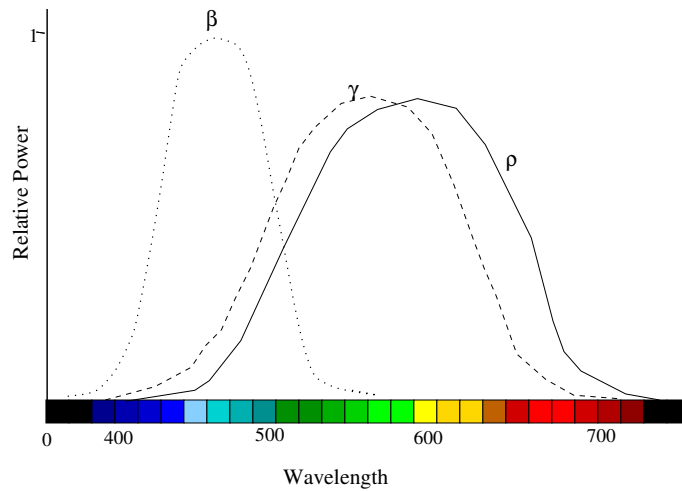


Figure A.5: Estimated spectral sensitivities of ρ , γ and β photo-receptors of the eye

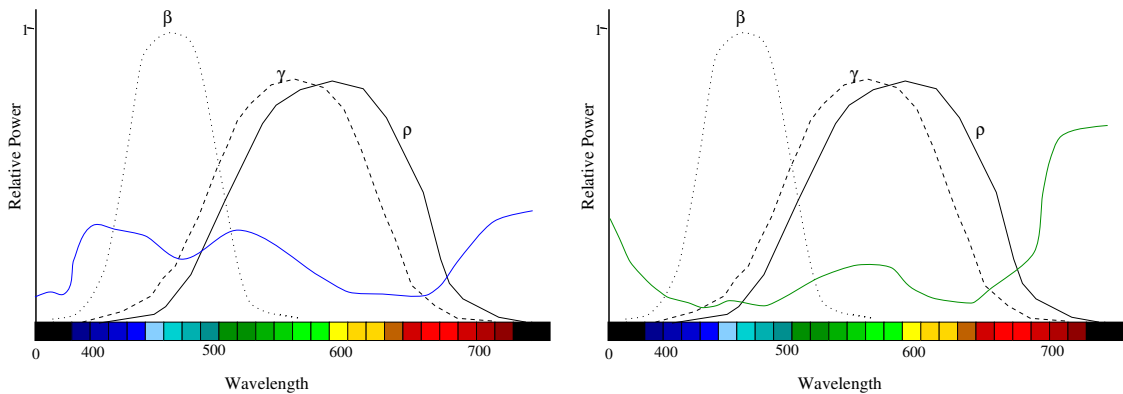


Figure A.6: Left: Color stimuli from ageratum flower appearing blue to the human eye. Right: Color stimuli from a particular fabric sample looking green to the human eye.

Note that human eye is insensitive to light of wavelength greater than $650nm$ and less than $400nm$. This shows that even though the color stimuli of an object suggest one color, the human perception may perceive a completely different color, based on the sensitivity of the photo-receptors in the retina of the eye.

For example, Figure A.6 shows the spectrum of the color stimuli from a flower ageratum. From the spectrum it appears that the color should look red, but it looks blue to the human eye. This is because the human eye is more sensitive to the blue component than the red component in this stimulus. Similarly, the stimuli produced by a fabric sample as shown in Figure A.6 seems green to the human observer though the color stimuli seems to indicate otherwise.

Because of the trichromatic nature of the human vision, it is very possible that two color stimuli, having different spectral power distribution will appear identical to the human eye. This is called

metamerism and two such stimuli are called *metameric pair*. In fact, metamerism is what makes color encoding possible. It is because of metamerism that there is no need to reproduce the exact spectrum of a stimuli, rather it is sufficient to produce a stimulus that is a *visual equivalent* of the original one. Note that, metamerism involves matching visual appearances of two *color stimuli*, and not two *objects*. Hence, two different objects with different reflectance properties can form a *metameric pair*, under some special lighting conditions.

A.2.5 Color Mixtures

Having considered the visual appearance of both achromatic and chromatic colors, now we turn towards production of colors.

Subtractive Mixture of Colors

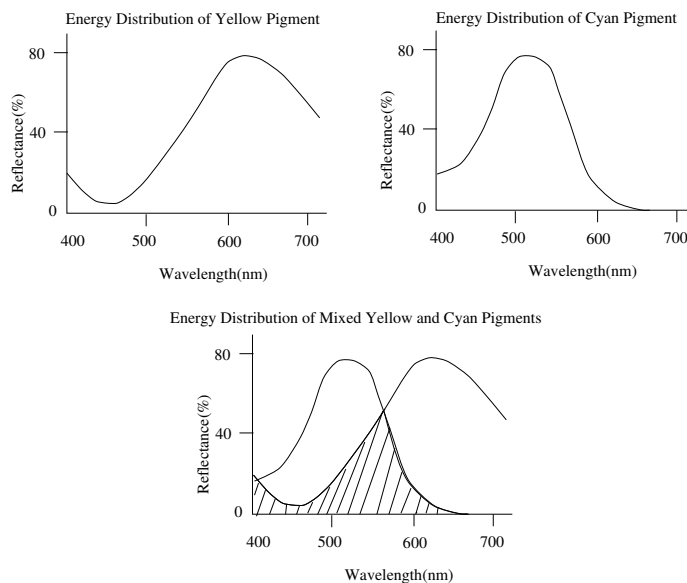


Figure A.7: Subtractive Color Mixture

The color of a surface depends on the capacity of the surface to reflect some wavelengths and absorb others. When a surface is painted with a pigment or dye, a new reflectance characteristic is developed based on the capacity of the pigment or dye to reflect and absorb the different wavelengths of light. Consider a surface painted with *yellow* pigment which reflects wavelengths 570 – 580nm and another surface painted with *cyan* pigment which reflects 440 – 540nm. If we mix both the pigments the resulting color will be *green*. This is because the yellow pigment absorbs the shorter wavelengths

below 500nm and some of the middle band wavelength from $500 - 550\text{nm}$. The cyan pigment absorbs all of the longer wavelengths 560nm and above. The energy distribution of all these are shown in Figure A.7. Thus the yellow absorbs the wavelengths evoking the sensation of blue while the cyan absorbs the wavelengths evoking the sensation of yellow. Hence, what is left behind after this is a sensation of green. This is called *subtractive color mixtures* since bands of wavelengths are subtracted or cancelled by the combination of *light absorbing materials*. The yellow, cyan and magenta is termed as the color primaries of the subtractive color mixtures, because these are the minimal number of pigments required to produce all other colors.

Additive Mixture of Colors

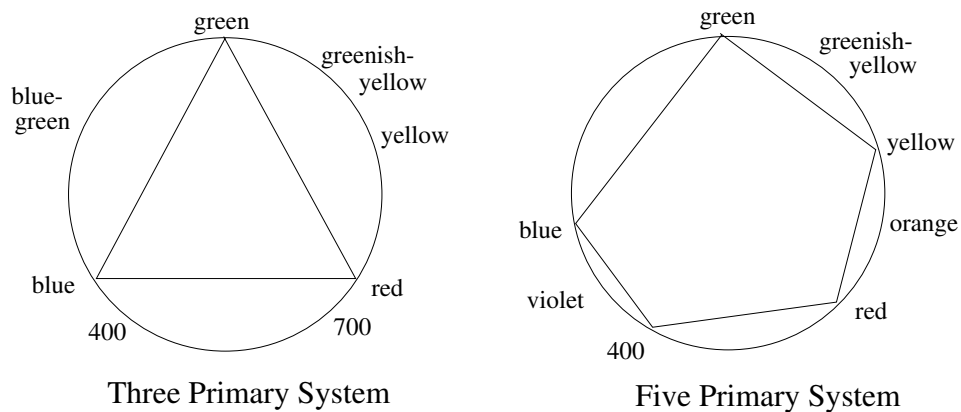


Figure A.8: Additive Color Mixture

Colors can be mixed in another fashion in which bands of wavelengths are added to each other. This is called *additive mixture of colors*. This is also the means by which color is produced in the color display. The surface of a color display is made up of hundreds of tiny dots of phosphor. Phosphors are compounds that emit light when bombarded with electrons and the amount of light given off depends on the strength of the electron beam. The phosphors on the screen are in groups of three, with one phosphor emitting longer wavelengths (red), one emitting the middle wavelengths (green) and one emitting the shorter wavelength (blue). All the three phosphors together produce a very broad band containing all of the visible wavelengths. Varying the intensity levels of the phosphors produce the different levels of lightness. Thus *red*, *green* and *blue* are called the primaries for the additive mixture of colors.

In Figure A.8, the spectrum of monochromatic colors is denoted by the outer circle. The primary colors are marked on that. Blue, Green and red are shown on this spectrum. The interior of the circle

denotes the color that will be formed by mixing two or more monochromatic light. The center of the circle denotes the white. Let us denote this point by O and the color it represents by W . Let us take a point P on the circumference of the circle denote the monochromatic color C . The line that joins O and P denotes the color C with different levels of saturation. With the three primaries, one can denote all the colors within the inner triangle. As is evident, these colors are unsaturated form of some monochromatic color. As is evident from the picture of three primary system in Figure A.8, we cannot produce any of the monochromatic colors (with the exception of the three primary colors) at high saturation level with only these three primaries. However, we can produce some unsaturated form of the monochromatic color. So people have tried with four or five primary colors as shown in Figure A.8. But experiments showed that the improvement in the color did not offset the increase in expenses and hence people generally use red, green and blue as primaries.

A.2.6 Colorimetry

CIE Standard

In 1931, a special committee of Commission Internationale de Eclairage (CIE) met to develop three standard primaries R_s , G_s and B_s . A major goal was to provide a numerical specification of additive color, to define a set of primaries, such that different amount of the trio produce the different colors in the visual spectrum. R_s , G_s and B_s are *imaginary* primaries devised by Maxwell, which encompassed the whole visual spectrum. The amount of these primaries required to reproduce all of the monochromatic light can be represented as a set of *color matching functions*, denoted by $\bar{x}(\lambda)$, $\bar{y}(\lambda)$ and $\bar{z}(\lambda)$ respectively (Figure A.9). Notice that they do not have any physical equivalence, and are not the spectral distributions of R_s , G_s and B_s , they are merely the auxiliary functions of how these three primaries should be mixed together to generate the metamer of the monochromatic colors.

CIE Tristimulus Values

It turns out that these three are the CIE standard color primaries model the response of the three photo-receptors in the human eye and is often referred as *Standard CIE Observer*. The *CIE tristimulus values* X , Y and Z , $X, Y, Z < 1.0$ are the amounts of R_s , G_s and B_s , required to generate a particular

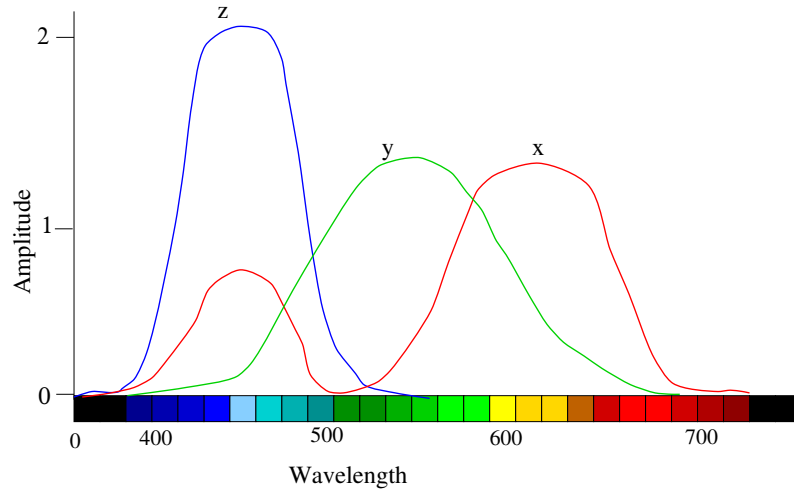


Figure A.9: A set of color matching functions adopted by the CIE to define a Standard Colorimetric Observer

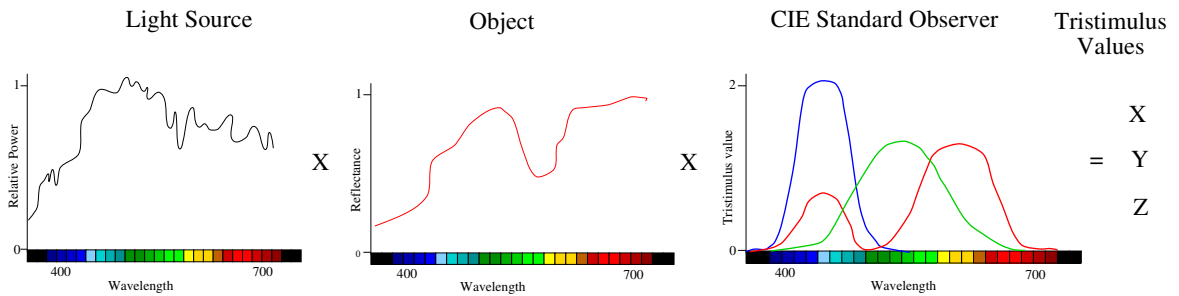


Figure A.10: Calculation of CIE tristimulus values

color C and is defined as follows. Let $S(\lambda)$ define the spectral power distribution of the light source. Let $R(\lambda)$ define the spectral reflectance distribution of the object. Then

$$X = k \sum_{\lambda=380}^{780} S(\lambda)R(\lambda)\bar{x}(\lambda)$$

$$Y = k \sum_{\lambda=380}^{780} S(\lambda)R(\lambda)\bar{y}(\lambda)$$

$$Z = k \sum_{\lambda=380}^{780} S(\lambda)R(\lambda)\bar{z}(\lambda)$$

and k is a normalizing factor. This is illustrated in Figure A.10.

A perfect white is an object that has a reflectance equal to unity throughout the visible spectrum. And also, it should be *isotropic*, i.e. it should reflect light in all directions uniformly. k can be chosen in two ways. It can be chosen such that $Y = 100$ when the object is a *perfect white*. Then k is called *percent factor*. If k is chosen such that Y value of a perfect white object is 1.00, it is called *factor values*.

A *colorimeter* is an instrument that can provide direct measurement of the CIE XYZ tristimulus values of a color stimuli. Y corresponds to *luminance* which is the measurement of the brightness. If X and Z are equal, stimuli with higher Y will look brighter. However, note that Y is not the luminance (as defined in Section A.1) itself.

A.2.7 Chromaticity Diagram

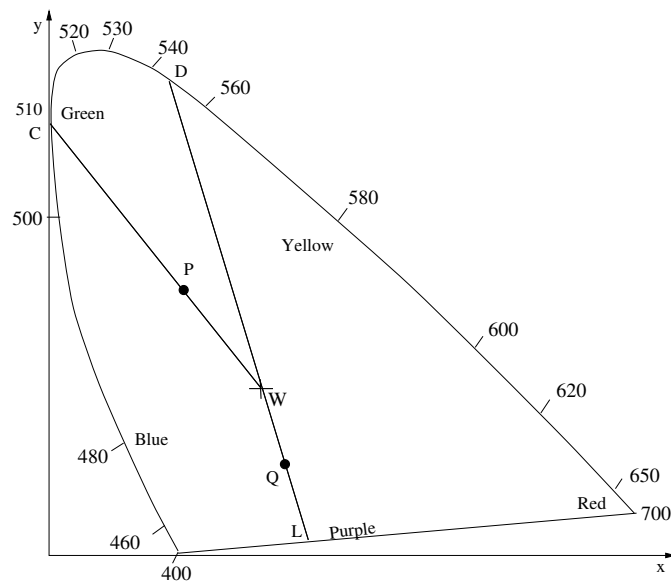


Figure A.11: CIE Chromaticity Diagram

We define *chromaticity values* x , y and z from the tristimulus values as follows.

$$x = \frac{X}{X + Y + Z}; y = \frac{Y}{X + Y + Z}; z = \frac{Z}{X + Y + Z}$$

Notice that $x + y + z = 1$. Thus, just by knowing x and y , we cannot calculate back X , Y and Z .

Figure A.11 shows the result of plotting x and y for all visible colors. This is called CIE chromaticity diagram and corresponds to chrominance. It has been shown that all colors with same hue and saturation (but different luminance) coincide at the same point on the chromaticity diagram.

The interior and the boundary of the horse shoe shaped region represent all the visible chromaticity values. A standard white light is formally defined at W where $x = y = z = \frac{1}{3}$. The monochromatic or the cent percent saturated colors form the outer border of this region while the colors in the interior of the horse-shoe are unsaturated colors. The straight line in the bottom represents the various shades of purple. This diagram is very useful since these factors out the luminance and shows

only the chrominance. So it *does not* show all the colors. When two colors are added together, the chrominance of the new color lies on the straight line joining the two original colors in the chromaticity diagram, the location of the new color depending on the proportion of the luminances of the two colors added.

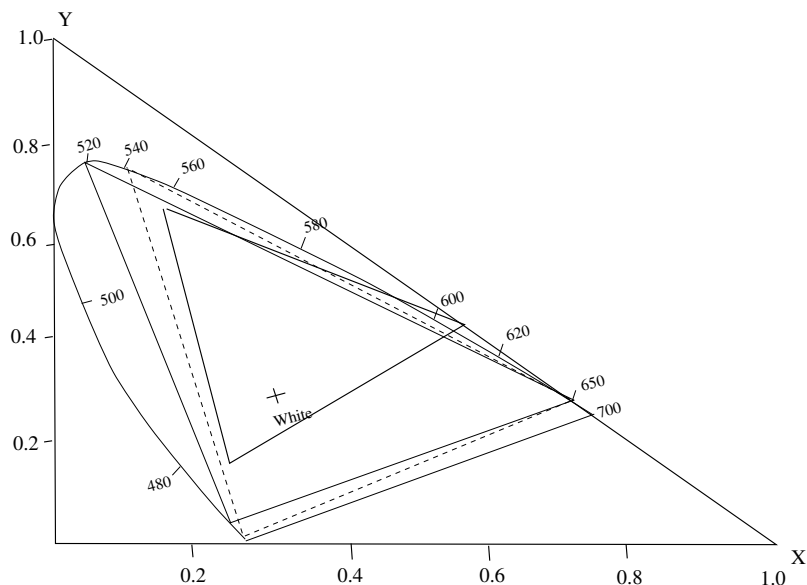


Figure A.12: CIE diagram showing three different color gamuts

Let P be a color in Figure A.11. The straight line joining white and P , meets the visual spectrum at C . Hence P is a unsaturated form of the pure monochromatic color C . The wavelength of C is called the *dominant wavelength* of P . However, all colors do not have a dominant wavelength. These colors are called *non-spectral*. For example Q does not have a dominant wavelength since the line from W to Q when extended meets the purple line. In such cases, the line is extended in the opposite direction and when it meets the visual spectrum, that wavelength is called the *complementary wavelength* for the color. In this case, the wavelength of D is the complementary wavelength of Q . Thus mixing D with Q will help us to get the achromatic color W . The *excitation purity* of any color possessing a dominant wavelength is an exactly defined ratio of the distances in the chromaticity diagram indicating how far the given color is displaced towards the spectrum color from the achromatic color. Thus the excitation purity of P is $\frac{|WP|}{|WC|}$. For a color without a dominant wavelength as Q , the excitation purity is $\frac{|WQ|}{|WL|}$.

Another use of the chromaticity diagram is that it helps us to specify *color gamuts*. If we draw a triangle joining any three colors in this diagram, all the color within the triangle can be represented by some combination of the three colors. This help us define the *real primaries* for reproducing color,

and needless to say, none of them can reproduce all the visible colors. Figure A.12 shows three such color gamuts devised by Wright and Guild respectively. Note that the smaller gamut cannot reproduce most of the shades of blue.

Advantage and Disadvantage of the CIE standard

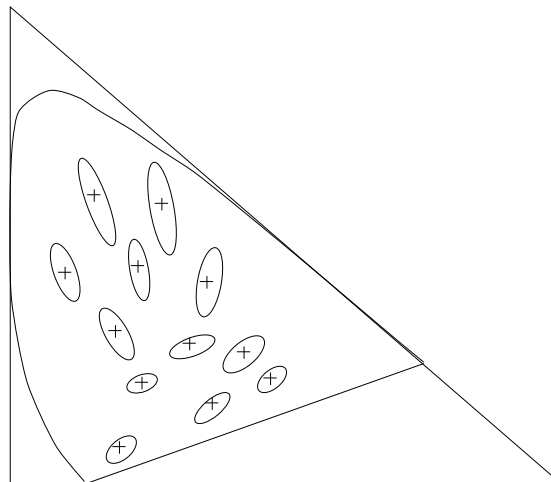


Figure A.13: *Least amount of change in color required to produce a change in hue and saturation*

The 1931 CIE standards have a few characteristics that render them useful for description of color in color hard copy and displays. The one obvious one is that the color produced by one set of primaries can be matched to the color produced by another set of primaries by adjusting them to produce the same CIE coordinates. Moreover, this models a standard human observer's photo-receptors sensitivity.

Despite these obvious facts, there are a few disadvantages of the CIE standard. The most important drawback is that the distance between two points on the CIE diagram tells nothing about the perceived color difference. In fact, from the perceptual perspective the CIE space is non-uniform. Figure A.13 depicts a study done by MacAdam in 1942 in which the least amount of color required to produce perceivable difference in hue and saturation is shown for samples taken from all over the CIE space. Two important aspects of this data need to be noted. First, the amount of change varies considerably for samples from different parts of the CIE space. Further, elliptical shape of the measurements indicates that the non-uniformity varies along the axis of the diagram. Recently, a transformation of the 1931 CIE standard color space has been adopted that produces a more uniform color space.

BIBLIOGRAPHY

- [Bern03] M. Bern and D. Eppstein. Optimized color gamuts for tiled displays. *ACM Computing Research Repository, cs.CG/0212007, 19th ACM Symposium on Computational Geometry, San Diego*, 2003.
- [Berns92a] R.S. Berns, M.E. Gorzynski, and R.J. Motta. Crt colorimetry, part ii: Metrology. *Color Research and Application*, 18(5):315–325, 1992.
- [Berns92b] R.S. Berns, R.J. Motta, and M.E. Gorzynski. Crt colorimetry, part i: Theory and practice. *Color Research and Application*, 18(5):299–314, 1992.
- [Buck00] Ian Buck, Greg Humphreys, and Pat Hanrahan. Tracking graphics state for networked rendering. *Proceedings of Eurographics/SIGGRAPH Workshop on Graphics Hardware*, 2000.
- [Cazes99] Albert Cazes, Gordon Braudaway, Jim Christensen, Mike Cordes, Don DeCain, Alan Lien, Fred Mintzer, and Steve L. Wright. On the color calibration of liquid crystal displays. *SPIE Conference on Display Metrology*, pages 154–161, 1999.
- [CC86] *Color and the Computer*. Academic Press INC, 1986.
- [Chen01] C. J. Chen and Mike Johnson. Fundamentals of scalable high resolution seamlessly tiled projection system. *Proceedings of SPIE Projection Displays VII*, 4294:67–74, 2001.
- [Chen02] Han Chen, Rahul Sukthankar, Grant Wallace, and Kai Li. Scalable alignment of large-format multi-projector displays using camera homography trees. *Proceedings of IEEE Visualization*, 2002.
- [Chorley81] R.A. Chorley and J. Laylock. Human factor consideration for the interface between electro-optical display and the human visual system. In *Displays*, volume 4, 1981.
- [CN93] Carolina Cruz-Neira, Daniel J. Sandin, and Thomas A. Defanti. Surround-screen projection-based virtual reality: The design and implementation of the CAVE. In *Proceedings of ACM Siggraph*, 1993.
- [Daly93] Scott Daly. The visual differences predictor : An algorithm for the assessment of image fidelity. *Digital Images and Human Vision, Editor: A.B. Watson, MIT Press*, pages 179–206, 1993.
- [Debevec97] Paul E. Debevec and Jitendra Malik. Recovering high dynamic range radiance maps from photographs. *Proceedings of ACM Siggraph*, pages 369–378, 1997.
- [D.H.Brainard89] D.H. Brainard. Calibration of a computer controlled color monitor. *Color Research and Applications*, 14(1):23–34, 1989.

- [ea97] N. Tsumura et. al. Color gamut mapping based on mahalanobis distance for color reproduction of electronic endoscope image under different illuminant, 1997.
- [Ferwerda97] James Ferwerda, S.N. Pattanaik, Peter Shirley, and Donald P. Greenberg. A model of visual masking for computer graphics. *Proceedings of SIGGRAPH'97*, pages 143–152, 1997.
- [Goldstein01] E. Bruce Goldstein. *Sensation and Perception*. Wadsworth Publishing Company, 2001.
- [Hereld02] Mark Hereld, Ivan R. Judson, and Rick Stevens. Dottyoto: A measurement engine for aligning multi-projector display systems. *Argonne National Laboratory preprint ANL/MCS-P958-0502*, 2002.
- [Humphreys99] G. Humphreys and P. Hanrahan. A distributed graphics system for large tiled displays. In *Proceedings of IEEE Visualization*, 1999.
- [Humphreys00] Greg Humphreys, Ian Buck, Matthew Eldridge, and Pat Hanrahan. Distributed rendering for scalable displays. *Proceedings of IEEE Supercomputing*, 2000.
- [Humphreys01] Greg Humphreys, Matthew Eldridge, Ian Buck, Gordon Stoll, Matthew Everett, and Pat Hanrahan. Wiregl: A scalable graphics system for clusters. *Proceedings of ACM SIGGRAPH*, 2001.
- [Kato96] N. Kato and M. Ito. Color gamut mapping for computer generated images, 1996.
- [Larson01] Gregory Ward Larson. Overcoming gamut and dynamic range limitation in digital images. *Siggraph Course Notes*, 2001.
- [Li00] Kai Li, Han Chen, Yuqun Chen, Douglas W. Clark, Perry Cook, Stefanos Damianakis, Georg Essl, Adam Finkelstein, Thomas Funkhouser, Allison Klein, Zhiyan Liu, Emil Praun, Rudrajit Samanta, Ben Shedd, Jaswinder Pal Singh, George Tzanetakis, and Jiannan Zheng. Early experiences and challenges in building and using a scalable display wall system. *IEEE Computer Graphics and Applications*, 20(4):671–680, 2000.
- [Lloyd02] Charles J. Lloyd. Quantifying edge blend quality: Correlation with observed judgements. *Proceedings of Image Conference*, 2002.
- [Lubin95] Jeffrey Lubin. A visual discrimination model for imaging system design and evaluation. *Vision Models for Target Detection and Recognition*, Editor: E. Peli, World Scientific, pages 245–283, 1995.
- [Majumder00] Aditi Majumder, Zue He, Herman Towles, and Greg Welch. Achieving color uniformity across multi-projector displays. *Proceedings of IEEE Visualization*, 2000.
- [Majumder01] Aditi Majumder and Greg Welch. Computer graphics optique: Optical superposition of projected computer graphics, 2001.

- [Majumder02a] Aditi Majumder and Rick Stevens. LAM: Luminance attenuation map for photometric uniformity in projection based displays. *Proceedings of ACM Virtual Reality and Software Technology*, 2002.
- [Majumder02b] Aditi Majumder. Properties of color variation across multi-projector displays. *Proceedings of SID Eurodisplay*, 2002.
- [Nakauchi96] S. Nakauchi. Color gamut mapping by optimizing perceptual image quality, 1996.
- [Pailthorpe01] B. Pailthorpe, N. Bordes, W.P. Bleha, S. Reinsch, and J. Moreland. High-resolution display with uniform illumination. *Proceedings Asia Display IDW*, pages 1295–1298, 2001.
- [Pattanaik98] S. N. Pattanaik, Mark D. Fairchild, James A. Ferwerda, and Donald P. Greenberg. Multiscale model of adaptation, spatial vision and color appearance. *Proceedings of IS&T and SID's 6th Color Conference, Arizona*, 1998.
- [Poynton96] Charles Poynton. *A Technical Introduction to Digital Video*. John Wiley and Sons, 1996.
- [Ramasubramanian99] Mahesh Ramasubramanian, S. N. Pattanaik, and Donald P. Greenberg. A perceptually based physical error metric for realistic image synthesis. *Proceedings of SIGGRAPH'99*, pages 73–82, 1999.
- [Raskar98] R. Raskar, G. Welch, M. Cutts, A. Lake, L. Stesin, and H. Fuchs. The office of the future: A unified approach to image based modeling and spatially immersive display. In *Proceedings of ACM Siggraph*, pages 168–176, 1998.
- [Raskar99a] Ramesh Raskar. Immersive planar displays using roughly aligned projectors. In *Proceedings of IEEE Virtual Reality 2000*, 1999.
- [Raskar99b] R. Raskar, M.S. Brown, R. Yang, W. Chen, H. Towles, B. Seales, and H. Fuchs. Multi projector displays using camera based registration. *Proceedings of IEEE Visualization*, 1999.
- [Samanta99] Rudro Samanta, Jiannan Zheng, Thomas Funkhouse, Kai Li, and Jaswinder Pal Singh. Load balancing for multi-projector rendering systems. In *SIGGRAPH/Eurographics Workshop on Graphics Hardware*, 1999.
- [Stone1a] Maureen C. Stone. Color balancing experimental projection displays. *9th IS&T/SID Color Imaging Conference*, 2001a.
- [Stone1b] Maureen C. Stone. Color and brightness appearance issues in tiled displays. *IEEE Computer Graphics and Applications*, 2001b.
- [Stupp99] Edward H. Stupp and Matthew S. Brennesholtz. *Projection Displays*. John Wiley and Sons Ltd., 1999.
- [Valois88] Russell L. De Valois and Karen K. De Valois. *Spatial Vision*. Oxford University Press, 1988.

- [Valois90] Russell L. De Valois and Karen K. De Valois. *Spatial Vision*. Oxford University Press, 1990.
- [Yang01] Ruigang Yang, David Gotz, Justin Hensley, Herman Towles, and Michael S. Brown. Pixelflex: A reconfigurable multi-projector display system. *Proceedings of IEEE Visualization*, 2001.